

STUDY OF SIMULATION MODELS TO ANALYZE STREAM BED VARIATIONS

A DISSERTATION

*Submitted in partial fulfillment of the
requirements for the award of the degree
of*

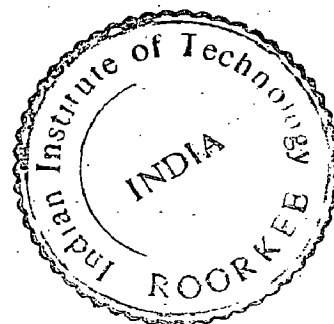
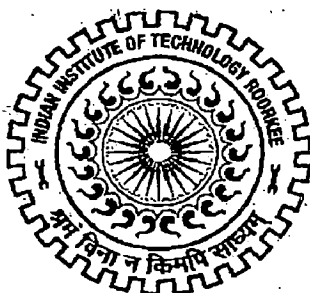
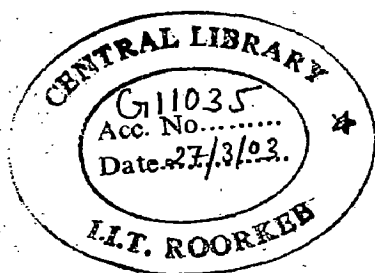
MASTER OF TECHNOLOGY

in

WATER RESOURCES DEVELOPMENT

By

MOTI RAJ GAUTAM



**WATER RESOURCES DEVELOPMENT TRAINING CENTRE
INDIAN INSTITUTE OF TECHNOLOGY ROORKEE
ROORKEE -247 667 (INDIA)
December, 2002**

10

627.072

GAU

CANDIDATE'S DECLARATION


I do hereby certify that this dissertation entitled "**STUDY OF SIMULATION MODELS TO ANALYZE STREAMBED VARIATIONS**" being submitted, in partial fulfillment of the requirements for the award of the degree of Master of Technology in **WATER RESOURCES DEVELOPMENT**, to Water Resources Development Training Centre, Indian Institute of Technology, Roorkee, is an authentic record of my own work carried out during the period from 16th July to 30th November, 2002 under the guidance of Dr. Nayan Sharma, Professor, Water Resources Development Training Centre, Indian Institute of Technology, Roorkee.

The matter embodied in this dissertation has not been submitted by me for the award of any other degree.


(MOTI RAJ GAUTAM)

This is to certify that the above statement made by the candidate is correct to the best of my knowledge.

Date: 6th Dec., 2002


(Dr. Nayan Sharma)
Professor
WRDTC, IIT-Roorkee

ACKNOWLEDGEMENT

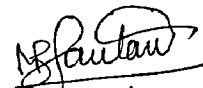
It is my great pleasure to express my sincere thanks with profound sense of respect and my gratitude to my guide Dr. Nayan Sharma, Professor, Water Resources Development Training Center (WRDTC), Indian Institute of Technology (IIT), Roorkee for his valuable guidance, constant encouragements atlast supervision and whole cooperation throughout the dissertation period.

I also extend my sincere gratitude to all the faculty members of the WRDTC, IIT, Roorkee for their valuable teaching, guidance, and encouragement and on time help rendered during the entire course of the study.

My special thanks goes to Dr. Howard H. Chang, Professor, Department of Civil and Environmental Engineering, San Diego University, USA for providing mathematical model FLUVIAL-12 and his expert advice during the study period.

The friendship developed and the help rendered by my batch mates can never be expressed in words.

Finally, I am extremely grateful to my mother who made innumerable sacrifices for me. No word would be enough to my loving wife Devaka Gautam and my children for encouragement and bearing patiently all the inconvenience caused during the study period.


6/12/2002

ABSTRACT

STUDY OF SIMULATION MODELS TO ANALYZE STREAM BED VARIATIONS

Quite often it becomes necessary to conduct computer-based hydraulic model study, especially for safe design of Hydraulic Structures against streambed variations. Several reputed international expert agencies such as Hydrologic Engineering Center (HEC), USA and Danish Hydraulic Institute (DHI), Denmark have developed versatile simulation models for reproduction of flow behavior of sediment laden-water on digital computers. This latest development of computer based simulation study of alluvial water courses has facilitated the engineering fraternity to conduct prompt hydraulic model testing to ascertain the safety of the structure against abrupt streambed variations. However, there is a need to investigate the response of simulation models from the standpoint of streambed variation under steady and transient conditions.

In this background, it is envisaged to undertake in this dissertation a study on three widely-used simulation models of international standing with regard to assessment of streambed variation. Further it is proposed that the phenomenon of streambed variation will be investigated for near-field and far-field concepts with the help of simulation models. The phenomenon of near-field streambed variation will be investigated on the model by considering for the general scour as well as local scour with hypothetical structure in position. The results of the proposed study will be useful for selection of simulation model for particular physical situation.

LIST OF SYMBOLS

a	=	Embankment width normal to the flow in bridge pier and abutment in scour formulae
A_e	=	Flow area of the approach cross section obstructed by the embankment, m^2
A_c	=	Net cross-sectional area in the inlet at the crossing, at mean water surface
		Cross-sectional area within reference frame, m^2 elevation, m^2
ΔA_b	=	Change in cross-sectional area obtained in sediment routing represents the correction for a time increment Δt that needs to be applied to the bed and banks, m^2
a, b	=	Pier width, m
C_d	=	Coefficient of discharge
C_1 to C_4	=	Various coefficients in Ackers and White's sediment transport formulae
D, d	=	Diameter of the bed material, mm or m
	=	Diameter of smallest nontransportable particle in the bed material, m
D_m, d_m	=	Effective mean diameter of the bed material in the bridge, mm or m
	=	$1.25 d_{50}$
D_{50}, d_{50}	=	Median diameter of the bed material, diameter which 50% of the sizes are smaller, mm or m
D_{84}, d_{84}	=	Diameter of the bed material of which 84% are smaller, mm or m
D_{90}, d_{90}	=	Diameter of the bed material of which 90% are smaller, mm or m
d_i	=	Geometric mean diameter, m
d_a	=	Arithmetic mean diameter, m
Fr	=	Froude Number [$V/(gy)^{1/2}$ or $u/(gy)^{1/2}$]
	=	Froude Number of approach flow upstream of the abutment
	=	Froude Number based on the velocity and depth adjacent to and upstream of the abutment
Fr_1	=	Froude Number directly upstream of a pier
F	=	A factor function of friction factor, f , m
F_c	=	critical Froude number for incipient motion
f	=	Darcy-Weisbach friction factor
	=	$8 g R S / u^2$
g	=	Acceleration of gravity, m / s^2
h_{1-2}	=	Head loss between sections 1 and 2, m
h_c	=	Average depth of flow in the waterway at mean water elevation, m
h_{ce}	=	Expansion or contraction loss, m
H	=	Height (i.e., height of a dune), m
H_b	=	Distance from the low chord of the bridge to the average elevation of the stream bed before scour, m
i	=	Number of cross-section counted upstream to downstream
j	=	Time t
$j+1$	=	Time $t+1$
K	=	Various coefficients in equations as described below
K	=	Various coefficients in equations as described below
	=	Conveyance in Manning's equation, $(AR^{2/3}) / n$, m^3/s

	=	Bottom width of the scour hole as a fraction of scour depth, m
K_o	=	Velocity head loss coefficient on the downstream side of the waterway
K_b	=	Velocity head loss coefficient on the bay or upstream side of the waterway
K_s	=	Shields coefficient
K_1	=	Correction factor for pier nose shape
	=	Coefficient for abutment shape
K_2	=	Correction factor for angle of attack of flow
	=	Coefficient for angle of embankment to flow
K_3	=	Correction factor for increase in equilibrium pier scour depth for bed condition
K_4	=	Correction factor for armoring in pier scour equation
k_1 & k_2	=	Exponents determined in Laursen's live-bed contraction equation, depends on the mode of bed material transport
k_s	=	Grain roughness of the bed. Normally taken as the d_{84} of the bed material, m
K	=	Karman's coefficient
	=	Transverse (radial) coordinate index
L	=	Length of pier or abutment, distance between sections, m
L_c	=	Length of the waterway, m
L_{lob}, L_{ch}, L_{rob}	=	Cross section reach lengths specified for flow in the left overbank, main channel, and right overbank, respectively, m
L_{-}	=	Length of abutment (embankment) projected normal to flow, m
n	=	Manning's n
n_1	=	Manning's n for upstream main channel
n_2	=	Manning's n for contracted section
Q	=	Discharge through the bridge or on the overbank at the bridge, m^3/s
Q_e	=	Flow obstructed by the abutment and approach embankment, m^3/s
Q_{max}	=	Maximum discharge in the inlet, m^3/s
Q_1	=	Flow in the upstream main channel transporting sediment, m^3/s
Q_2	=	Flow in the contracted channel, m^3/s . Often this is equal to the total discharge unless the total flood flow is reduced by relief bridges or water overtopping the approach roadway
Q_{100}	=	Storm-event having a probability of occurrence of one every 100 years, m^3/s
Q_{500}	=	Storm-event having a probability of occurrence of one every 500 years, m^3/s
Q_{lob}, Q_{ch}, Q_{rob}	=	Arithmetic average of the flows between sections for the left overbank, main channel, and right overbank, respectively, m
q	=	Discharge per unit width, discharge of lateral inflow, $m^3/s / m$
	=	Discharge in conveyance tube, m^3/s
Q_s	=	Sediment discharge at cross-section, m^3/s
q_b	=	Sediment discharge per unit channel width, $m^3/s / m$
q_s	=	Lateral inflow of sediment, $m^3/s / m$
R	=	Hydraulic radius, radius of curvature, m
	=	Coefficient of resistance
Re	=	Renold's Number
	=	uy / ν
r	=	radius of curvature, m

SBR	=	Set-back ratio of each abutment
S_1	=	Slope of energy grade line of main channel, m/m
S_f	=	Slope of the energy grade line, m/m
S_o	=	Average bed slope, m/m
S_s	=	Specific gravity of bed material. For most bed material this is equal to 2.65.
	=	Shields' Coefficient
	=	Side slope of embankment, 1 vertical : S_s horizontal
s	=	Curvilinear length of channel, m
S	=	Total energy gradient in curved channel
S'	=	Longitudinal energy gradient in curved channel
S''	=	Energy gradient due to secondary current in curved channel
Δt	=	Time increment, seconds
V_{av}, V_u	=	Average velocity, m / s
	=	Characteristic average velocity in the contracted section for estimating a median stone diameter, D_{50} , m/s
u_{max}, V_{max}	=	Q_{max}/A' , or maximum velocity in the inlet, m / s
u_1, V_1	=	Average velocity at upstream main channel, m / s
	=	Mean velocity of flow directly upstream of the pier, m / s
u_2, V_2	=	Average velocity in the contracted section, m / s
V_c, u_c	=	Critical velocity, m/s, above which the bed material of size d, d_{50} , etc. and smaller will be transported
V_{c50}, u_{c50}	=	Critical velocity for d_{50} bed material size, m / s
V_{c90}, u_{c90}	=	Critical velocity for d_{90} bed material size, m / s
V_e	=	Q_e/A_e , m/s
V_f	=	Average velocity of flow zone below the top of the footing, m / s
V_i, u_i	=	Approach velocity when particles at a pier begin to move, m / s
V_{max}, u_{max}	=	Maximum average velocity in the cross section at Q_{max} , m / s
VR	=	Velocity ratio
V^*, u^*	=	Shear velocity in the upstream section, m / s
	=	$(\tau/\rho)^{1/2} = (gy_1 S_1)^{1/2}$
W	=	Bottom width of the bridge less pier widths, or overbank width (set back distance less pier widths), m
	=	Topwidth of the scour hole from each side of the pier of footing, m
W_1	=	Bottom width of the upstream main channel, m
W_2	=	Bottom width of the main channel in the contracted section less pier widths, m
ω	=	Fall velocity of the bed material of a given size, m/s
x	=	Distance along the flow direction, m
y	=	Depth of flow, m. This depth is used in the Neill's and Laurson's equation as the upstream channel depth to determine V_c or u_c .
	=	Depth of flow in the contracted bridge opening for estimating a median stone diameter, d_{50} , m
ya	=	Average depth of flow on the floodplain, m
yf	=	Distance from the bed to the top of the footing, m
yo	=	Existing depth of flow, m
yps	=	Depth of pier scour, m

y_s	=	Average contraction scour depth, m
y_s	=	Local scour depth, m
y_s	=	Depth of vertical contraction scour relative to mean bed elevation, m
y_{sc}	=	Depth of contraction scour, m
y_1	=	Average depth in the upstream main channel or on the floodplain prior to contraction scour, m
	=	Depth of flow directly upstream of the pier, m
	=	Depth of flow at the abutment, on the overbank or in the main channel for abutment scour, m
y_2	=	Average depth in the contracted section (bridge opening) or on the overbank at the bridge, m
	=	Average depth under lower cord, m
Z	=	Vertical offset to datum, m
τ_2, τ_0	=	Average bed shear stress at the contracted section, Pa or N / m^2
τ_c, τ_{cr}	=	Critical bed shear stress at incipient motion, N / m^2
τ^*c	=	Non dimensional critical shear stress
	=	u_*c / v
γ	=	Specific weight of water, N / m^3
ρ	=	Density of water, Kg / m^3
ρ_s	=	Density of sediment, kg / m^3
ϕ	=	Angle of repose of the bed material (ranges from about 30° to 44°)
	=	Skew angle of abutment (embankment) with respect to flow
ν	=	Kinematic viscosity of water, m^2 / s
λ	=	Porosity coefficient
ϕ_T	=	Total load parameter
α	=	Energy correction factor
β	=	Momentum correction factor

CONTENTS

CANDIDATES DECLARATION	(i)
ACKNOWLEDGMENT	(ii)
ABSTRACT	(iii)
LIST OF SYMBOLS	(iv-vii)
TABLE OF CONTENTS	(viii-x)
LIST OF TABLES	(xi)
LIST OF FIGURES	(xii-xiii)
1. INTRODUCTION	1-5
1.1 General	1
1.2 Objectives	2
1.2.1. To identify and Review of the Attribute of Widely used Simulation Models	2
1.2.2. Testing of Simulation Models for Streambed Variations	3
1.2.3. Simulation of General and Local Scour	4
1.2.4. Analysis of Simulation Models	4
1.3. General Comments on Results	4
1.4. Limitations of the Study	4
1.5. Organization of Thesis	5
2. BASIC THEORETICAL CONCEPTS	6-31
2.1. General	6
2.2. General and Local Scour	6
2.3. Contraction Scour Equation	8
2.3.1. Live-bed Contraction Scour Equation	8
2.3.2. Clear-Water Contraction Equation	10
2.3.3. Backwater	12
2.3.4. Confluence Scour	12
2.3.5. Bend Scour	12
2.3.6. Critical Velocity of Bed Materials	13
2.4. Local Scour	13
2.4.1 Computation of Pier Scour	14
2.4.2 Pressure Flow Scour	17
2.4.3 Scour from Debris	18
2.4.4 Width of Scour Hole	18
2.5. Local Scour at Abutments	18
2.5.1. Live-bed Scour at Abutments	20
2.5.2. Clear-Water Scour at Abutments	22

2.6.	Streambed Variation Equations	22
2.6.1.	Water Routing	22
2.6.2.	Sediment Routing	24
2.6.3.	Determination of Sediment Discharge	24
2.6.4.	Numerical Solution of Continuity Equation for Sediment	26
2.6.5.	Simulation of Changes in Channel Width	27
2.6.6.	Direction of Width Adjustment	27
2.6.7.	Rate of Width Adjustment	28
2.6.8.	Simulation of Changes in Channel-bed Profile	29
2.6.9.	Simulation in Changes due to Curvature Effects	30
3.	PROMINENT MATHEMATICAL MODELS	32-37
3.1.	General	32
3.2.	Review of Models	32
3.2.1.	FLUVIAL-12	32
3.2.2.	CHARIMA and ILLUVIAL	33
3.2.3.	MIKE 11	33
3.2.4.	HEC-6	34
3.2.5.	WSPRO	34
3.2.6.	HEC-RAS	35
4.	DESCRIPTION OF MODELS USED	38-66
4.1.	General	38
4.2.	FLUVIAL-12	38
4.3.	HEC-RAS	39
4.3.1.	Steady Flow Water Surface Profiles	40
4.3.2.	Unsteady Flow Simulations	40
4.3.3.	Bridges and Culverts	40
4.3.3.1.	Entering Geometric Data	41
4.3.3.2.	Cross-section Locations	41
4.3.3.3.	Contraction and Expansion Losses	44
4.3.4.	Bridge Hydraulic Calculations	45
4.3.4.1.	Low Flow Computations	45
4.3.4.2.	Pressure Flow Computations	53
4.3.4.3.	Weir Flow Computation	57
4.3.4.4.	Combination Flow	60
4.4.	FHWA WSPRO	60
4.4.1.	General	60
4.4.2.	Pier Scour	61
4.4.3.	Local Scour at Abutments	63
4.4.4.	Contraction Scour	64
4.4.5.	Clear-Water Contraction Scour	65
4.5.	Critical Shear Stress Approach	66
4.6.	Critical Velocity Approach	66

5. SIMULATION STUDY	67-100
5.1. Simulation study of Streambed Variation	67
5.2. Data Required	67
5.3. Input Data	67
5.4. Computing Procedure	68
5.5. Output Description	68
5.6. Description of Maan River	68
5.6.1. Location	68
5.6.2. Physical Conditions	69
5.6.3. Streambed Variations	69
5.7. Simulation and Results	70
5.7.1. Changes in River Channel Configurations	70
5.7.2. Changes in Sediment Size and Hydraulic Sorting	77
5.7.3. Streambed Variation in Relation to Power Expenditure	78
5.7.4. Water Surface Profiles	79
5.8. Streambed Variation of Babai River	80
5.8.1. Physical condition	80
5.8.2. Simulation and Results	81
5.8.3. Change in River Channel Configuration	81
5.8.4. Changes in Sediment Load and Hydraulic Parameters	87
5.8.5. Changes in Sediment Size and Hydraulic Sorting	87
5.8.6. Streambed Variation in Relation to Power Expenditure	89
5.8.7. Water Surface Profiles	89
5.8.8. Flow Resistance	91
5.9. Simulation of General and Local Scour	91
5.9.1. General	91
5.9.2. Data Required	92
5.9.3. Scour Depth Simulation Using HEC-RAS	92
5.9.3.1. Geometric Data Editor	92
5.9.3.2. Entering Bridge Data	94
5.9.3.3. Unsteady Flow Data	95
5.9.3.4. Unsteady Flow Analysis	96
5.9.3.5. Hydraulic Design Function	96
5.9.4. Scour Depths Under Steady Flow Conditions	100
5.9.5. FHWA WSPRO Method	100
6. SUMMARY AND CONCLUSIONS	101-104
6.1. Water Surface Profiles	101
6.2. Total Sediment Transport Rate	101
6.3. Energy Gradient and Power Expenditure	102
6.4. Variation in Streambed Profile	102
6.5. Scour Depths	104
6.6. Conclusions	105
REFERENCES	107
APPENDIX-A	109
APPENDIX -B	122
APPENDIX -C	134

LIST OF TABLES

Table No. Title	Page
2.1 Values of k1 and k2 Sediment Load Conditions	9
2.2 Variation of ks with Bed Material Size	11
2.3 Correction k1 for Pier Nose Shape	16
2.4 Correction Factor k2 for Angle of Attack 'θ' of the Flow	16
2.5 Factor k3 for Increase in Equilibrium Pier Scour Depths for Bed Conditions	16
2.6 Limits for Bed Material Size and K4 Values	17
2.7 Abutment Shape Coefficient k1	21
3.1 Summary of Some Alluvial River Models	36
4.1 Ranges of Expansion Ratios	43
4.2 Subcritical Flow Contraction and Expansion Coefficients	44
4.3 Typical Drag Coefficients for Pier Shape	49
4.4 Yarnell's Pier Coefficient for Various Pier Shapes	50
5.1 Time and Spatial Variations of grain Size	77
5.2 Time and Spatial Variations of Energy Gradient	78
5.3 Time and Spatial Variations of Froude Number	80
5.4 Time and Spatial Variations of Froude Number	90
5.5 Time and Discharge Variations of Contraction Scour Depths	98
5.6 Time and Discharge Variations of Abutment Scour Depths	99
5.7 Time and Discharge Variations of Pier Scour Depths	99
5.8 Scour Depths under Steady Flow Conditions	100
5.9 Scour Depths Simulated by WSPRO	100
6.1 Spatial Variation of Energy Gradient (Mann River) at Peak Floods	102
6.2 Maximum Contraction Scour Depths	104
6.3 Maximum Abutment Scour Depths	104
6.4 Maximum Pier Scour Depths	105

LIST OF FIGURES

Fig. No.	Title	Page No.
2.1	Pier Scour Depth in Sand-bed as Function of Time	8
2.2	Schematic Presentation Scour around Cylindrical Pier	14
2.3	Abutment Scour Schematic Presentation	20
4.1	Cross-section Locations	41
4.2	Typical Cross-section Near Bridges	42
4.3	Cross-section Near and Inside the Bridge	47
4.4	A Bridge Under Sluice Gate Type of Pressure Flow	55
4.5	Coefficient of Discharge for Sluice Gate Type of Flow	55
4.6	A Bridge under Fully Submerged Flow	56
4.7	Bridge with Pressure and Weir Flow	58
4.8	Discharge Reduction due to Submergence	60
4.9	Equal Conveyance Tubes	62
4.10	Sketch Showing two Possible Choices of Abutment Approach Depths	64
5.1	Inflow Hydrograph of Maan River	70
5.2	Time Variation of Cross-section, No Significant Changes	71
5.3	Time Variation of Cross-section, Degradation of Channel	71
5.4	Time Variation of Cross-section, Aggradation and Lateral Migration of Channel	72
5.5	Time Variation of Cross-section, Aggradation and Width Reduction	72
5.6	Time Variation of Cross-section, Aggradation and Width Reduction	73
5.7	Time Variation of Cross-section, Lateral Migration of Channel	73
5.8	Time Variation of Cross-section, Aggradation	74
5.9	Time Variation of Cross-section, Aggradation and Lateral Migration of Channel	74
5.10	Time and Spatial Variation of Sediment Load	76
5.11	Time and Spatial Variation of Water Surface Profiles	76
5.12	Time and Spatial Variation of Velocity	76
5.13	Time and Spatial Variation of Power Expenditure	79
5.14	Inflow Hydrograph of Babai River	81
5.15	Time Variation of Cross-section, Degradation and Width Reduction	82

5.16 Time Variation of Cross-section, Aggradation and Width Reduction	82
5.17 Time Variation of Cross-section, Aggradation and Lateral Migration of Channel	83
5.18 Time Variation of Cross-section, Aggradation, Widening and Lateral Migration	83
5.19 Time Variation of Cross-section, Aggradation and Widening	84
5.20 Time Variation of Cross-section, Aggradation and Widening	84
5.21 Time Variation of Cross-section, Aggradation and Widening	85
5.22 Time Variation of Cross-section, Degradation and Lateral Migration of Channel	85
5.23 Time Variation of Cross-section, Degradation, Width Reduction and Lateral Migration of Channel	86
5.24 Time and Spatial Variation of Velocity	86
5.25 Time and Spatial Variation of Sediment Load	87
5.26 Time and Spatial Variation of Median Diameter, d_{50}	88
5.27 Time and Spatial Variation of Energy Gradient (Power Expenditure)	88
5.28 Time and Spatial Variation of Water Surface Profile	90
5.29 Time and Spatial Variation of Manning's 'n'	91
5.30 River Schematic Drawn in Geometric Data Editor	93
5.31 Upstream and Downstream Cross-section of the Bridge	94
5.32 Unsteady Flow Data Editor and Flood Hydrograph Plotted by the HEC-RAS	96
5.33 Hydraulic Design Function	97
5.34 Plot of General and Local Scour Depths	98
6.1 Spatial Variations of Water Surface Profiles of Maan River at Peak Flood	101
6.2 Time and Spatial Variation of Streambed of Babai River Simulated by FLUVIAL-12	103
6.3 Time and Spatial Variation of Streambed of Maan River Simulated by FLUVIAL-12	103

INTRODUCTION

1.1. General

Alluvial rivers are self-regulatory in that they adjust their characteristics in response to any change in the environment. These environment changes may occur naturally, as in the case of climatic variation or change in vegetative cover, may be result of such human activities as damming, river training, diversion, sand and gravel mining, channelization, bank protection and bridge and highway construction. Such changes distort the natural quasi equilibrium of a river; in the process of restoring the equilibrium, the river will adjust new conditions by changing its slope, roughness, bed material size, cross-sectional shape, or meandering pattern. Within the existing constraints, any one or combination of these characteristics may adjust as the river seeks to maintain the balance between its ability to transport and the load provided.

River channel behavior often needs to be studied for its natural state and responses to the aforementioned human activities. Studies of river hydraulics, sediment transport and river channel changes may be through physical modeling or mathematical modeling or both. Physical modeling has been relied upon traditionally to obtain the essential design information. It nevertheless often involves large expenditure and is time consuming in model construction and experimentation. What limits the accuracy of physical modeling is the scale distortion, which is almost unavoidable whenever it involves sedimentation.

Mathematical modeling of erodible channels has been advanced with progress in the physics of fluvial processes and computer techniques. Since the actual size of river is employed in mathematical modeling there is no scale distortion. The applicability and accuracy of a model depends on the physical foundation of numerical techniques employed.

1.2. Objectives

A number of mathematical models have been developed by different investigators in the field of river engineering for the specific purpose or general purposes since 1970's (see table 3.1). Streambed variation can be divided into viz. long-term aggradation and degradation, contraction scour and local scour around hydraulic structures. The study of some widely used and readily available, simulation models to compute or simulate various parameters of streambed variation components is the aim of this work. The objective of this study can be summarized as given below.

1.2.1. To Identify and Review the Attributes of Widely used Simulation Models

Mathematical models for the study will be selected for the study of the following components of streambed variations:

- 1 Water routing
- 2 Sediment routing
- 3 Changes in channel width
- 4 Changes in channel bed profile
- 5 Changes in geometry due to curvature effects
- 6 Bridge hydraulics (computation of contraction scour and local scour)

1. Water routing component should contain the evaluation of flow resistance due to the longitudinal and transverse flow.
2. Sediment routing component should be reviewed for the following features:
 - (i) Computation of sediment transport capacity using suitable formula for physical conditions.
 - (ii) Determination of actual sediment discharge by making corrections for sorting and diffusion.
3. Width change in alluvial rivers are characterized by widening of channel bed during aggradation (or fill) and reduction in width at the time of degradation (or scour). For a time increment, the amount of width change depends on the sediment rate, bank configuration and bank erodibility. The slope of erodible bank is limited by the angle of repose of the material. The rate of width change depends

on the rate at which sediment material is removed or deposited. Therefore, in the study, the model will be reviewed for its capability to simulate the variations of the lateral dimensions of the channel.

4. The process of variation of width (due to scour or fill) are associated with the streambed profile changes. Generally speaking, deposition in the bed is often accompanied by channel widening, while channel-bed erosion is usually associated with the channel width reduction, consequently channel-bed profile variation in both the cases.
5. Sediment transport, in the presence of transverse flow, has a component in that direction. Sediment movement in transverse direction contributes to the adjustment of transverse bed profile. In any unsteady flow, the transverse profile varies with time, and it is constantly adjusted towards equilibrium through scour or deposition. Selected models will be reviewed in response to these effects.
6. The presence of hydraulic structure across any stream can distort its present state of transient equilibrium. The river tries to attain its lost state of equilibrium, in doing so a huge amount of sediment is removed from the riverbed around the structures. The safety of the structure depends on the amount of potential scour that it would experience during its life span. Estimation of potential scour around any hydraulic structures is a great concern for hydraulic engineers for the safety of the structure. Streambed variation simulating models should be capable of estimating these quantities. In the study, bridge hydraulics component of simulation model will be investigated.

1.2.2. Testing of Simulation Models for Streambed Variation

The accuracy of mathematical models depends on the physical foundation, numerical techniques, and physical relations for momentum, flow resistance and sediment transport. Testing and calibration are important steps for more effective use of a model. The major items that require calibration include the roughness coefficient, sediment transport equation, bank erodibility factor, bed erodibility factor etc. The selected models for the study shall be employed for the simulation of the various components of streambed variation and hydraulic parameters with real-life data.

1.2.3. Simulation of General and Local Scours

General and local scour depths around bridge pier and abutments will be simulated assuming a hypothetical bridge across the stream in the study.

1.2.4. Analysis of Adopted Simulation Models

The selected models will be analyzed for their capabilities, attributes and their limitations.

1.3. General Comments on the Results

In this dissertation an erodible-boundary model, FLUVIAL-12 was employed in the case studies of mobile boundary channels, for simulating components of streambed variations (water routing sediment routing, width and profile variation). Simulated results are supported by the general observations in the field. The results incorporate interrelated changes in channel-bed profile, width and lateral migration of channel-bends. During aggradation channel-bed widens and during degradation channel-bed becomes narrower. These changes reflect in part, rivers adjustments in power expenditure.

In the case studies general and local scours were simulated using the HEC-RAS and WSPRO in a hypothetical bridge. Water surface profiles computed by these models were compared with the values computed by the FLUVIAL-12. These studies demonstrate that in the case of severely disturbed rivers, flood level computation using HEC-RAS and WSPRO may be quite inaccurate and improved accuracy can be provided by the FLUVIAL –12.

1.4. Limitations of the Study

Present dissertation is only an attempt to assess the general capabilities and attributes of simulation models in the form of case studies. It is only a visualization of streambed variation, general and local scour around a hypothetical bridge simulated by the mathematical models in mobile boundary channels. In these case studies sediment data from the grain-size distribution of bed material are only representative at the extremities of the study reach, and bank and bed erodibility factors are recommended values, water surface profiles are not verified by the measurement data.

The calibration and test of a model are important steps to be taken for more effective use of a model. Because of the sensitivity of simulated results to each relation or empirical coefficient more attention to be paid to those that generate sensitive results. Major items that require calibration include the roughness coefficient, sediment transport equation, bank erodibility factor, bed erodibility factor and so on.

1.5. Organization of Thesis

Chapter Two –Basic Theoretical concepts: In this chapter the basic concepts of general and local scours around pier and abutments, and streambed variations (viz., aggradation and degradation, variation of channel geometry and lateral migration of channel etc.) and governing equations are discussed in details.

Chapter Three - Prominent Mathematical Models: In this chapter mathematical models developed by different investigators in the field of river modeling their attributes and capabilities are explained.

Chapter Four – Mathematical Models Used: Mathematical models used in the case studies, the FLUVIAL-12, HEC-RAS and WSPRO algorithm used in the models, principles and methods of simulation are described.

Chapter Five–Simulation Studies and Results: This chapter comprises two parts, in the first part simulation of streambed bed variation for Babai and Maan Rivers by employing the FLUVIAL-12, and discussions of results of all the components of streambed variation have been presented. In the second part, simulation of general and local scours around a hypothetical bridge piers and abutments, and discussions of the simulated results have been presented.

Chapter Six - Summary and Conclusions: In this chapter summary of results simulated by the FLUVIAL-12, HEC-RAS and WSPRO, and comparison of profiles, flow resistance and power expenditure, are discussed. At the end summary of simulated results and conclusions are given.

Appendix – Sample input and out of FLUVIAL-12, WSPRO and HEC-RAS are shown end of the thesis.

BASIC THEORETICAL CONCEPTS

2.1. General

The streambed was seen to rise during the floods, while bed was lowered after the flood receded in alluvial rivers. On few other streams, exactly opposite happening was observed. These changes may be rapid. The variation of riverbed during flood is dependent on the difference between sediment supply into the reach and transporting capacity of the reach; if the supply is less than the capacity of the reach, bed is scoured. Such cases are observed in narrow reaches. On the other hand, in wide reaches situated downstream of narrow reaches, the sediment supply during floods would be in excess of the capacity and thus the bed rises during the rising stage.

Hydraulic Structure that obstruct the flow pattern in the vicinity of structure may cause localized erosion or scour. Changes in flow characteristics (velocity and turbulence) lead to change in sediment transport capacity and hence local disequilibrium between actual sediment transport and the capacity of flow to transport sediment. A new equilibrium eventually be reached as hydraulic conditions are adjusted through scour. Scour which may occur, at structure may be divided into general and local scour. These possible processes have the different time scales. Overall streambed variation results from modification to the stable regime condition to which the river has adjusted. This may be the result of changes in water or sediment flow in a river.

2.2. General and Local Scour

In an alluvial channel the scour around bridge piers, abutments, spur-dikes and other local obstructions is first initiated by the interference to the flow and sediment transport. The erodible bed deforms until it reaches an equilibrium scour configuration for which the rate of sediment supplied to the scour area is balanced by the rate of transport out of the area that is $(Q_s)_{in} = (Q_s)_{out}$. According to H. H. Chang, 1988[8], "the sediment transport through the scour hole is also effected by the horse shoe vortices, which, as turbulent motion, increase the particle mobility. The sediment transport rate is an inverse function of the particle size. Because sediment rates flowing into and out of

scour area change with size, at nearly the same proportion, the scour depth, is not significantly affected by the sediment size, which is therefore missing in most formulas for local scour”.

Since the pattern of scour is very much complicated by the configuration of the obstruction it is often necessary to utilize model studies in order to establish equilibrium scour depth as a function of pertinent variables. Such model studies have been made at the university of Iowa, Laursen, 1956 [10], and 1960, University of Roorkee Garde et al.,1961 [3] and Kothyari, 1992,Ettema,1992 [7], Kothyari et al.,1992 [4], Shen et al. 1969 [9], Melville and Sutherland,1988 [6] and Jain and Fisher,1980 [5], Breusers and Raudkivi,(1991). More than ten formulas have been developed for predicting local scours around bridge piers, based on essentially laboratory data. Despite the large number of such formulas contain a limited number of variables, namely, approach flow depth, effective pier width, Froude Number, shear stress and critical shear stress. Some of these formulae are for rectangular bridge piers. H. H. Chang, 1976 [8], analyzed data of different source and found, “The scour depth of circular pier is about 90 percent of that for rectangular pier and for sharp nose piers it is about 80 percent.”

Although a large amount of literature has been published on the local scour of cohesionless bed sediment around a pier, yet the studies by Melville (1975) and Hopkin et al. (1975) show that too often, glaring disparities have occurred between the actual depths of local scour and measured in the field and the local scour predicted from the diverse range of design relationships that were in use at that time [8].

The Colorado State University 1975[8] or CSU, formula reported in the Federal Highway Administration manual as a best fit to the data available is the most widely used formula. Froehlich developed a pier scour equation in uniform sediment under live bed condition from field measurements of local scour. Jain and Fisher 1979 [5] studied scour around circular piers at higher Froude numbers and proposed formula for scour depth calculation.

2.3. Contraction Scour Equation

There is two terms of contraction scour depending upon the competence of the uncontracted approach flow to transport bed material into the contraction.

Live-bed scour occurs when there is streambed sediment being transported into contracted section from upstream. In this case the scour hole reaches equilibrium when the transport of the bed material out of the scour hole is equal to the transported into the scour hole from upstream.

Clear-water scour occurs when the bed material sediment transport in the uncontracted approach flow is negligible or material being transported in the upstream reach is transported through the downstream reach at less than the capacity of flow. In this case the scour hole reaches equilibrium when the average bed shear stress is less than that required to incipient motion of the bed materials.

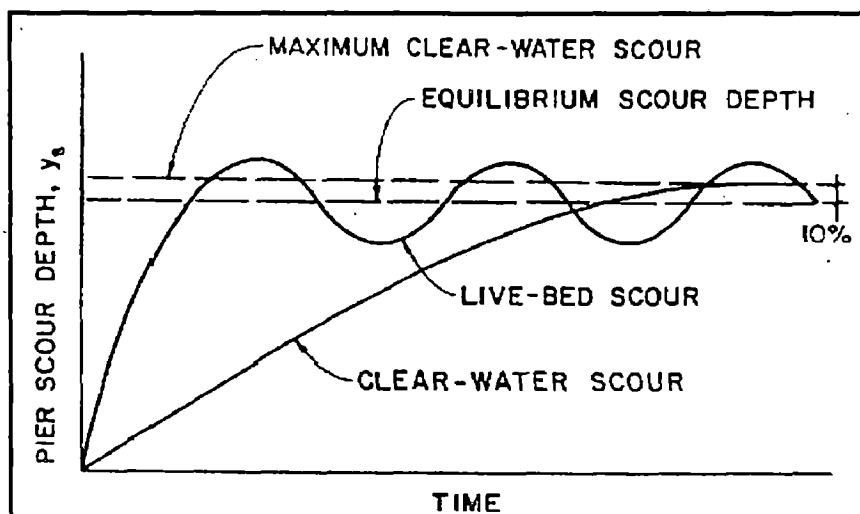


Fig. 2.1 Pier Scour Depth in Sand bed Stream as a Function of Time [20]

2.3.1. Live-bed Contraction Scour Equation

Laursen, (1960) derived the following contraction scour equation for live-bed scour

$$y_2 / y_s = (Q_2 / Q_1)^{6/7} (W_1 / W_2)^{k_1} (n_2 / n_1)^{k_2} \quad (2.1)$$

$$y_s = y_2 - y_0 \quad (2.2)$$

Where, y_s = equilibrium scour depth, m

y_1 = average depth in upstream main channel, m

y_2 = average depth in contracted section, m

y_o = existing depth in contracted section before scour, m

Q = flow in the upstream channel, cumec often this is equal to the total discharge unless the total flood flow is reduced relief bridges, water overtopping the approach road way or in the setback area.

W_1 = bottom width of upstream main channel, m

W_2 = bottom width of downstream main channel, m

n_1 = Manning's roughness coefficient for upstream uncontracted section

n_2 = Manning's roughness coefficient for contracted section

k_1, k_2 = exponent determined below depending the mode of bed material transport

The location for y_1, W_1, Q_1 and n_1 equal to one bridge opening distance from the upstream face of the bridge.

Table 2.1 [20]

Values of k_1 and k_2 and			Sediment Load Conditions
u_* / ω	k_1	k_2	Mode of bed material transport
< 0.50	0.59	0.066	Mostly contact bed material discharge
0.50 to 2.00	0.64	0.21	Some suspended bed material discharge
> 2.00	0.69	0.37	Mostly suspended bed material discharge

$u_* = \sqrt{(g y_1 S_f)}$, Shear velocity in the upstream section, N / m^2

ω = median fall velocity of the bed material based on the d_{50} , m / s

g = acceleration due to gravity, m / s^2

2.3.2. Clear-Water Contraction Equation

Clear water contraction occurs in the bridge opening when, (1) there is no bed material transport from the upstream reach into the downstream reach. And (2) material being transported in the upstream reach is transported through the downstream reach mostly in suspension at less than the capacity of flow. With clear water contraction scour the area of contracted section increases until, in the limit, the velocity of flow (u) or shear stress (τ_o) on the bed is equal to the critical velocity (u_c) or critical stress (τ_c) of a certain particle size (d) in the bed material.

Normally the width (W) of contracted section and depth (y) increases until limiting conditions are reached. Following development given by Laursen, (1960) equation for determining the clear water contraction scour in a long contraction was developed.

For the equilibrium in the contracted reach:

$$\tau_o = \tau_c \quad (2.3)$$

Where, τ_o = average bed shear stress in contracted section, N / m²

τ_c = critical shear stress at incipient motion, N/ m²

The average bed shear stress using y for hydraulic radius (R) and Manning's equation to determine the slope (S_f) can be expressed as follows:

$$\tau_o = \gamma_f y S_f = \rho g n^2 u^2 / y^{1/3} \quad (2.4)$$

For noncohesive bed material and fully developed clear water contraction scour, the critical shear stress can be determined using Shields' relation

$$\tau_c = k_s (\rho_s - \rho_f) g \quad (2.5)$$

The bed in long contraction scour until $\tau_o = \tau_c$ resulting in

$$\rho g n^2 u^2 / y^{1/3} = k_s (\rho_s - \rho_f) g d \quad (2.6)$$

Solving for the depth (y) in contracted section gives

$$y = [n^2 u^2 / \{k_s (\rho_s / \rho_f - 1) d\}]^3 \quad (2.7)$$

In terms of discharge (Q) the depth is given by

$$y = [n^2 Q / \{k_s (\rho_s / \rho_f - 1) d W^2 \}]^{3/7} \quad (2.8)$$

Where, y = average equilibrium depth in contracted section after contraction scour, m

S_f = slope of the energy grade line, m/m

u = average velocity in contracted section

d = diameter of smallest non – transportable particle in the bed material, m

W = bottom width of contracted section, m

k_s = Shields' coefficient

γ_f = unit weight of water, (9800 N/ m³)

ρ_f = density of water, (1000 kg / m³)

ρ_s = density of sediment (2647 kg / m³)

Table 2.2 [20]

Variation of k_s with Bed Material Size		
k_s	Size of bed material	Froude number, Fr
0.047	0.065 mm to 2.00 mm	< 0.800
0.030	2.00 mm < d_{50} < 40 mm	
0.020	d_{50} > 40 mm	

HIRE recommends the use of effective mean bed material size, (d_m) in place d_{50} ,

$$d_m = 1.25 d_{50}$$

The Strickler's equation gives $n = 0.040 (d_m)^{1/6}$ and $k_s = 0.039$ then depth (y) is given as:

$$y = u^2 / (40 d_m^{2/3})^3 \quad (2.9)$$

$$y = [Q^2 / (40 d_m W^2)]^{3/7} \quad (2.10)$$

$$y_s = y - y_o \text{ (average scour depth)} \quad (2.11)$$

2.3.3. Back Water

The live-bed contraction scour equation is derived assuming uniform reach above the long contractions where sediment transport into the downstream reach equal to the sediment transport out. The clear-water contraction equations are derived assuming that depth at bridge increases until shear stress and velocity are decreased so that there is no longer sediment transport. With the clear-water equations it is assumed that flow goes from one uniform flow condition to another. Both equations calculate contraction depth assuming a level water surface ($y_s = y_2 - y_0$). A more consistent computation would be to write energy balance equation before and after the scour. For live-bed, energy balance would be between approach section (1) and contracted section (2), whereas, for clear-water scour it would be the energy at the same section before (1) and after (2) of the contraction scour. These options are available in HEC- RAS and WSPRO.

2.3.4 Confluence Scour

When two branches of river meet, both the angle of confluence and water level may differ. Though mathematical models are available at present, because of one dimensional modeling these are of limited value. Bresuers and Raudkivi, (1991) proposed the following relationship to calculate scour at downstream of confluence:

$$y_s / y_0 = c_o + 0.037 \theta \quad (2.12)$$

Where,

c_o = Coefficient depending on bed material properties
= 1.29-2.24

y_0 = Average flow depth of the two branches, m

y_s = Equilibrium scour depth, m

θ = Angle between two upstream branches

Kassen and Vermeer, (1983) recommended for Jamuna river in Bangladesh $c_o = 1.29$ for fine sand. Based on field data Ashmore and Parker, (1983) found $c_o = 2.24$.

2.3.5 Bend Scour Depth

In general bend scour depends on local parameters (bend, curvature, flow depth and grain size) and upstream influences (redistribution of flow and sediment transport).

In outer part of bend excess scour occurs as the result of spiral flow. Struiksmā, et.al, (1985) showed that excess bed scour is due to this spiral flow and an overshoot phenomenon. Thorne, (1993) on the basis of flume experiment and prototype experiments in large rivers (flow depth upto 17 m), in which, the mean particle diameter varied from 0.3 to 63 mm suggested the following relationship:

$$y_s / y_o = 1.07 - \ln (R / B - 2) \text{ for } 2 < R / B < 22 \quad (2.13)$$

Where, R = Radius of curvature for center line, m

B = Bed width, m

Time scale, T_{as} for changes of cross-sectional profile can be given as:

$$T_{as} = 0.85 B^2 \sqrt{S_s} / (\pi^2 q) \quad (2.14)$$

Where, S_s = Shields' parameter

q = Sediment transport per unit width, m^2 / s

2.3.6. Critical Velocity of the Bed Material

Velocity and depth in equation (2.6) are associated with initiation of motion of the indicated particle size (d) . The critical velocity (u_c) for the initiation of the motion of bed material size (d), from equation (2.6) results in

$$u_c = [k_s (S_s - 1)^{1/2} d^{1/2} y^{1/6} / n] \quad (2.15)$$

Using specific gravity of sand, $S_s = 2.65$, Shields' Coefficient $k_s = 0.039$

And, $n = 0.041 (d)^{1/6}$ the above equation (2.15) reduces into

$$u_c = 6.19 y^{1/6} d^{1/2} \quad (2.16)$$

Where, u_c = critical velocity which above the bed material of size d and smaller will be transported, m / s

d = size of the bed materials, m

y = depth of flow, m

n = Manning's roughness coefficient

2.4 Local Scour Equation

The basic mechanism causing local scour at piers and abutments is the formation of vortices (known as horse-shoe vortex) at their base. In addition to the horse-shoe vortex around the base of the pier, there are vertical vortices downstream of the pier

called wake vortex (figure 2.2). Both horse-shoe and wake vortices remove material from the pier base region. However intensity of the wake vortex diminishes rapidly as the distance of the downstream from the pier increases.

Factors, which affect the magnitude of local scour depth at piers and abutments, are:

1. Velocity of the approach flow,
2. Depth of the flow,
3. Width of pier,
4. Discharge intercepted by the abutment and return in the main channel at the abutment (in laboratory flume this discharge is function of projected length of an abutment into the flow),
5. Length of the pier if skewed to the flow,
6. Size and gradation of material,
7. Angle of attack of approach to the pier or abutment,
8. Shape of the pier and abutment,
9. Bed configuration and
10. Ice formation or jam or debris.

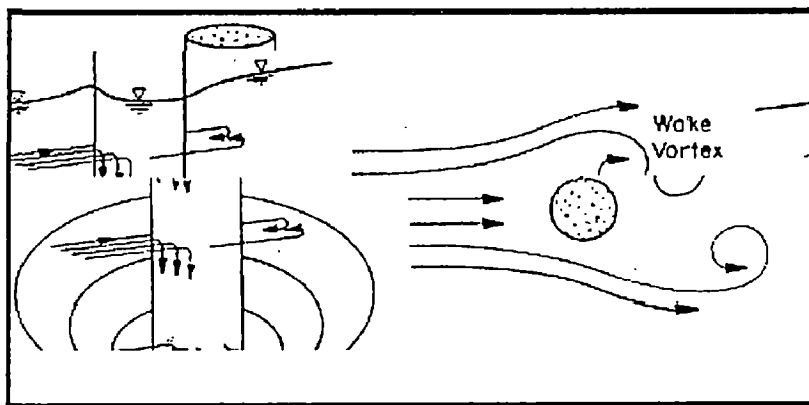


Fig. 2.2 Schematic Presentation of Scour around Cylindrical

2.4.1. Computation of Pier Scour

To determine pier scour, an equation based on the Colorado State University (CSU) formula is recommended by Hydraulic Engineering Center circular (HEC-18), FHWA [20], for the live-bed and clear-water, is used. The equation predicts the maximum pier scour depths and is given as:

$$y_s / y_1 = 2.0 k_1 k_2 k_3 k_4 (a / y_1)^{0.65} (Fr)^{0.43} \quad (2.17)$$

For round nose piers aligned with the flow:

$$y_s \leq 2.4 \text{ times the pier width (a) for Froude Number, } Fr \leq 0.80 \quad (2.18)$$

$$y_s \leq 3.0 \text{ times the pier width (a) for Froude Number, } Fr > 0. \quad (2.19)$$

In terms of y_s / a equation (2.17) can be written as:

$$y_s / a = 2.0 k_1 k_2 k_3 k_4 (y_1 / a)^{0.35} (Fr)^{0.43} \quad (2.20)$$

Where, y_s = Scour depth, m

y_1 = Flow depth directly upstream of the pier, m

k_1 = Correction factor for pier nose shape

k_2 = Correction factor for angle of attack of flow

k_3 = Correction factor for channel bed condition

k_4 = Correction factor for armoring by bed material size

a = Pier width, m

Fr = Froude Number directly upstream of the pier

$$= u_1 / (gy_1)^{1/2}$$

u_1 = Mean velocity of flow directly upstream of the pier, m/s

g = Acceleration due to gravity, (9.81 m/s²)

The correction factor k_2 for angle of attack of the flow, given in Table 2.4, can be calculated using the following equation:

$$k_2 = (\cos\theta + L / a \sin\theta)^{0.55} \quad (2.21)$$

If L / a is ≥ 12 use $L / a = 12$

Table 2.3

Correction Factor for Pier Nose Shape	
Shape of Pier Nose	K₁
(a) Square	1.1
(b) Round Nose	1.0
(c) Circular Nose	1.0
(d) Circular Cylinder	1.0
(e) Group of Cylinder	1.0
(f) Sharp Nose	0.9

Table 2.4

Correction Factor k₂ for Angle of Attack 'θ' of the Flow			
Angle	L / a = 4	L / a = 8	L / a = 12
0	1.0	1.0	1.0
15	1.5	2.0	2.5
30	2.0	2.75	3.5
45	2.3	3.3	4.3
90	2.5	3.9	5.0

Table 2.5

Factor k₃ for Increase in Equilibrium Pier Scour Depths for Bed Conditions		
Bed Conditions	Dune Height, m	k₃
Clear- Water Scour	N / A	1.1
Plane Bed and Antidune Flow	N / A	1.1
Small Dunes	3.0 > H ≥ 0.6	1.1
Medium Dunes	9.0 > H ≥ 3.0	1.2 to 1.1
Large Dunes	H ≥ 9.0	1.3

The correction factor k_4 decreases scour depths for armoring of the scour hole for bed materials that have d_{50} equal to or larger than 0.06m ($d_{50} \geq 0.06$ m). The correction factor results from recent research for FHWA by Molinas at CSU which showed that when the approach velocity, u_1 is less than the critical velocity (u_{c90}) of the d_{90} size of the bed material and there is a gradation in sizes in the bed material, the d_{90} will limit the scour depth. The equation developed by Jones from analysis of data is:

$$k_4 = [1 - 0.89 (1 - VR)^2]^{0.5} \quad (2.22)$$

$$VR = (u_1 - u_i) / (u_{c90} - u_i) \quad (2.23)$$

$$u_i = 0.645 (d_{50} / a)^{0.053} u_{c50} \quad (2.24)$$

Where, VR = Velocity ratio

u_1 = Approach velocity, m / s

u_i = Approach velocity when particles at pier begins to move, m / s

u_{c90} = Critical velocity for d_{90} material size, m / s

u_{c50} = Critical velocity for d_{50} material size, m / s

$$u_c = 6.19 y^{1/6} d_c^{1/3} \quad (2.25)$$

d_c = Critical particle size for the critical velocity u_c , m

Limiting k_4 values and bed material size are given in table 2.6

Table 2.6

Limits for Bed Material Size and k_4 Values			
Factor	Minimum Bed Material size	Minimum k_4 Value	VR > 1.0
K_4	$D_{50} \geq 0.06$ m	0.70	1.0

2.4.2. Pressure Flow Scour

Pressure flow is denoted as orifice flow, occurs when the surface elevation at the upstream face of the bridge is greater than or equal to low chord of the bridge structure. Pressure flow under the bridge results from a pile up of water on the upstream bridge face, and plunging of the flow downward and under bridge it has been discussed in chapter four.

2.4.3 Scour from Debris

Debris lodged in pier also increases the local scour at a pier. The debris may increase pier width and deflect a component of flow downward. This increases transport of sediment out of the scour hole. When floating debris is lodged on the pier, the scour depth can be estimated by assuming that the pier width is larger than the actual width. The problem is in determining the increase in pier width to use in the pier scour equation. Furthermore, at larger depths the effects of the debris on scour should diminish.

2.4.4. Width of Scour Hole

The top width of scour hole in cohesionless bed material from one side of a pier or footing can be estimated from the following equation:

$$W = y_s (k + \cot\phi) \quad (2.26)$$

Where, W = Top width of scour hole from each side of the pier or footing, m

y_s = Scour depth, m

k = Bottom width of scour hole as a fraction of scour depth

ϕ = Angle of repose of bed material ranging from 30° to 44°

The angle of repose for cohesionless material in air ranges from about 30° to 44° . Therefore, if the bottom width of scour hole is equal to the depth of scour (y_s) top width in cohesionless sand vary from 2.07 to 2.08 y_s . At the extreme, if $k = 0.0$, the top width would vary from 1.04 to 1.73 y_s . Thus top width ranges from 1.04 to 2.80 y_s and will depend on bottom width of the scour hole and composition of bed material. In general, deeper the scour hole, the smaller the bottom width. In water angle of repose of cohesionless material is less than the values given for air. Therefore, top width of 2.0 y_s is suggested for practical purposes.

2.5 Local Scour at Abutments

Local scour at abutment occurs when abutment obstructs the flow. The obstruction of flow forms a horizontal vortex starting at upstream end of the abutment, and running along the toe of the abutment, and a vertical wake vortex at the downstream end of the abutment. The vortex at the toe of the abutment is similar to horse-shoe vortex

that forms at piers, and the vortex that forms at the downstream end is similar to the wake vortex that forms downstream of a pier, or that forms downstream of any flow separation.

Equations for predicting abutment scour depths such as Liu, et al.'s Laursen's [10], Froehlich's and Melville's are based on entirely laboratory data. The problem is that little field data on abutment scour exist. Liu et al.'s equation was developed by dimensional analysis of the variables with best-fit line drawn through the laboratory data. Laursen's equations are based on inductive reasoning of the change in transport relations due to the accelerations of flow caused by the abutment. Froehlich's equations were derived from dimensional analysis and regression analysis of the available laboratory data. Melville's equations were derived from dimensional analysis and development of relations between dimensional parameters using best-fit line through laboratory data.

"All equations in literature were developed using abutment and roadway approach length as one of the variables and result in excessive conservative estimates of scour depth" [20]. Richardson and Richardson pointed this out in a discussion of Melville's, (1992), paper, "The reason the equations in the literature predict excessive conservative abutment scour depths for the field situation is that in the laboratory flume, the discharge intercepted by the abutment is directly related to the abutment length; whereas, in the field it is rarely the case" [22].

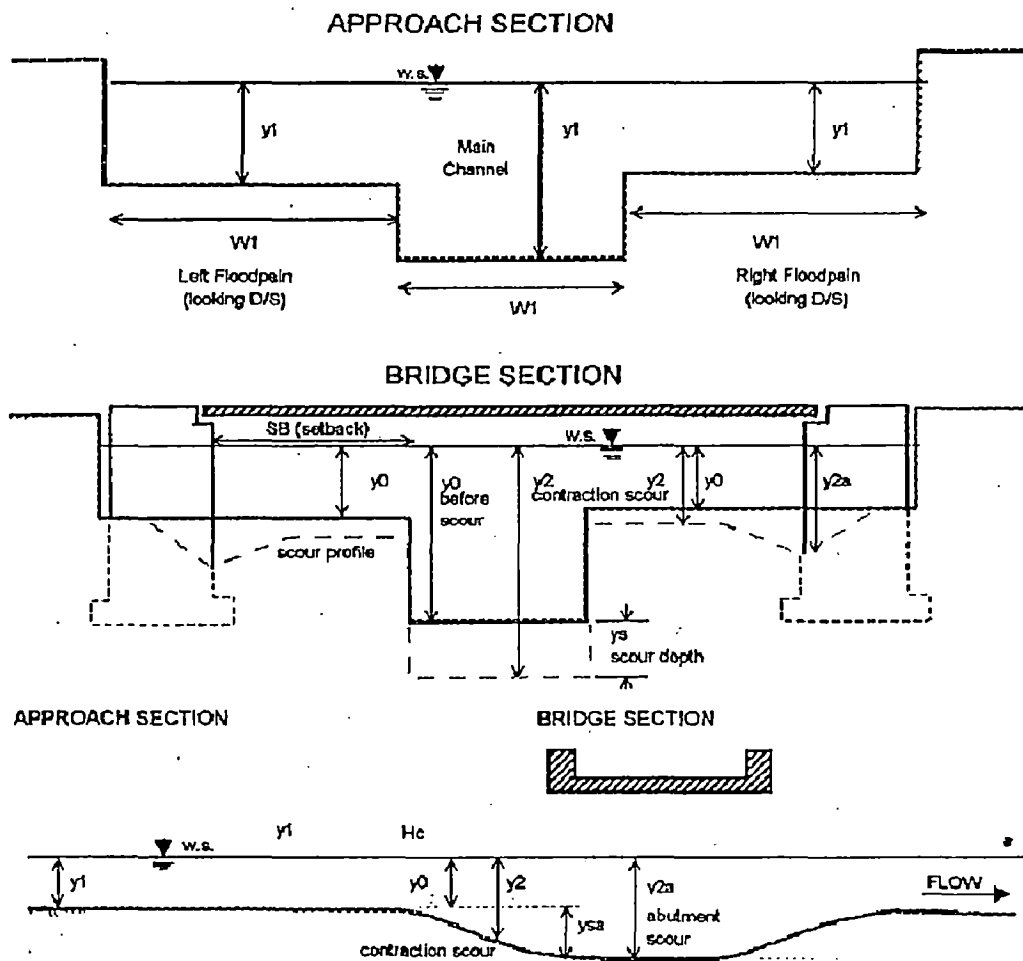


Fig. 2.3 Abutment Scour Schematic Presentation

2.5.1. Live-Bed Scour at Abutments

As a check on the potential depth of scour to aid in the design of the foundation and placement of riprap or guide banks, Froehlich's live bed scour equation or an equation from the HIRE can be used. Froehlich analyzed 170 live-bed scour measurements in laboratory flumes by regression analysis to obtain the following equation:

$$y_s / y_a = 2.27 k_1 k_2 (L' / y_a)^{0.43} (Fr)^{0.61} + 1.0 \quad (2.27)$$

Where, k_1 = Coefficient for abutment shape

k_2 = Coefficient for angle for abutment to the flow

$$k_2 = (\theta / 90^\circ)^{0.13}$$

$\theta < 90^\circ$ if abutment points downstream

$\theta > 90^\circ$ if abutment points upstream

L' = Length of abutment (embankment) projected normal to the flow, m

A_e = Flow area of approach cross- section obstructed by abutment, m^2

Fr = Froude Number of approach flow upstream of the abutment

$$= u_e / \sqrt{(g y_a)}$$

$$u_e = Q_e / A_e, \text{ m / s}$$

Q_e = Flow obstructed by the abutment and approach embankment, m^3 / s

y_2 = Average depth of flow on the flood plain, m

y_s = Scour depth, m

It should be noted that equation (2.27) is not consistent with the fact that as L' tends to zero, y_s also tends to zero. The 1.0 was added to the equation so as to envelop 98 percent of the data.

Table 2.7

Abutment Shape Coefficient, k_1	
Description	k_1
Vertical Wall Abutment	1.0
Vertical Wall Abutment with Wing Wall	0.82
Spill Through Abutment	0.55

HIRE equation (4.19) can be used when the ratio of projected abutment length (L') to the flow depth (y) is greater than 25.

$$y_s = 4 Fr^{0.33} k_1 / 0.55 \quad (2.28)$$

Where, y_s = Scour depth, m

y_1 = Depth of flow at the abutment on the over bank or in the main channel, m

F_r = Froude Number based on velocity and depth adjacent to and upstream of the abutment

k_1 = Abutment shape coefficient

2.5.2. Clear-Water Scour at Abutments

For clear-water scour at abutment equation (2.27) and equation (2.28) are used because clear-water scour equation potentially decrease scour at abutments due to the presence of coarser material. This decrease is unsubstantiated by the field data.

2.6. Streambed Variations Equations

The basic equations for treating the transient problem in alluvial streams can be written for one-dimensional flow in the following manner. The basic equations will be discussed for water routing, sediment routing and for boundary conditions separately.

2.6.1. Water Routing

Water routing provides temporal and spatial variations of the stage, discharge, energy gradient and other hydraulic parameters in the channel. The water routing component has the following three major features:

- (1) Numerical solution of the continuity and momentum equations for longitudinal flow,
- (2) Evaluation of flow resistance due to longitudinal and transverse flows, and
- (3) Upstream and downstream boundary conditions.

The continuity and momentum equations in the longitudinal direction are:

$$\partial A / \partial t + \partial Q / \partial s - q = 0 \quad (2.29)$$

$$1 / A (\partial Q / \partial t) + g (\partial H / \partial s) + 1 / A [\partial / \partial s (Q^2 / A)] + g S - (Q / A^2) q = 0 \quad (2.30)$$

Where, Q = Discharge, m^3 / s

A = Cross- sectional area of flow, m^2

t = Time, sec

s = Curvilinear coordinate along discharge center line measured from the upstream entrance

q = Lateral inflow rate, m^3 / s per unit length

H = Stage or water surface elevation, m

S = Energy gradient, m / m

According to H. H. Chang, (1983) in curved channel, total energy gradient, S in equation (2.30) can be partitioned into the longitudinal energy gradient, S' , and the transverse energy gradient, S'' , due to the secondary currents, i.e.

$$S = S' + S'' \quad (2.31)$$

The longitudinal gradient can be evaluated using any valid flow resistance relationship. Chang, suggests to use Brownlie's formula, (1983), for alluvial bed roughness.

Transverse energy gradient Chang, (1983, 1984) can be calculated as given below:

$$V_{i+1} = \left[V_i + F_1(f) \frac{U}{r_c} \exp[F_2(f)\Delta s] \Delta s \right] \exp[-F_2(f)\Delta s] \quad (2.32)$$

Where, V is the transverse surface velocity along discharge centerline, U is the average velocity of a cross section, i and $i+1$ are s -coordinate indices, F_1 and F_2 are functions of f (friction factor) and depth. Equation (2.32) provides the spatial variation in v_1 from which the mean flow curvature may be obtained using the transverse velocity profile. Form the transverse velocity profile Kikkawa, et al. (1976), the mean flow curvature, r_f , is related to the transverse surface velocity as:

$$r_f = \frac{D_c}{k} \frac{U}{v} \left[\frac{10}{3} \frac{15}{k9} \left(\frac{f}{2} \right)^{1/2} \right] \quad (2.33)$$

Where, D_c is the flow depth at discharge centerline (thalweg) and k is the Karman constant. At each time step, the mean flow curvature at each cross section is obtained using Eqs. (2.32) and (2.33). Accuracy of computation for the finite-difference equation (Eq.2.31) is maintained if the step size $\Delta s \leq 2D_c$. For this reason, the distance

between two adjacent cross sections is divided into smaller increments if necessary. Flow parameters for these increments are interpolated from values known at adjacent cross sections.

If the temporal terms in Equations (2.29) and (2.30) are ignored; water routing may be simplified by computing water-surface profiles at successive time steps. Computation of the water-surface profile at each time step is based upon the standard-step method (Chow, 1957). For many cases, spatial variation in discharge due to channel storage is small and this technique produces closely similar results as the unsteady routing.

2.6.2. Sediment Routing

The sediment routing has the following components

Computation of sediment transport capacity using a suitable formula for the physical conditions,

Determination of actual sediment discharge by making corrections for sorting and diffusion,

Upstream conditions for sediment inflow, and

Numerical solution of the continuity equation for sediment.

2.6.3. Determination of Sediment Discharge

To treat the time-dependent and non-equilibrium sediment transport, the bed material at each section is divided into several, say five, size fractions; the size for each fraction is represented by its geometric mean. For each size fraction, sediment transport capacity is first computed using a sediment-transport formula.

- (1) Engelund-Hansen formula (1967),
- (2) Yang's unit stream power formula (1972, 1986),
- (3) Graf's formula (1970),
- (4) Ackers-White formula,
- (5) Parker, et al. formula for gravel (1982), and
- (6) Meyer-Peter and Muller bedload formula or any other sediment transport formula.

The actual sediment rate is obtained by considering sediment material of all size fractions already in the flow as well as the exchange of sediment load with the bed using the method by Borah et al. (1982). If the stream carries a load in excess of its capacity, it will deposit the excess material on the bed. In the case of erosion, any size fraction available for entrainment at the bed surface will be removed by the flow and added to the sediment already in transport. During sediment removal, the exchange between the flow and the bed is assumed to take place in the active layer at the surface. Thickness of the active layer is based upon the relation defined by Borah, et al. This thickness is a function of the material size and composition, but also reflects the flow condition. During degradation, several of these layers may be scoured away, resulting in the coarsening of the bed material and formation of an armor coat. However, new active layers may be deposited on the bed in the process of aggradations. Materials eroded from the channel banks, excluding that portion in the wash load size range, are included in the accounting. Bed armoring develops if bed shear stress is too low to transport any available size.

The non-equilibrium sediment transport is also affected by diffusion, particularly for finer sediments. Because of diffusion, the deposition or entrainment of sediment is a gradual process and it takes certain travel time or distance to reach the transport capacity for a flow condition. Therefore, the actual sediment discharge at a section depends not only on the transport capacity at the section but also on the supply from upstream and its gradual adjustment toward the flow condition of this section. In the model, the sediment discharge is corrected for the diffusion effects on deposition and entrainment using the method by Zhang, et al. (1983). The procedures for computing sediment transport rate, sediment sorting and diffusion are applied to the longitudinal and transverse directions. They are also coupled with bed-profile evolution.

Sediment discharge may be limited by availability, as exemplified by the flow over a grade-control structure or bedrock. The very high transport capacity at such a section, associated with the high velocity, is limited by the supply rate from upstream; that is, the sediment discharge at such a section is under upstream control.

2.6.4. Numerical Solution of Continuity Equation for Sediment

Changes in cross-sectional area, due to longitudinal and transverse imbalances in sediment discharge, are obtained based upon numerical solution of continuity equations for sediment in the respective directions. First, the continuity equation for sediment in the longitudinal direction is

$$(1 - \lambda) \frac{\partial A_b}{\partial t} + \frac{\partial Q_s}{\partial s} - q_s = 0 \quad (2.34)$$

Where λ is the porosity of bed material, A_b is the cross-sectional area of channel within some arbitrary frame, Q_s is the bed-material, and q_s is the lateral inflow rate of sediment per unit length. According to this equation, the time change of cross-sectional area $\partial A_b / \partial t$ is related to the longitudinal gradient in sediment discharge $\partial Q_s / \partial s$ and lateral sediment inflow q_s . In the absence of q_s , longitudinal imbalance in Q_s is absorbed by channel adjustments toward establishing uniformity in Q_s .

The change in cross-sectional area ΔA_b for each section at each time step is obtained through numerical solution of Eq. (2.34). This area change will be applied to the bed and banks following correction techniques for channel width and channel-bed profile.

From Eq. (2.34), the correction in cross-sectional area of channel bed for a time increment can be written as

$$\Delta A_b = - \frac{\Delta t}{1 - \lambda} \left(\frac{\partial Q_s}{\partial s} - q_s \right) \quad (2.35)$$

At a section i , the lateral sediment inflow may be written as:

$$q_{s_i} = \frac{1}{2} (q_{s_i}^j + q_{s_i}^{j+1}) \quad (2.36)$$

Where superscripts j and $j+1$ are the times at t and $t + \Delta t$, respectively. The model employs an upstream difference in s and a centered difference in t for the partial derivative, $\partial Q_s / \partial s$, in Eq.(2.34), i.e.

$$\frac{\partial Q_s}{\partial s} = \frac{2}{\Delta s_i + \Delta s_{i-1}} \frac{Q_{s_i}^j + Q_{s_i}^{j+1}}{2} - \frac{Q_{s_{i-1}}^j + Q_{s_{i-1}}^{j+1}}{2} \quad (2.37)$$

Where Δs_i is the distance between sections i and $i+1$, Δs_{i-1} is the distance between $i-1$ and i . With this upstream difference for $\partial Q_s / \partial s$, the change in bed area at a section i depends on sediment rates at this section and its upstream section $i-1$; it is independent of the sediment rate at the downstream section. In other words, it is under upstream control. Contrary to this, the upstream stage; i.e., the stage is under downstream control in a sub critical flow.

2.6.5. Simulation of Changes in Channel Width

The change in cross-sectional area ΔA_b , obtained in sediment routing represent the correction for a time increment Δt that needs to be applied to the bed and banks. With ΔA_b being the total correction, it is possible for both the bed and banks to have deposition or erosion; it is also possible to have deposition along the banks but erosion in the bed and vice versa. The direction of width adjustment is determined following the stream power approach and the rate of change is based upon bank erodibility and sediment transport described in the follow:

2.6.6. Direction of Width Adjustment

For a time step, width corrections at all cross sections are such that the streamwise distribution of stream power for the reach moves toward uniformity. These corrections are subject to the physical constraint of rigid banks and limited by the amount of sediment removal or deposition along the banks within the time step. A river channel undergoing changes usually has non-uniform spatial distribution in power expenditure or γQS . Usually the spatial variation in Q is small, but that in S is pronounced. An adjustment in width reflects the river's adjustment in flow resistance, that is, in power expenditure. A reduction in width at a cross section is usually associated with a decrease in energy gradient for the section, whereas an increase in width is accompanied by an increase in energy gradient. To determine the direction of width change at a section I , the energy gradient at this section, S_i , is compared with the weighted average of its adjacent sections, S_i . Here

$$S_i = \frac{S_{i+1}\Delta S_{i-1} + S_{i-1}\Delta S_i}{\Delta S_i + \Delta S_{i-1}} \quad (2.38)$$

If the energy gradient S_i is greater than S_{i+1} , channel width at this section is reduced so as to decrease the energy gradient. On the other hand, if S_i is lower, channel width is increased in order to raise the energy gradient. These changes are subject to the rate of width adjustment and physical constraints.

Width changes in alluvial rivers are characterized by widening during channel-bed aggradations (or fill) and reduction in width at the time of degradation (or scour). Such river channel changes represent the river's adjustment in resistance to seek equal power expenditure along its course. A degrading reach usually has a higher channel-bed elevation and energy gradient than do its adjacent sections. Formation of a narrower and deeper channel at the degrading reach decreases its energy gradient due to reduced boundary resistance. On the other hand, an aggrading reach is usually lower in channel-bed elevation and energy gradient. Widening at the aggrading reach increases its energy gradient due to increasing boundary resistance. These adjustments in channel width reduce the spatial variation in energy gradient and total power expenditure of the channel.

2.6.7. Rate of Width Adjustment

For a time increment, the amount of width change depends on the sediment rate, configuration and bank erodibility. The slope of erodible bank is limited by the angle of repose of the material. The rate of width change depends on the rate at which sediment material is removed or deposited along the banks. For the same sediment rate, width adjustment at a tall bank is not as rapid as that at a low bank. The rates of width adjustment for cases of width increase and decrease are somewhat different as described below separately.

An increase in width at a channel section depends on sediment removal along the banks. The maximum rate of widening occurs when sediment inflow from the upstream section does not reach the banks of this section while bank material at this section is being removed. River-banks have different degrees of resistance to erosion; therefore, the rate of sediment removal along a bank needs to be modified by a coefficient. For this purpose, the bank erodibility factor is introduced as an index for the erosion of bank

material and the four bank types reflecting the variation in erodibility are classified as follows.

- (1) Non-erodible banks.
- (2) Erosion-resistant, banks characterized by highly cohesive material or substantial vegetation, or both.
- (3) Moderately erodible banks having medium bank cohesion.
- (4) Easily erodible banks with noncohesive material.

Values of the bank erodibility factor vary from 0 for the first type to 1 for the last type of banks. The values of 0.2 and 0.5 have been empirically determined for the second and third types, respectively, based upon test and calibration of the model using field data from rivers in the western U.S. However, the bank erodibility factor should still be calibrated whenever data on width changes are available.

A decrease in channel width is accomplished by sediment deposition along the banks or by a decrease in stage, or both. For practical reasons, deposition does not exceed the stage in the model. The maximum amount of width reduction at a section occurs when sediment inflow from the upstream section is spread out at this section and the sediment removal from the bank areas at this section is zero. Within the limit of width adjustment, changes in width are made at all cross sections in the study reach toward establishing uniformity in power expenditure.

2.6.8. Simulation Changes in Channel-Bed Profile

After the banks are adjusted, the remaining correction for ΔA_b is applied to the bed. Distributions of erosion and deposition, or scour and fill, at a cross section are usually not uniform. Generally speaking, deposition tends to start from the low point and is more uniformly distributed because it tends to build up the channel bed in nearly horizontal layers. This process of deposition is often accompanied by channel widening. On the other hand, channel-bed erosion tends to be more confined with greater erosion in the thalweg. This process is usually associated with a reduction in width as the banks slip back into the channel. Such characteristic channel adjustments are effective in reducing the stream-wise variation in stream power as the river seeks to establish a new

equilibrium. In the model, the allocation of scour and fill across a section during each time step is assumed to be a power function of the effective tractive force $\tau_0 - \tau_c$, i.e.

$$\Delta z = \frac{(\tau_0 - \tau_c)^m}{\sum_B (\tau_0 - \tau_c)^m \Delta y} \Delta A_b \quad (2.39)$$

Where Δz is the local correction in channel-bed elevation, τ_0 (given by γDS) is the local tractive force, τ_c is the critical tractive force, m is an exponent, and y is the horizontal coordinate, and B is the channel width. The value of τ_c is zero in the case of fill.

The m value in Eq. (2.39) is generally between 0 and 1; it affects the pattern of scour-fill allocation. The value of m is determined at each time step such that the correction in channel-bed profile will result in the most rapid movement toward uniformity in power expenditure, or linear water surface profile, along the channel. Equation (2.39) may only be used in the absence of channel curvature. The change in bed area at a cross section in a curved reach is

$$\Delta A_b = \frac{1}{r_f} \int r dz \quad (2.40)$$

Where, r_f is the radius of curvature at the discharge centerline or thalweg. Because of the curvature, adjacent cross-sections are not parallel and the spacing Δs between them varies across the width. Therefore, the distribution of Δz given in Eq. (2.39) needs to be weighted according to the r -coordinate with respect to the thalweg radius, r_f/r , i.e.

$$\Delta z = \frac{(\tau_0 - \tau_c)^{m/r}}{\sum_B (\tau_0 - \tau_c)^{m/r} \Delta r} \Delta A_b \quad (2.41)$$

2.6.9 Simulation of Changes Due to Curvature Effects

Simulation of curvature-induced scour and deposition is based upon the flow curvature for which the stream-wise variation is given by Eq. (2.32). The major features of transverse sediment transport and changes in bed topography are described below.

Sediment transport, in the presence of transverse flow, has a component in that direction. Sediment movement in the transverse direction contributes to the adjustment of transverse bed profile. In an unsteady flow, the transverse bed profile varies with time,

and it is constantly adjusted toward equilibrium through scour and deposition. The transverse bed load per unit channel length q_b' can be related to the stream-wise transport q_b . Such a relationship by Ikeda (1982) can be written in parametric form as

$$\frac{q_b'}{q_b} = F\left(\tan \delta, \frac{\partial z}{\partial r}\right) \quad (2.42)$$

Where δ is the angle of deviation of bottom currents from the stream-wise direction. The near-bed transverse velocity is a function of the curvature, and it is computed using the flow curvature.

Eq. (2.42) relates the direction of bed-load movement to the direction of near-bed velocity and transverse bed slope $\partial z / \partial r$. As transverse velocity starts to move sediment away from the concave bank, it creates a transverse bed slope that counters the transverse sediment movement. An equilibrium is reached, i.e., $q_b' = 0$, when the effects of these opposing tendencies are in balance. Transverse bed-profile evolution is related to the variation in bed-material load. Ikeda and Nishimura (1986) developed a method for estimating transport and diffusion of fine sediments in the transverse direction by vertical integration of suspended load over the depth. Their model for predicting the transverse bed slope is also employed.

Changes in channel-bed elevation at a point due to transverse sediment movement are computed using the transverse continuity equation for sediment

$$\frac{\partial z}{\partial t} + \frac{1}{1-\lambda} \frac{1}{r} \frac{\partial}{\partial r} (r q_s') = 0 \quad (2.43)$$

Written in finite difference form with a forward difference for q_s' , this equation becomes

$$\Delta z_k = \frac{\Delta t}{1-\lambda} \frac{2}{r_k} \frac{r_{k+1} q'_{xk+1} r_k q'_{sk}}{r_{k+1} - r_{k-1}} \quad (2.44)$$

Where, K is the radial (transverse) coordinate index measured from the center of radius. Equation (2.44) provides the changes in channel-bed elevation for a time step due to transverse sediment movement. These transverse changes, as well as the longitudinal changes, are applied to the streambed at each time step. Bed-profile evolution is simulated by repeated iteration along successive time steps.

PROMINENT MATHEMATICAL MODELS**3.1. General**

A mathematical modeling in river is the simulation of flow conditions based on formulation and solution of mathematical relationships expressing known hydraulic principles. Development of river simulation software has undergone many changes since it was initiated in the early 1960s. Earlier uniform sized sediments were assumed and assumption of quasi-steady flow was made so that $\partial U/\partial t = \partial y/\partial t = 0$ even though flow may be unsteady. In recent years more sophisticated models have developed by considering sediment non-uniformity, flow unsteadiness and treating suspended load and bed load separately. In simpler method of computations the system of equations are solved in two phases (in uncoupled mode) where water surface computations are first performed at all the sections then sediment transport rates are calculated. By routing the sediment Δz is obtained in each section, the new slope is determined and computations for water surface elevation is repeated. In coupled mode, these computations are performed together in each time step. In this chapter, briefly few prominent mathematical models in the field of river engineering will be reviewed.

3.2. Review of Models**3.2.1. FLUVIAL-12**

FLUVIAL-12 mathematical model was developed by Dr. Howard H. Chang, Professor San Diego University, USA, (1976) .It was modified several times and latest version was modified in 1998. It is calibrated with the field data and used extensively in water surface profile computations and study of river morphology.

The FLUVIAL-12 model is one-dimensional erodible-boundary model, and it can simulate inter-related changes in channel-bed profile, channel width and bed topography induced by channel curvature. The main features of FLUVIAL- 12 are:

- (i) Unsteady flow model
- (ii) A strong coupling of change in geometry and slope
- (iii) Friction updating and inclusion of sorting and armoring.
- (iv) This model does not require sediment rating curve and it can compute sediment load based on the hydraulics of the flow.
- (v) Capability of simulating effect of curvature on total sediment transport.
- (vi) Options available for six sediment transport equations described in section 5. according to the actual physical conditions.
- (vii) Inclusion of sediment in non erodible boundary reaches or rock out crops
- (viii) Losses due to bridge and weirs can be computed.
- (ix) HEC- 2 format data can be used with slight modifications.

3.2.2. CHARIMA and ILLUVIAL

Karim and Kennedy developed these two models, at Iowa University, Iowa USA in 1982. Several modifications have been done till to date and their main features are:

- (i) Strong coupling between resistance and total load transport.
- (ii) Inclusion of active surface layer where exchange of sediment takes place.
- (iii) Suspended sediment source term in mass balance equation.
- (iv) Friction updating and inclusion of sorting and armoring.
- (v) Provision of additional local head loses due to weirs, bridges, sills etc.
- (vi) Sediment transport over non-erodible reaches or rock outcrops.

3.2.3. MIKE 11

MIKE11 is a comprehensive one dimensional flow model for simulating flows, water quality, sediment transport in estuaries, rivers, irrigation channels and other water bodies. It was developed by Danish Hydraulic Institute (DHI), Denmark.

MIKE11 is a dynamic model. Hydrodynamic(HD) module is the main feature of the MIKE11 modeling system and forms the basis for most modules including Flood Forecasting, Advection-Dispersion, Water Quality and non-cohesive sediment transport

modules. The MIKE11 HD module solves the vertically integrated equations for the conservation of continuity and momentum, i.e. Saint Venant's equations.

Applications related to the MIKE11 HD module includes:

- (i) Flood forecasting and reservoir operation
- (ii) Simulation of flood control measures
- (iii) Operation of irrigation and surface irrigation system
- (iv) Design of channel system
- (v) Tidal and storm surge studies in rivers and estuaries.

In addition to the HD module described above, MIKE11 includes add-on module for:

- (i) Hydrology
- (ii) Advection-Dispersion
- (iii) Models for different aspects for water quality
- (iv) Cohesive sediment transport
- (v) Non-cohesive sediment transport.

3.2.4. HEC- 6

The computer program HEC-6 is one dimensional steady state model designed to analyze long term scour and deposition in river and reservoir. It is an erodible bed model. Numerical program incorporates one dimensional energy equation to compute water surface profile by using standard energy step and Manning's equation. This model was developed by Hydrologic Engineering Center, US Army Corps of Engineers (USAC).

3.2.5. WSPRO

WSPRO is one-dimensional model, to compute water surface profile and contraction scour and local scour scours. The program can compute 20 equal-conveyance "tubes" and hydraulic properties by sub-areas as well as analyses weir flow over an embankment and bridge hydraulics for pressure flow. The equal-conveyance "tubes" and hydraulic properties by sub-area provide information that can be used to estimate the various components of local scour. The scour equation recommended by

HEC circular no18 is utilized in the program to compute bridge scour parameters. Further details are given in chapter four.

3.2.6. HEC- RAS

HEC- RAS is an integrated system software designed for interactive use in a multi-tasking, multi-user's environment. This system is comprised of graphical user interface, separate hydraulic analysis components, data storage and management capabilities, graphics and reporting facilities. Present form of HEC-RAS two one-dimensional hydraulic analysis components.

- (i) Steady flow water surface profile computations
- (ii) Unsteady flow water surface profile computations

The model is capable of hydraulic calculations for

- (i) Cross-section, bridge, culvert and other hydraulic structures
- (ii) Inclusion of channel dredging, levee and channel modifications.
- (iii) Calculation of local head loses
- (iv) Evaluation of flood plain encroachments
- (v) Split flow optimization
- (vi) Multiple Profile computations
- (vii) Evaluating profiles at confluence
- (viii) Compatible with GIS
- (ix) Local and general scour computation using CSU and Froehlich's equations.

HEC – RAS explained in detail in chapter four.

Table 3.1 Summary of Some Alluvial River Models [1]

No	Model	Investigators and country	Year	Type	
				I	II
1.	LPM	De Vries DHL, Netherlands Soni et al. Mehta et al. Roorkee, India	1973 1980 1983	SM SM SM	A A A
2.	LHM	De Vries DHL, Netherlands	1973	SM	A
3.	NLPM	Jaramilo et al. Iowa, U.S.A. Zhang Hou	1984	SM	N&A
4.	NHLM	Ribberink, Netherlands	1987	SM	A
5.	DHL	De Vries DHL, Netherlands	1973	SM	FD
6.	SOGREAH	Cunge et al., France	1973	QS	FD
7.	PREDICTOR-CORRECTOR	Swamee et al., UOR Roorkee	1974	QS	FD
8.	HEC-6	Thomas, USA	1977	QS	FD
9.	HEC 2 SR	Simons et al., USA	1980	QS	FD
10.	FLUVIAL	Chang et al., San Diego University, USA	1976	QS	FD
11.	KUWASER	Simons et al., USA	1979	QS	FD
12.	KOMURA-SIMONS	USA	1971	QS	FD
13.	IALLUVIAL	Karim et al., Iowa, USA	1982	QS	FD

Explanations:

A	=	Analytical	N	=	Numerical method
FD	=	Finite difference method	FEM	=	Finite element method
SM	=	Simplified models	QS	=	Quasi-steady
US	=	Unsteady	CFD	=	Coupled finite difference model
LPM	=	Linear Parabolic model	LHM	=	Linear Hyperbolic model
NLPM	=	Nonlinear Parabolic model	NLHM	=	Nonlinear Hyperbolic model

No	Model	Investigators and country	Year	Type	
				I	II
14.	VISTULA	Witkopwska, Hana Poland	1971	QS	FD
15.	YONG	Yong, Taiwan	1984	QS	FD
16.	HRS, Wallingford	Bettess et al., Wallingford	1979	QS	FD
17.	USGS	Bennet et al., USA	1977 1983	US	FD
18.	VUWSR	Tucci et al., USA	1979	US	FD
19.	SEDIMENT-4H	Arithural Ranjan, USA	1977	US	FEM
20.	DASS-SIMONS	Dass et al., USA	1975	US	FEM
21.	BOGNAR	Dass et al., USA	1986	US	FD
22.	ABDELLA	Abddia et al., France	1986	US	FD
23.	CHEN	Chen, USA	1973	US	FD
24.	MOBED	Krishnappan et al., Canada	1977	US	FD
25.	PARANA RIVER MODEL	Ceirano et al., Argentina	1982	QS	FD
26.	SYSTEM-11 MIKE-11	Havano et al., DHI, Denmark	1989	US	FD
27.	CARICHAR	Rahuel et al., France, USA, China	1988	US	CFD
28.	CHARIMA	Holly, Jr. Iowa, USA	1988	US	CFD
29.	SEDICOUP	BAW, Germany	1992	US	CFD
30.	MARC	Tianjin Institute of Water Transport, China	1990	US	FD
31.	ARM	Palaniappan, Roorkee, India	1991	QS	FD
32.	CHAR-2	Sogreah, France	1992	QS	FD
33.	FCM	Corriea et al. Switzerland	1992	US	CFD

DESCRIPTION OF MODEL USED

4.1. General

For the study of streambed variations we have to estimate long-term aggradation and degradation, general scour and local scour. To simulate long-term streambed variations erodible boundary models are best suited and for the study of local scour and general scour, bridge hydraulics component must be available in the model. In this context models were examined critically, then it was found that Charima and Illuvial MIKE11, and FLUVIAL-12 were found to be erodible boundary models and to simulate general scour and for local scour HEC-RAS and WSPRO were found to be suitable. Out of five models only HEC-RAS is available in the WRDTC. To obtain other models, request was sent to the model developer and, FLUVIAL-12 and WSPRO could be available others did not respond. Therefore, in this chapter, mathematical models used in this study namely WSPRO, HEC-RAS and FLUVIAL- 12 will be described.

4.2. FLUVIAL – 12

Mathematical model FLUVIAL- 12 was developed by Dr. Howard H. Chang, Professor, Department of Civil and Environmental Engineering, San Diego University, USA, in 1976. It is a unsteady finite difference model.

The FLUVIAL-12 model is an erodible-boundary model; it can simulate inter-related changes in channel-bed profile, channel width and bed topography induced by the channel curvature. The FLUVIAL –12 model has the following five major components:

- (1) Water Routing
- (2) Sediment Routing
- (3) Changes in Channel Width
- (4) Changes in Channel Bed Profile and
- (5) Changes in Geometry Due to the Curvature Effects.

This model employs space-time domain in which the space domain is represented by the discrete cross-sections along the channel; time domain represented by discrete time increments. Temporal and spatial variation in flow, sediment transport and channel geometry are computed following an iterative procedure. Water routing, which is coupled with the changing curvature, is assumed to be uncoupled from the sediment process because sediment movement and changes in channel geometry are slow in comparison to the flow hydraulics.

All the above components of streambed variations are simulated by FLUVIAL-12 using methods described in sections 2.6.1 to 2.6.7.

The geometric data and hydraulic data if they are available in HEC-2 format can be used here, with slight modification in record identifiers. Sediment transport data can be entered in the form of sediment discharge inflow hydrograph or in the form of sediment grain-size distribution curve, by partitioning the whole sample into five to eight geometric diameter group and their percent in the sample.

Boundary conditions for water routing required is discharge hydrograph at the upstream boundary of the reach and downstream boundary condition can be either stage discharge curve or any energy gradient. For the dynamic wave routing is downstream time versus stage curve must be given as downstream boundary. Bridge hydraulics component of FLUVIAL-12 is also available. By calculating conveyance and head loss potential scour depth can also predicted, for this some manual calculations are required.

4.3. HEC-RAS

HEC-RAS is an integrated system of software, designed for interactive use in a multi-tasking, multi-user environment. The system is comprised of graphical user interface, separate hydraulic analysis components, data storage and management capabilities, graphic and reporting facilities.

The present version of HEC-RAS contains two one-dimensional hydraulic analysis components for:

- (i) Steady flow water surface profile components,
- (ii) Unsteady flow simulation and
- (iii) It is a fixed boundary model and mobile-bed model is being added in near future

4.3.1. Steady Flow Water Surface Profiles

Steady flow water surface profiles component of modeling system is intended for calculating profiles for steady gradually varied flow. The system can handle a full network of channel, a dendritic system, or a single river reach. The steady flow component is capable of modeling subcritical, super-critical, and mixed flow regime water surface profiles.

The basic computational procedure is based on the solution of one-dimensional energy equation. Energy losses are evaluated by friction (Manning's equation) and contraction / expansion (coefficient multiplied by the change in the velocity head). The momentum equation is utilized in the situations where the water surface profile is rapidly varied. These situations include mixed flow regime calculations (hydraulic jumps), hydraulics of bridges evaluating profiles at river confluences (stream junctions).

The effects of various obstructions such as bridges, culverts, weirs, and structures in the flood plain may be considered in the computations. The steady flow system is designed for application of floodplain management and flood insurance studies to evaluate floodway encroachments. Also the capabilities are available for assessing the change in water surface profiles due to channel improvements, and levees.

4.3.2. Unsteady Flow Simulation

This component of the HEC-RAS modeling system is capable of simulating one-dimensional unsteady flow simulation through a full network of open channels. The unsteady flow equation solver is adopted from Robert L. Barkau's UNET model (Barkau, 1992 and HEC, 1997). This unsteady flow component was developed primarily for subcritical flow regime calculations.

The hydraulic calculations for cross-sections, bridges, culverts, and other hydraulic structures that were developed for steady flow component are incorporated into the unsteady flow module.

4.3.3. Bridges and Culverts

Bridges and culverts modeling of HEC-RAS is performed as follows:

4.3.3.1 Entering Geometric Data

Geometric data are entered through geometric data editor either in the form of HEC-2 data format (if available in the data storage file) or in the form of (y, z) coordinates for each cross-section. Here y stands for the distance from the reference point on the leftbank facing towards downstream of the river and z stands for the elevation from the datum. Along with cross-section co-ordinates Manning's 'n' values for the left overbank, the main channel and the right overbank are entered. Expansion and contraction coefficients are entered if required between the two consecutive cross-sections. Distance between the two consecutive cross-section along the left overbank, the main channel and the right overbank are also entered in the geometric data editor.

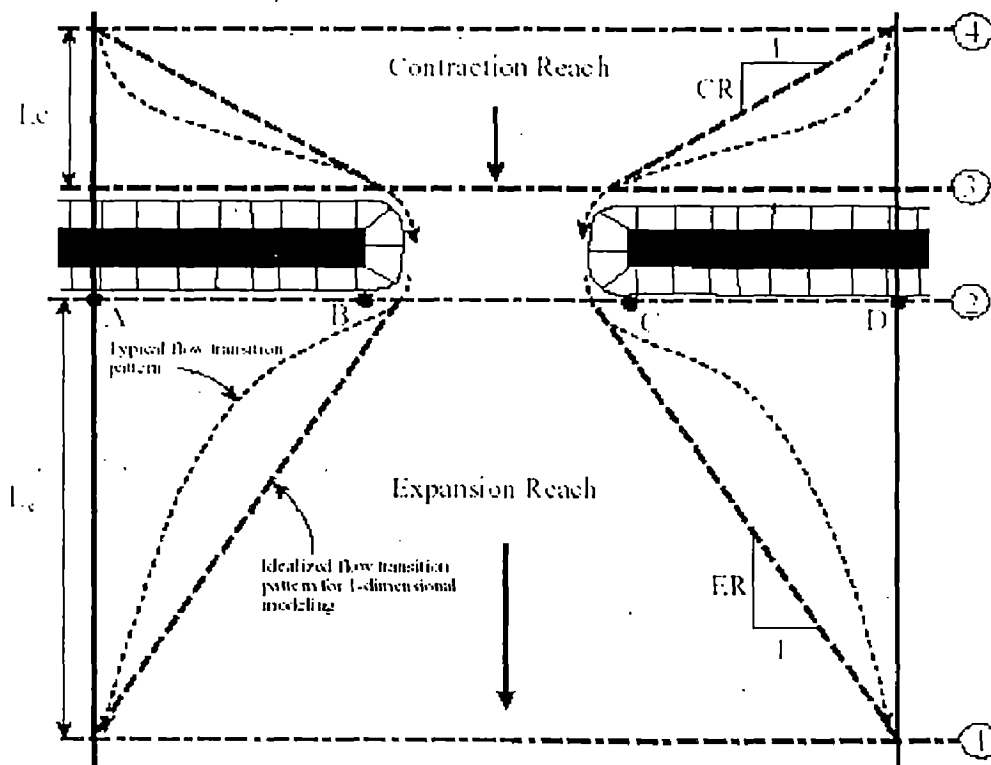
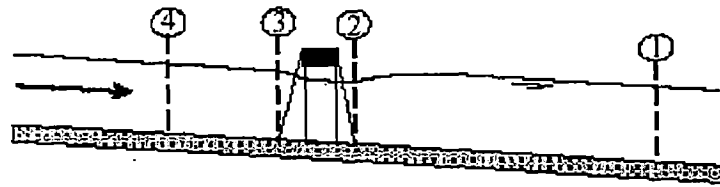


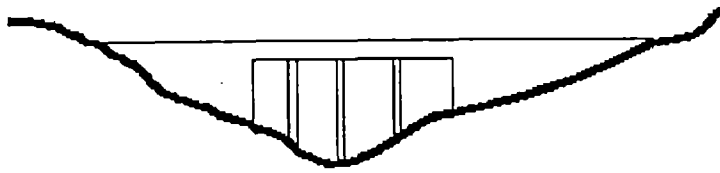
Fig.4.1 Cross-section Location

4.3.3.2. Cross-section Locations

The bridge and culvert routine utilizes four user defined cross-sections in the computations of energy losses. A plan view of the basic cross-section is shown in Fig. 4.1.



A. Channel Profile and cross section locations



B. Bridge cross section on natural ground



C. Portion of cross sections 2 & 3 that is ineffective for low flow

Fig.4.2 Typical Cross-sections Near Bridge

Cross-section 1: is located sufficiently downstream of the structure so that the flow is not affected by the structure (i.e. flow is fully expanded). This expansion distance will vary depending upon the degree of constriction, shape of the constriction, magnitude of the flow, and velocity of the flow. Table 4.1 offers range of expansion ratios, which can be used for different degree of constriction, different slopes, and different ratios of the overbank roughness (n_{ob}) to the main channel roughness (n_c). The downstream distance of expansion reach (L_e) is found out multiplying by expansion ratio by the average obstruction length (the average of the distances A to B and C to D from figure 4.1).

Cross-section 2: is located immediately downstream of the bridge (i.e. within a few feet). This cross-section represents the natural ground just out side the bridge. This is normally located at the toe of the downstream bridge embankment.

Cross-section 3: should be located just upstream from the bridge. The distance between the bridge and cross-section 3 should be relatively short. This distance should only reflect the length required for the abrupt acceleration and contraction of the flow that occurs in the immediate area of the opening. Cross-section 3 represents the natural ground just

upstream of the bridge. This section is normally located at the toe of the upstream bridge embankment.

Table 4.1 Ranges of Expansion Ratio

	$n_{ob} / n_c = 1$	$n_{ob} / n_c = 2$	$n_{ob} / n_c = 4$
b / B = 0.10 S = 1 ft /mile S = 5 ft /mile S = 10 ft /mile	1.4 - 3.6	1.3 - 3.0	1.2 - 2.1
	1.0 - 2.5	0.8 - 2.0	0.8 - 2.0
	1.0 - 2.2	0.8 - 2.0	0.8 - 2.0
b / B = 0.25 S = 1 ft /mile S = 5 ft /mile S = 10 ft /mile	1.60 - 3.0	1.40 - 2.5	1.20 - 2.0
	1.50 - 2.5	1.30 - 2.0	1.30 - 2.0
	1.50 - 2.0	1.30 - 2.0	1.30 - 2.0
b / B = 0.50 S = 1 ft /mile S = 5 ft /mile S = 10 ft /mile	1.40 - 2.6	1.30 - 1.90	1.20 - 1.40
	1.30 - 2.0	1.20 - 1.60	1.0 - 1.40
	1.30 - 2.0	1.20 - 1.50	1.0 - 1.40

Where b / B is the ratio of bridge opening width to total floodplain width.

Cross-section 4: is an upstream cross-section where flow lines are approximately parallel and the cross-section is fully effective. In general, flow contraction over a shorter distance than flow expansions. The distance between the cross-sections 3 and 4 (contraction length, L_c) is generally one bridge length (recommended by WSPRO manual). A detailed of flow contraction and expansion at bridge was undertaken by Hydrologic Engineering Center (HEC) the results are available in "Flow Transition in Bridge Back Water Analysis" (RD-42, HEC, 1995).

4.3.3.3. Contraction and Expansion Losses

Losses due to contraction and expansion of flow between cross sections are determined during the standard step profile calculations. Manning's equation is used to calculate friction losses, and all other losses are described in terms of a coefficient times the absolute value of the change in velocity head between adjacent cross sections. When the velocity head increases in the downstream direction, a contraction coefficient is used; and when the velocity head decreases, an expansion coefficient is used.

As shown in Figure 7.1, the flow contraction occurs between cross sections 4 and 3, while the flow expansion occurs between sections 2 and 1. The contraction and expansion coefficients are used to compute energy losses associated with changes in the shape of river cross-sections (or effective flow areas). The loss due to expansion of flow is usually larger than the contraction loss, and losses from short abrupt transitions are larger than losses from gradual transitions. Typical values for contraction and expansion coefficients under subcritical flow conditions are shown in Table 4.2 below:

Table 4.2

Subcritical Flow Contraction and Expansion Coefficients		
Transition	Contraction	Expansion
No transition loss computed	0.0	0.0
Gradual transitions	0.1	0.3
Typical Bridge sections	0.3	0.5
Abrupt transitions	0.6	0.8

The maximum value for the contraction and expansion coefficient is 1.0.

A detailed study was completed by the Hydrologic Engineering Center entitled "Flow Transitions in Bridge Backwater Analysis"(HEC, 1995). According to these studies, contraction and expansion coefficients for supercritical flow should be lower than subcritical flow. For typical bridges that are under class C flow conditions (totally

supercritical flow), the contraction and expansion coefficients should be around 0.1 and 0.3 respectively. For abrupt bridge transitions under class C flow, values of 0.3 and 0.5 may be more appropriate.

4.3.4. Bridge Hydraulic Computations

4.3.4.1. Low Flow Computations

For low flow computations the program first uses the momentum equation to identify the class of the flow. This is accomplished by first calculating the momentum at critical depth inside the bridge at the upstream and downstream ends. The end with the higher momentum (therefore, the most constricted section) will be the control section in the bridge. The momentum at critical depth in the controlling section is then compared to the momentum of the flow downstream of the bridge when performing a subcritical profile (upstream of the bridge for a supercritical profile). If the momentum downstream is greater than the critical depth momentum inside the bridge, the class of flow is considered to be completely subcritical (i.e., class a low flow). If the momentum downstream is less than the critical depth momentum inside the bridge, then it is assumed that constriction will cause the flow to pass through critical depth and hydraulic jump will occur at some distance downstream (i.e., class B low flow). If the profile is completely super critical through the bridge then this is class C low flow. Depending on the class of flow the program will do the following:

Class A low flow: Class A low flow exists when the water surface through the bridge is completely subcritical (i.e., above the critical depth). Energy losses through the expansion (section 2 to 1) are calculated as friction losses and expansion losses. Friction losses are based on a weighted friction slopes times weighted reach lengths between section 1 and 2. The average friction slope is based on one of the four available alternatives in the HEC-RAS, with the average conveyance method being the default. The average length is used in the calculation based on discharge-weighted reach length.

There are four methods for computing loss through the bridge (from section 2 to 3):

- Energy equation (standard step method).
- Momentum balance
- Yarnell equation
- FHWA WSPRO method

Energy loss through the contraction section (sections 3 to 4) are calculated as friction loss and contraction loss. These losses between sections 3 to 4 are calculated the same as friction and expansion losses between sections 1 and 2.

Energy Equation (standard step method): The energy-based method treats a bridge in the same manner as a natural river cross-section, except the area of the bridge below the water surface is subtracted from the total area, and the wetted perimeter is increased where the water is in contact with the bridge structure. As described previously, the program formulates two cross sections inside the bridge by combining the ground information of sections 2 and 3 with the bridge geometry. As shown in Figure 4.3, for the purposes of discussion, these cross sections will be referred to as sections BD (Bridge Downstream) and BU (Bridge Upstream). The sequence of calculations starts with a standard step calculation from just downstream of the bridge (section 2) to just inside of the bridge (section BD) at the downstream end. The program then performs a standard step through the bridge (from section BD to section BU). The last calculation is to step out of the bridge (from section BU to section 3).

The energy-based method requires Manning's n values for friction losses and contraction and expansion coefficients for transition losses. The estimate of Manning's n values is well documented in "Open Channel Hydraulics" by V. T. Chow, 1959, as well as several research studies. Contraction and expansion coefficients are provided in Table 4.2. Detailed output is available for cross sections inside the bridge (sections BD and BU) as well as the user entered cross sections (sections 2 and 3).

Momentum Balance Method: The momentum method is based on performing a momentum balance from cross section 2 to cross-section 3. The momentum balance is performed in three steps. The first step is to perform a momentum balance from

cross-section 2 to cross-section BD inside the bridge. The equation for this momentum balance is as follows:

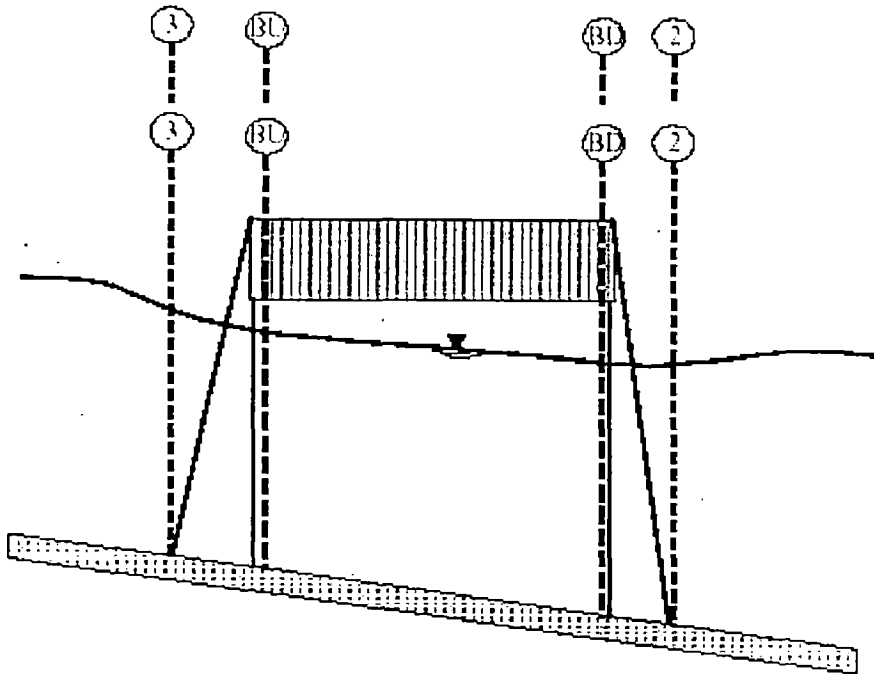


Fig. 4.3 Cross-section Near and inside the Bridge

$$A_{BD} Y_{BD} + \beta_{BD} Q_{BD}^2 / (g A_{BD}) = A_2 Y_2 + \beta_2 Q_2^2 / (g A_2) - A_{PBD} Y_{PBD} + F_f - W_x \quad (4.1)$$

Where, A_2, A_{BD} = Active flow area at section 2 and BD, respectively, m^2

A_{PBD} = Obstructed area of pier on downstream side, m^2

Y_2, Y_{BD} = Vertical distance from water surface to center of gravity of flow area A_2 and A_{BD} , respectively, m

Y_{PBD} = Vertical distance from water surface to center of gravity of wetted pier area on downstream side, m

β_2, β_{BD} = Velocity weighing coefficient for momentum equation at section 2 and BD, respectively

Q_2, Q_{BD} = Discharge at section 2 and BD, respectively, m^3 / sec

F_f = External force due to friction, per unit weight of water, $N / (N / m^3)$

W_x = Force due to weight in the direction of the flow, per unit weight of water,
 N / (N / m³.)

The second step is momentum balance from section BD to BU (see Fig. 4.3). The relation for this step is as follows:

$$A_{BU} Y_{BU} + \beta_{BU} Q_{BU}^2 / (g A_{BU}) = A_{BD} Y_{BD} + \beta_{BD} Q_{BD}^2 / (g A_{BD}) + F_f - W_x \quad (4.2)$$

The final step is a momentum balance from section BU to section 3 (see Fig. 4.3). The equation for this step is as follows:

$$A_3 Y_3 + \beta_3 Q_3^2 / (g A_3) = A_{BU} Y_{BU} + \beta_{BU} Q_{BU}^2 / (g A_{BU}) + A_{PBU} Y_{PBU} + 1 / 2 [C_D A_{PBU} Q_3^2 / (g A_3^2)] + F_f - W_x \quad (4.3)$$

Where, C_D = Drag coefficient for flow going around the pier.

The momentum balance method requires the use of roughness coefficients for the estimation of the friction force and a drag coefficient for the force of drag on piers. Drag coefficients are used to estimate the force due to the water moving around the piers, the separation of the flow, and the resulting wake that occurs downstream. Drag coefficients for various cylindrical shapes have been derived from experimental data (Lindsey, 1938). The following table shows some typical drag coefficients that can be used for piers:

Table 4.3

Typical drag coefficients for various pier shape	
Pier Shape	Drag Coefficient C
Circular pier	1.20
Elongated piers with semi-circular ends	1.33
Elliptical piers with 2:1 length to width	0.60
Elliptical piers with 4:1 length to width	0.32
Elliptical piers with 8:1 length to width	0.29
Square nose piers	2.00
Triangular nose with 30 degree angle	1.00
Triangular nose with 60 degree angle	1.39
Triangular nose with 90 degree angle	1.60
Triangular nose with 120 degree angle	1.7

During the momentum calculations, if the water surface (at sections BD and BU) comes into contact with the maximum low chord of the bridge, the momentum balance is assumed to be invalid and the results are not used.

Yarnell's Equation: The Yarnell equation is an empirical equation that is used to predict the change in water surface from just downstream of the bridge (section 2 of Figure 4.3) to just upstream of the bridge (section 3). The equation is based on approximately 2600

lab experiments in which the researchers varied the shape of the piers, the width, the length, the angle, and the flow rate. The Yarnell equation is as follows (Yarnell, 1934):

$$H_{3-2} = 2K (K + 10w - 0.6) (\alpha + 15\alpha^4) u_2^2 / (2g) \quad (4.4)$$

Where, H_{3-2} = Drop in water surface elevation from section 3 to 2, m

K = Yarnell's pier shape coefficient

= Obstructed area of pier by total unobstructed area at section 2

= Ratio of velocity head to depth at section 2

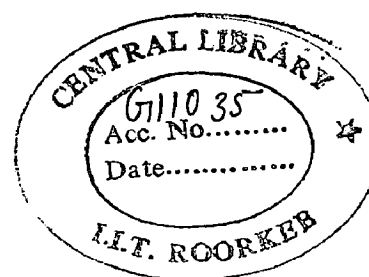
u_2 = Velocity downstream at section 2, m / s

α = Energy correction factor

The computed upstream water surface elevation (section 3) is simply the downstream water surface elevation plus H_{3-2} . With the upstream water surface known the program computes the corresponding velocity head and energy elevation for the upstream section (section 3). When the Yarnell method is used, hydraulic information is only provided at cross sections 2 and 3 (no information is provided for sections BU and BD). The Yarnell equation is sensitive to the pier shape (K coefficient), the pier obstructed area, and the velocity of the water. The method is not sensitive to the shape of the bridge opening, the shape of the abutment or the width of the bridge.

Table 4.4

Yarnell's pier coefficient, K, for various pier shapes	
Pier Shape	Yarnell K Coefficient
Semi-circular nose and tail	0.90
Twin-cylinder piers with connecting diaphragm	0.95
Twin-cylinder piers without diaphragm	1.05
90 degree triangular nose and tail	1.05
Square nose and tail	1.25
Ten pile trestle bent	2.50



FHWA WSPRO Method:

The low flow hydraulic computations of the Federal Highway Administration's (FHWA) WSPRO computer program, has been adapted as an option for low flow hydraulics in HEC-RAS. The WSPRO methodology had to be modified slightly in order to fit into the HEC-RAS concept of cross-section locations around and through a bridge. The WSPRO method computes the water surface profile through a bridge by solving the energy equation. The method is an iterative solution performed from the exit cross section (1) to the approach cross-section (4). The energy balance is performed in steps from the exit section (1) to the cross section just downstream of the bridge (2). From just downstream of the bridge (2) to inside of the bridge at the downstream end (BD); from inside of the bridge at the downstream end (BD) to inside of the bridge at the upstream end (BU). From inside of the bridge at the upstream end (BU) to just upstream of the bridge (3); and from just upstream of the bridge (3) to the approach section (4). A general energy balance equation from the exit section to the approach section can be written as follows:

$$h_4 + \alpha_4 u_4^2 / (2g) = h_1 + \alpha_1 u_1^2 / (2g) + h_{L1-4} \quad (4.4)$$

Where, h_1 = Water surface elevation at section 1, m

h_4 = Water surface elevation at section 4, m

u_1 = Velocity at section 1, m / s

u_4 = Velocity at section 4, m / s

h_{L1-4} = Energy loss from section 4 to 1, m

α_1, α_4 = Energy correction factor for non-uniform flow at section 1 and 4, respectively.

The incremental energy losses from section 4 to 1 are calculated as follows:

From Section 1 to 2:

Losses from section 1 to section 2 are based on friction losses and an expansion loss. Friction losses are calculated using the geometric mean friction slope times the flow weighted distance between sections 1 and 2. following equation is used for friction losses from 1 to 2:

$$h_{f1-2} = BQ^2 / (K_1 K_2) \quad (4.5)$$

Where B is the flow weighted distance between sections 1 and 2, and K_1 and K_2 are the total conveyance at sections 1 and 2 respectively. The expansion loss from section 2 to section 1 is computed by the following equation:

$$h_e = Q^2 / (2gA_1^2) [\{ |2\beta_1 - \alpha_1 - 2\beta_2 | A_1 / A_2 \} + \alpha_2 A_1 / A_2] \quad (4.6)$$

Where, β_1, β_2 = Momentum correction factor for non-uniform flow at section 1 and 2, respectively.

$$\alpha_1 = \Sigma (K_i^3 / A_i^2) / (K_T^3 / A_T^2) \quad (4.7)$$

$$\beta_1 = \Sigma (K_i^2 / A_i) / (K_T^2 / A_T) \quad (4.8)$$

α_1 and β_1 are related to bridge geometry and are defined as follows:

$$\alpha_1 = 1 / C^2 \quad (4.9)$$

$$\beta_1 = 1 / C \quad (4.10)$$

Where, C is an empirical discharge coefficient for the bridge, which was originally developed as part of the Contracted Opening method by Kindswater, Carter, and Tracy (USGS, 1953), and subsequently modified by Matthai (USGS, 1968). The computation of the discharge coefficient, C, is explained in detail in appendix D of "HEC-RAS Reference Manual 2001".

From Section 2 to 3:

Losses from section 2 to section 3 are based on friction losses only. The energy balance is performed in three steps: from section 2 to BD; BD to BU; and BU to 3. Friction losses are calculated using the geometric mean friction slope times the flow weighted distance between sections. The following equation is used for friction losses from BD to BU:

$$h_{f(BU-BD)} = L_B Q^2 / (K_{BU} K_{BD}) \quad (4.11)$$

Where K_{BU} and K_{BD} are the total conveyance at sections BU and BD respectively, and L_B is the length through the bridge. Similar equations are used for the friction losses from section 2 to BD and BU to 3.

From Section 3 to 4:

Energy losses from section 3 to 4 are based on friction losses only. The equation for computing the friction loss is as follows:

$$h_{f(3-4)} = L_{av} Q^2 / (K_3 K_4) \quad (4.12)$$

Where L_{av} is the effective flow length in the approach reach, and K3 and K4 are the total conveyances at sections 3 and 4. The effective flow length is computed as the average length of 20 equal conveyance stream tubes (FHWA, 1986). The computation of the effective flow length by the stream tube method is explained in appendix D of “HEC-RAS Reference Manual 2001”.

Class B low flow: Class B low flow can exist for either subcritical or supercritical profiles. For either profile, class B flow occurs when the profile passes through critical depth in the bridge constriction. For a subcritical profile, the momentum equation is used to compute an upstream water surface above critical depth and a downstream water surface below critical depth, using momentum balance through the bridge. For a supercritical profile, the bridge is acting as control and is causing the upstream water surface elevation to be above critical depth. Momentum is used again to calculate an upstream water surface above critical depth and a downstream water surface below critical depth. The program will proceed with forewater calculations downstream the bridge.

Class C low flow: Class C low flow exists when the water surface through the bridge is completely supercritical. The program can use either the energy or momentum equation to compute the water surface through the bridge.

4.3.4.2. Pressure flow Computations

Pressure flow occurs when the flow comes into contact with the low chord of the bridge. Once the flow comes into contact with the upstream side of the bridge, a backwater occurs and orifice flow is established. The program will handle two cases of orifice flow: the first is when only the upstream side of side of the bridge is in contact with the water; and second is when the bridge constriction is flowing completely full. For the first case, a sluice gate type of equation is used, as described in, “Hydraulics of Bridge Waterways” (FHWA, 1978). In the second case, the standard full flowing orifice equation is used. The program will begin checking for the possibility of pressure flow when energy grade line goes above the maximum low chord elevation. Once pressure flow is computed, pressure flow answer is compared with low flow answer and higher of

the two is used. The user has the option to tell the program to use the water surface, instead of energy, to trigger the pressure flow calculation.

Pressure and Weir Flow Method:-

A second approach for the computation of high flows is to utilize separate hydraulic equations to compute the flow as pressure and/or weir flow. The two types of flow are presented below.

Pressure Flow Computations:-

Pressure flow occurs when the flow comes into contact with the low chord of the bridge. Once the flow comes into contact with the upstream side of the bridge, a backwater occurs and orifice flow is established. The program will handle two cases of orifice flow; the first is when only the upstream side of the bridge is in contact with the water; and the second is when the bridge opening is flowing completely full. The HEC-RAS program will automatically select the appropriate equation, depending upon the flow situation. For the first case (see Figure 4.4), a sluice gate type of equation is used (FHWA, 1978):

$$Q = C_d A_{BU} [Y_3 - Z / 2 + \alpha_3 u_3^2 / (2g)]^{1/2} \quad (4.13)$$

Where, Q = Total discharge through the bridge opening, m^3 / s

C_d = Coefficient of discharge for pressure flow

A_{BU} = Area of bridge opening at section BU, m^2

Y_3 = Hydraulic depth at section 3, m

Z = Vertical distance from maximum bridge log chord to the mean river bed elevation at section BU, m

The discharge coefficient C_d , can vary depending upon the depth of water upstream. Values for C_d range from 0.27 to 0.5, with a typical value of 0.5 commonly used in practice. The user can enter a fixed value for this coefficient or the program will compute one based on the amount that the inlet is submerged. A diagram relating C_d to Y_3/Z is shown in Figure 4.5.

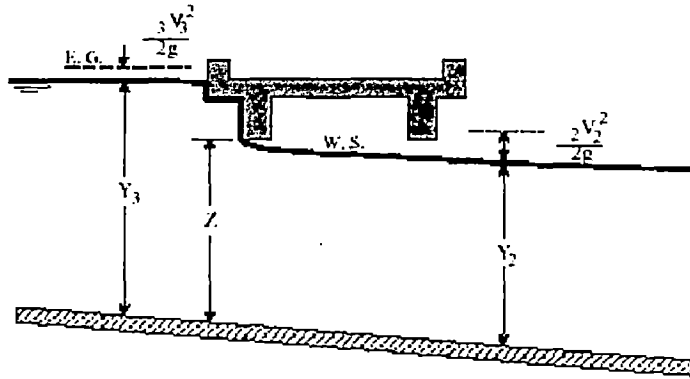


Fig. 4.4 A Bridge Under Sluice Gate Type of Pressure Flow

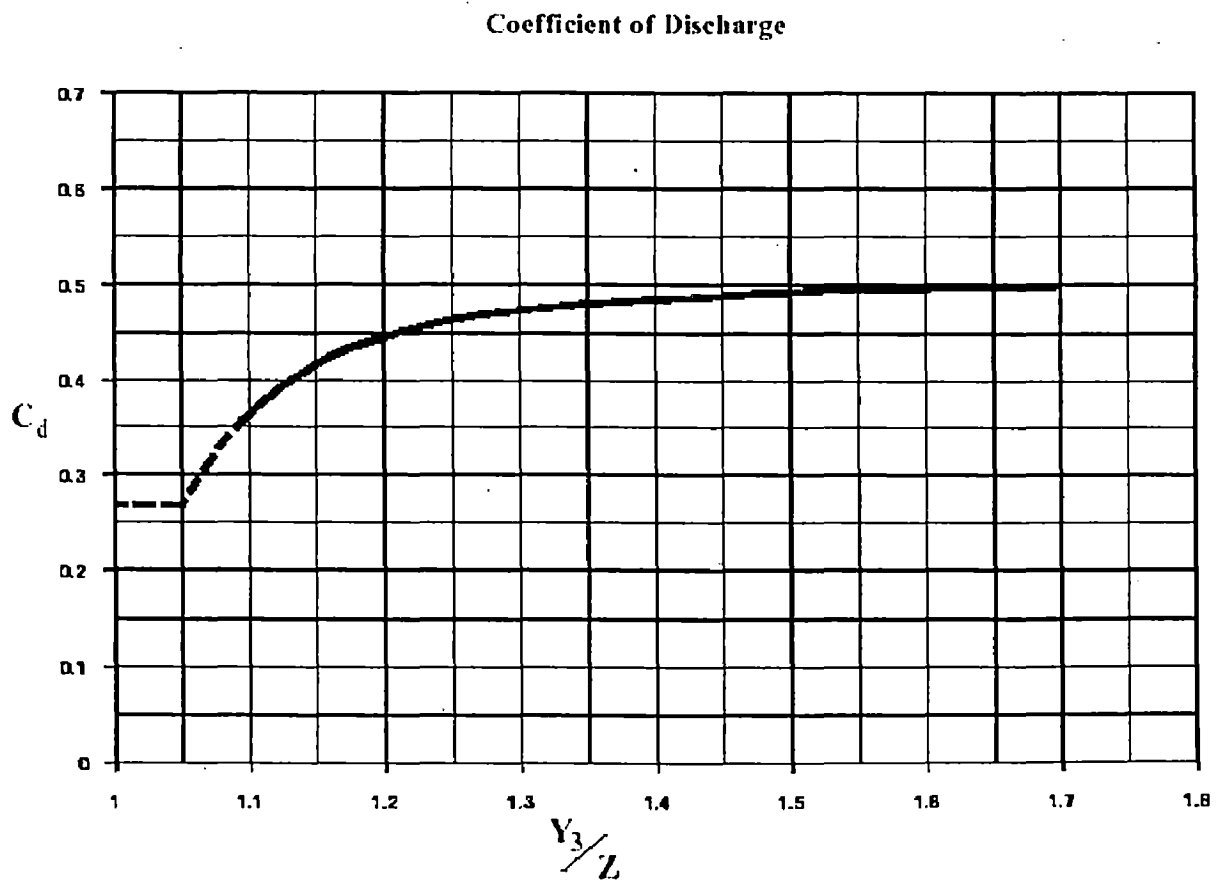


Fig. 4.5 Coefficient of Discharge for Sluice Gate type of Flow

loss coefficient, which comes from the form of the orifice equation that is used in the HEC-2 computer program (HEC, 1991):

$$C = A \sqrt{(2gH / k)} \quad (4.15)$$

Where, k = Total loss coefficient

Conversion from k to C is:

$$C = \sqrt{(1 / k)} \quad (4.16)$$

The program will begin checking for the possibility of pressure flow when the computed low flow energy grade line is above the maximum low chord elevation at the upstream side of the bridge. Once pressure flow is computed, the pressure flow answer is compared to the low flow answer, the higher of the two is used. The user has the option to tell the program to use the water surface, instead of energy, to trigger the pressure flow calculation.

4.3.4.3. Weir Flow Computations

Flow over the bridge, and the roadway approaching the bridge, is calculated using the standard weir equation (see Figure 4.7):

$$Q = C L (H)^{3/2} \quad (4.17)$$

Where, Q = Total flow over the weir, m^3 / s

C = Coefficient of discharge for weir flow

L = Effective length of the weir, m

H = Difference between energy upstream and road crest, m

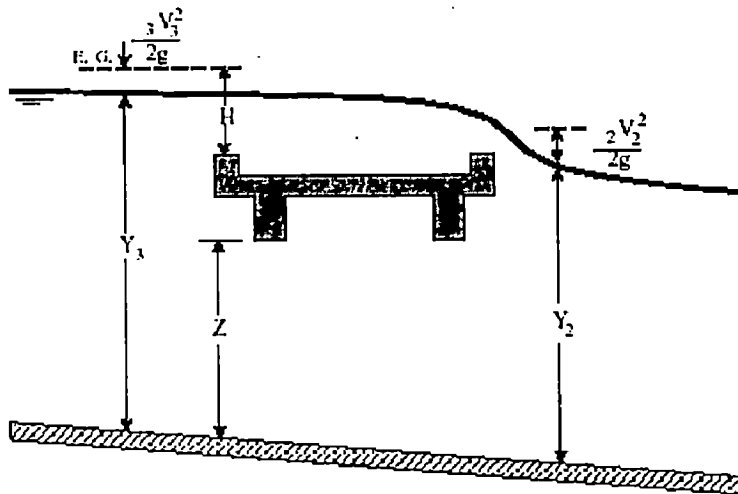


Fig.4.7 Bridge with Pressure and Weir Flow

The approach velocity is included by using the energy grade line elevation in lieu of the upstream water surface elevation for computing the head, H . Under free flow conditions (discharge independent of tailwater) the coefficient of discharge C , ranges from 2.5 to 3.1 (1.38 - 1.71 metric) for broad-crested weirs depending primarily upon the gross head on the crest (C increases with head). Increased resistance to flow caused by obstructions such as trash on bridge railings, curbs, and other barriers would decrease the value of C .

Tables of weir coefficients, C , are given for broad-crested weirs in King's Handbook (King, 1963), with the value of C varying with measured head H and breadth of weir. For rectangular weirs with a breadth of 15 feet and a H of 1 foot or more, the given value is 2.63 (1.45 for metric). Trapezoidal shaped weirs generally have a larger coefficient with typical values ranging from 2.7 to 3.08 (1.49 to 1.70 for metric).

"Hydraulics of Bridge Waterways" (FHWA, 1978) provides a curve of C versus the head on the roadway. The roadway section is shown as a trapezoid and the coefficient rapidly changes from 2.9 for a very small H to 3.03 for $H = 0.6$ feet. From there, the curve levels off near a value of 3.05 (1.69 for metric).

With very little prototype data available, it seems the assumption of a rectangular weir for flow over the bridge deck (assuming the bridge can withstand the forces) and a coefficient of 2.6 (1.44 for metric) would be reasonable. If the weir flow is over the roadway approaches to the bridge, a value of 3.0 (1.66 for metric) would be consistent

with available data. If weir flow occurs as a combination of bridge and roadway overflow, then an average coefficient (weighted by weir length) could be used.

For high tailwater elevations, the program will automatically reduce the amount of weir flow to account for submergence on the weir. Submergence is defined as the depth of water above the minimum weir elevation on the downstream side (section 2) divided by the height of the energy gradeline above the minimum weir elevation on the upstream side (section 3). The reduction of weir flow is accomplished by reducing the weir coefficient based on the amount of submergence. Submergence corrections are based on a trapezoidal weir shape or optionally an ogee spillway shape. The total weir flow is computed by subdividing the weir crest into segments, computing L, H, a submergence correction, and a Q for each section, then summing the incremental discharges. The submergence correction for a trapezoidal weir shape is from "Hydraulics of Bridge Waterways" (Bradley, 1978). Figure 4.8 shows the relationship between the percentage of submergence and the flow reduction factor.

When the weir becomes highly submerged the program will automatically switch to calculating the upstream water surface by the energy equation (standard step backwater) instead of using the pressure and weir flow equations. The criteria for when the program switches to energy based calculations is user controllable. A default maximum submergence is set to 0.95 (95 percent).

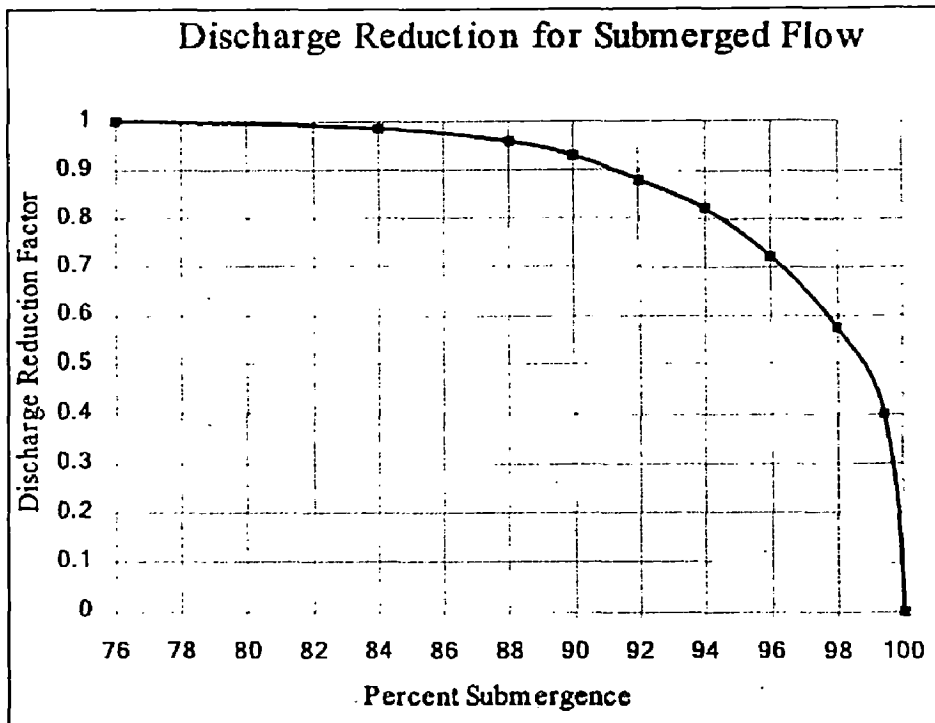


Fig. 4.8 Discharge Reduction due to Submergence

4.3.4.4. Combination Flow

Sometimes combinations of low flow or pressure flow occur with weir flow. In these cases an iterative procedure is used to determine the amount of each type of flow.

4.4. FHWA WSPRO

4.4.1. General

The WSPRO is a computer Program developed by Federal Highway Authority in association with USGS (United States Geological Society) for computation of scour, both locally at piers and abutments and through contracted openings, for many federal, state, and local organizations that are involved with the design and construction of bridges. Equations that can be used to estimate scour are fairly easy to apply, however, many times difficulty comes when trying to estimate appropriate values for the variables that are required in the equations.

FHWA's Hydraulic Engineering Circular No. 18, Evaluating Scour at Bridges, and Hydraulic Engineering Circular No. 20, Stream Stability at Highway Structures

presents information and equations that can be used to evaluate scour at bridges which consists of long term aggradations or degradation, contraction scour, and local scour at piers and abutments.

The FHWA/USGS bridge backwater program, WSPRO, has many features that can be used to estimate the hydraulic parameters needed for scour computations. The program can compute equal-conveyance “tubes” and hydraulic properties by subareas as well as analyze weir flow over an embankment and bridge hydraulics for pressure flow. The equal-conveyance “tubes” and hydraulic properties by subareas provide information that can be used to estimate the various components of local scour. The ability of the program to model weir and pressure flow provides additional insight into potential scour problems at bridge crossings.

4.4.2. Pier Scour

The pier scour equation of WSPRO is as given by equation (2.17) in chapter 2, in which, k_3 and k_4 are taken unity each.

Ideally, one would use the flow depth and velocity, described in equation (2.17) three pier widths upstream of the pier, but seldom is that information readily available. WSPRO can provide the depths and velocities in front of the pier which, is an acceptable approximation of the desired parameters.

One of the improvements the WSPRO computer program has over other one – dimensional computer programs that are used to analyze bridge hydraulics is the use of an improved estimate of friction loss in the contracting reach upstream of the bridge. This estimate is based on an effective flow length, which is computed by dividing the “approach” and “bridge” cross-sections into 20 equal-conveyance “tubes” and computing the average length of the “tubes.” The division of a cross-section into equal-conveyance “tubes” is illustrated in Fig. 4.9

At each cross section where the “tubes” are to be computed, the program outputs for each individual “tube” the left and right edge, the cross-sectional area, and velocity. The average, or hydraulic, depth can be computed by dividing the area of the “tube” by the top width of the “tube.” By evaluating the output and selecting the “tube(s)” that include the pier being analyzed, one can obtain the depth and velocity at that pier.

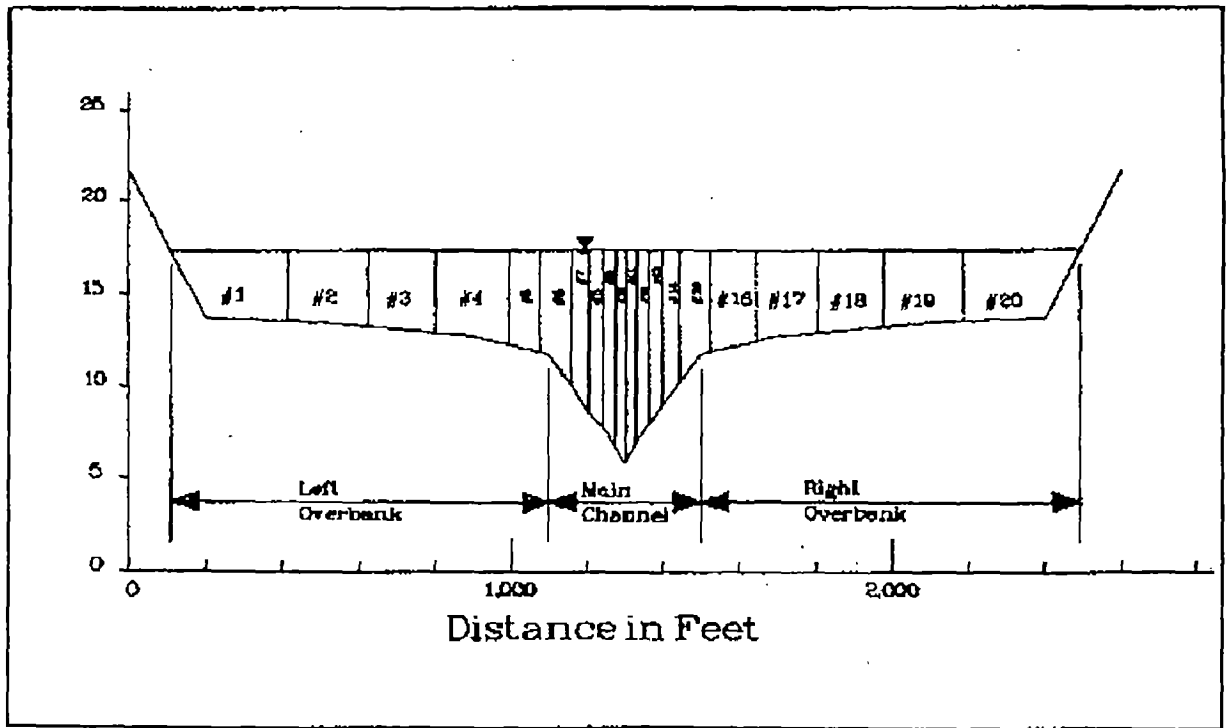


Fig. 4.9 Equal Conveyance Tubes

$$WSEL_u = WSEL_d + HF_{us-ds} \quad (4.18)$$

$WSEL_{ds}$ = Water surface elevation at the downstream side of the bridge, m.,

$WSEL_{us}$ = Water surface elevation at the upstream side of the bridge, m, and

HF_{us-ds} = Friction loss between the upstream and downstream faces of the bridge, m.

One can then assume that the depth of flow in front of the pier is equivalent to the water surface elevation ($WSEL_{us}$) at the upstream face of the bridge minus the ground elevation at the pier.

WSPRO is a one-dimensional fixed-bed hydraulic model that does not consider the fact that the channel may migrate with time. Channel migration could alter the velocity distribution in the bridge opening and the shape of the cross-section. In addition, if the cross-section is on a bend, the velocity distribution will be incorrect.

4.4.3. Local Scour at Abutments

Using WSPRO the abutment scour is computed using equation (2.24). Q_e , A_e , u_e , and y_a can be determined for use in the above equation. Assuming that the “approach” cross-section is representative of the cross-section at the embankment, the “approach” cross-section located one bridge length from the upstream face of the bridge is the best source for most of the information. If the “approach” cross-section is not representative of the cross-section at the embankment, the “full-valley” cross-section should be used. The “full-valley” cross-section is the cross-section upon which the bridge opening is superimposed in design mode. By selecting the equal-conveyance “tubes” at the “approach” cross-section that would be blocked by the embankment and then summing the conveyance and area in the “tubes”, Q_e and A_e is determined.

If weir flow over the embankment occurs program subtracts the discharge associated with the road overflow, Q_{road} , from Q_e . This flow is not obstructed by the embankment and does not flow past the abutment. The elevation of the water surface at the upstream side of the embankment is computed from the water surface elevation at the “approach” cross-section and the following relationship:

$$H_f = (Q^2 / K^2) L \quad (4.18)$$

Where, H_f = The friction loss based on the straight line flow distance between the “approach” cross-section and the upstream face of the bridge, m.,

Q = Total flow at the “approach” cross-section, $m^3/s.$,

K = Total conveyance at the “approach” cross-section, $m^3/s.$, and

L = Length between the “approach” cross-section and the upstream face of the bridge, m

Q_e and A_e are developed by plotting both the equal-conveyance “tubes” and the embankment on a plot of the “approach” cross-section and computing the flow and flow area blocked by the embankment.

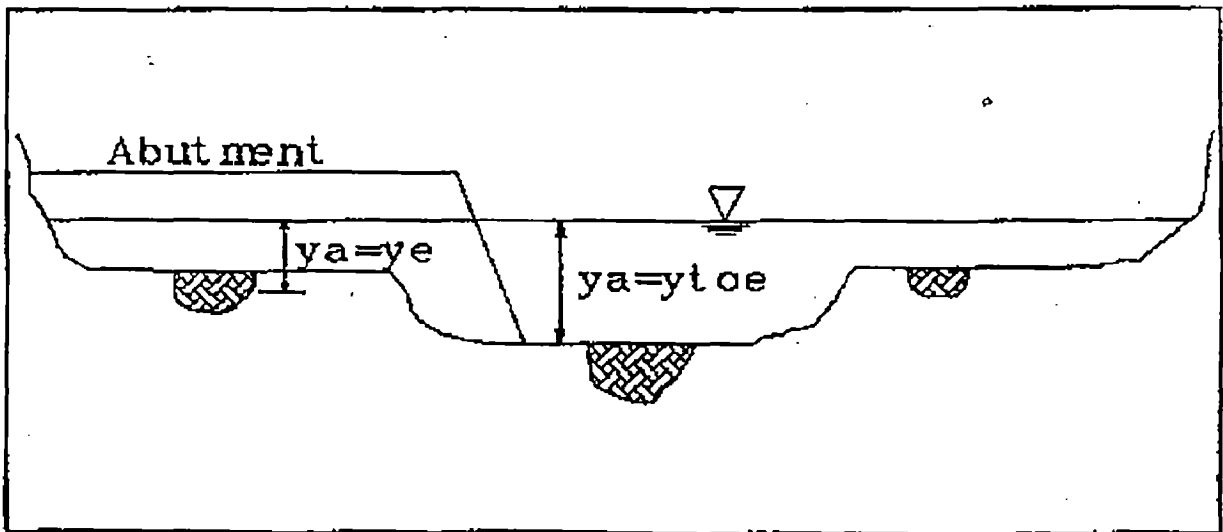


Fig. 4.10 Sketch Showing Possible Choices of Abutment Approach Depth, y_a

Program computes an average flow depth as follows:

$$y_a = A_c / L' \quad (4.19)$$

4.4.4. Contraction Scour

Live-Bed: The live-bed contraction scour equation recommended in HEC-18 is:

$$y_2 / y_1 = (Q_{mc2} / Q_{mc1})^{6/7} (W_{c1} / W_{c2})^{k_1} (n_2 / n_1)^{k_2} \quad (4.20)$$

Where,

y_1 = Average depth in the main channel at the "approach" cross-section, m.,

y_2 = Average depth in the contracted section, m.,

Q_{mc1} = Flow in the approach main channel that is transporting sediment, m^3/s ,

Q_{mc2} = Flow in the contracted main channel which is often Q_{total} but not always, m^3/s ,

W_{c1} = Average bottom width of the main channel at the "approach" cross-section, m.,

W_{c2} = Average bottom width of the contracted section, m.,

n_2 = Manning's n for the contracted section,

n_1 = Manning's n for the main channel, and

k_1 & k_2 = Exponents described in chapter 3.

The estimated contraction scour, y_s , can then be estimated by

Subtracting y_1 from y_2 , ie. $y_s = y_2 - y_1$, m

In a flood, the flow is typically into the overbank during the event for which the contraction scour is to be estimated. The above relationship assumes that the material being transported is in the main channel, therefore, the flow parameters needed for the computation are for the main channel only. The estimated contraction scour, y_s , can then be determined by subtracting y_1 from y_2 ie. $y_s = y_2 - y_1$.

4.4.5. Clear-Water Contraction Scour

Clear-water contraction scour, when part of the opening experiences, clear water-scour are calculated as:

$$y_{ob2} = [Q_{ob2}^2 / D_{50}^{2/3} W_{setback}^2] \quad (4.21)$$

$$\text{and } y_{sob} = y_{ob2} - y_{ob1} \quad (4.22)$$

Where,

y_{ob1} = Average depth in the left or right overbank at the uncontracted "approach" cross-section, m.

y_{ob2} = Flow depth in the left or right overbank in the contracted section, m.,

y_{sob} = Depth of scour in the left or right overbank of the contracted section, m.,

Q_{ob2} = Discharge in the left or right overbank portion of the contracted section, m^3 / s ,

D_{50} = Sediment size in the overbank portion of the contracted section, m., and

$W_{setback}$ = Distance the abutment is set back from the main channel, m.,

The depth of scour, y_{sob} , in the left or right overbank of the contracted section is computed y_{ob1} from y_{ob2} . The above equation applies to the case where the abutment is set back into the overbank and there is no live-bed scour in the overbank portion of the contracted section. Often it is difficult to determine whether or not the scour is a result of live-bed or clear-water sediment transport. Several methods exist to determine the scour mechanism.

4.5. Critical Shear Stress Approach

A critical shear stress approach can be used to determine whether or not there is sufficient shear stress in the channel to transport material from the bed. The average shear stress on the bed of the channel can be estimated as follows:

$$\tau_0 = \gamma R S_f \quad (4.23)$$

Where, τ_0 = Average shear stress, N/m^2 ,

γ = Specific weight of water, 62.4 N/m^3 ,

R = Area divided by wetted perimeter for the portion of the channel for which the shear stress is to be calculated, m, and

S_f = Slope of the energy grade line, m. / m.

In general, material transported in overbank tends to be a result of clear-water scour while material in the main channel is a result of live-bed scour. The slope of the energy grade-line, S_f can be determined as:

$$(EGL_{us} - EGL_{ds}) / L_{(us-ds)} = S_f \quad (4.24)$$

4.6. Critical Velocity Approach

An equation has been developed by Neill, (1968) which can be used as an indicator of live-bed or clear-water scour. The equations are given in chapter 2 (2.15) and (2.16). If the critical velocity, u_c , is smaller than the mean velocity in the overbank or main channel, then live-bed sediment transport is assumed.

SIMULATION STUDY

5.1. Simulation Study of Streambed Variation

As mentioned earlier in chapter 1, streambed variation comprises five components viz., water routing, sediment routing, width variation, lateral migration of channel, and channel-bed profile variation. In this chapter the phenomenon of streambed variations by analyzing field data have been discussed. For this purpose data from Maan and Babai Rivers have been used.

5.2. Data Required

The following data are required for the studies on long-term streambed variation:

Cross-section of river in the study reach

Longitudinal section of the river in the study reach, or frictional slope or riverbed slope

Radius of curvature, if effect of curvature is to be considered

Thickness of erodible bed layer

Information about non erodible bank or bed or rock out-crop

Manning's coefficient of roughness 'n'

Flow hydrograph into the reach

Sediment inflow data, or

Grain size distribution data at the two extremities of the reach.

The mathematical model FLUVIAL-12 has been used for the study on long term streambed variations.

5.3. Input Data

Input to the model include the initial cross- sections, channel roughness, initial bed-material composition, inflow hydrograph and physical constraints such as check dams, rigid banks, bed rock outcrops, etc. The input data follow the HEC-2 data format.

5.4. Computing Procedures

Major steps of computation in the model include the following:

1. Enter input data.
2. Compute water surface elevation and sediment loads at all cross-sections.
3. Set time $t = t + \Delta t$.
4. Determine changes in channel cross-sectional using techniques for sediment routing.
5. Compute and apply changes in channel width.
6. Obtain new channel-bed profiles.
7. Compute and make changes in cross-sectional profile due to lateral migration for those sections in channel bends.
8. Update bed-material compositions.

After step 8, the computation returns to step 2 for another time step. The iteration continues until required time step is covered.

5.5. Output Description

Output of the model include initial bed-material compositions, time and spatial variations of the water surface profiles, channel width, flow depth, flood discharge, velocity, energy gradient, roughness coefficient, median sediment size, and bed material load. In addition, cross-sectional profiles are printed at different time intervals.

5.6. Description of Maan River

5.6.1. Location

River Maan is located in the Bardia district, Bheri Zone of the Mid-Western Development region of Nepal. Geographical coordinates of the river in the study reach are latitude $28^{\circ} 15' N$ and longitude $71^{\circ} 28' E$. The study reach lies between the East-West Highway Bridge and Nepalgunj-Gularia (the district head quarter) road bridge.

5.6.2. Physical Conditions

The study reach is 5 Km. downstream of the East-West Highway Bridge. The perennial channel is narrow with wide flood plain, natural slope of about 1: 3000 on an average and bed material size decrease significantly in the downstream direction. Bed-material in the study reach varies from coarse sand ($d_{50} = 2.19$ mm) at upstream end to medium sand ($d_{50} = 0.65$ mm) downstream end.

The configuration of the channel was distorted prior to study flood event by man's activities including sand mining. As a result of sand mining several large borrow pits with a depth as great as 2 m were created. The banks are erodible at the both the sides in the study reach from the river station 12 Km. downstream. There are two parallel channels (farmer's inundation canal through flood plain) along the river. Farmers take water during winter season (or low flow season) and in the rainy season both are filled with sediment. Inflow hydrograph of the river is available for the year 1998-1999 at the East-West Highway Bridge and no other tributaries enter into the river in the study reach. The peak flood was 550 cumec in 7 July 1998, (see Fig. 5.1).

A hypothetical bridge was considered to exist at river station 9.385 Km. for the study of local and general scour. The presence of the bridge modifies the present state of equilibrium of the river.

5.6.3. Streambed Variations

Significant variations in streambed was observed after the floods. The main changes in streambed were aggradation of borrow pits and convex bank at river station 11.0 Km. Degradation of concave bank at the river station 11.0 Km. was observed. The thalweg of channel shift towards the concave bank, was observed. A significant change in streambed slope was observed due to the degradation at the curved reach and aggradation at downstream of the curvature although quantitatively data measured in the field are not available for the comparison of the results.

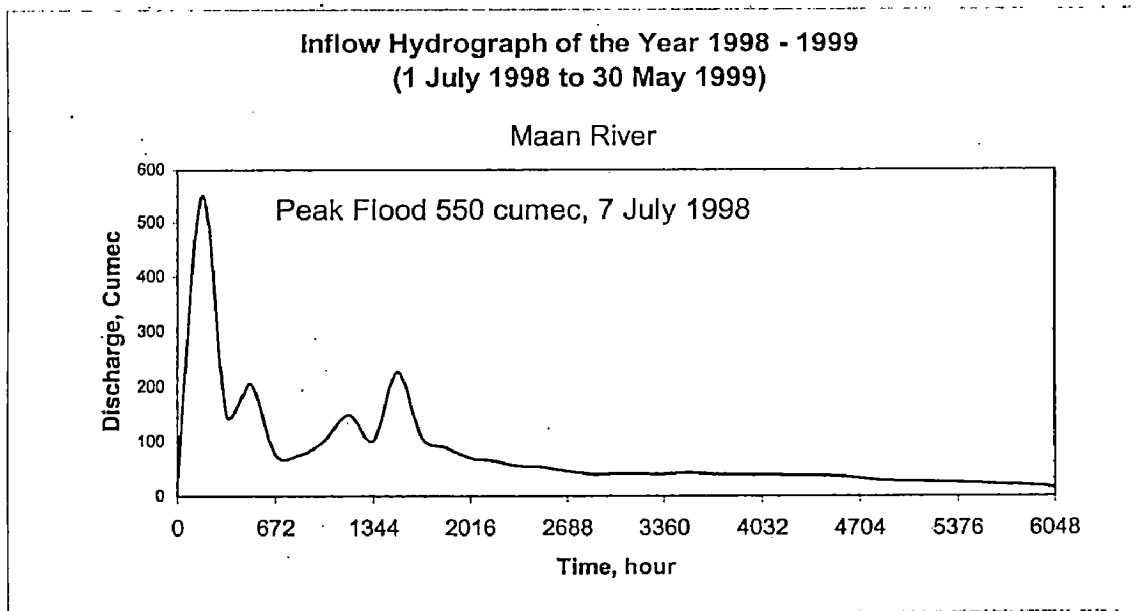


Fig. 5.1 Inflow Hydrograph

5.7. Simulation and Results

The mathematical model FLUVIAL-12 was used to simulate streambed variations in the Maan River during 1998 flood as mentioned earlier. Engelund-Hunsen formula was used in computing sediment movement. Channel roughness in terms of Manning's n was selected to be 0.035 in consideration of channel irregularity and minor-vegetation growth; it was assumed to be 0.05 for triggering initial computations. The contraction and expansion ratios were assumed to be 0.1 and 0.3 respectively. Bank erodibility factor was assumed to be 0.50 i.e., moderately erodible banks. Brownlie's formula was used to compute Manning's n in successive computations. There is a bend at 11.0 Km.. Streambed variation was simulated by the model, and results are presented in Fig. 5.2 to 5.9.

5.7.1. Changes in River Channel Configuration

River channel changes, including those in channel-bed profile, channel width, and lateral migration, as simulated by the computer model, are described herein.

Longitudinal Channel-bed Profile: Changes in longitudinal channel-bed profile are characterized by aggradation in depressions, and degradation at mounds and higher grounds, and gradual formation of a more or less smooth channel-bed profile at the end of the peak floods. However, small to medium sand-dunes are observed after the floods particularly in the downstream of river stations 11.0 and 9.250 Km.. In that process, considerable variation in the longitudinal channel-bed elevation through the downstream portion of the reach is predicted at and after the peak floods. Longitudinal channel-bed profile is also considerably affected due to bends.

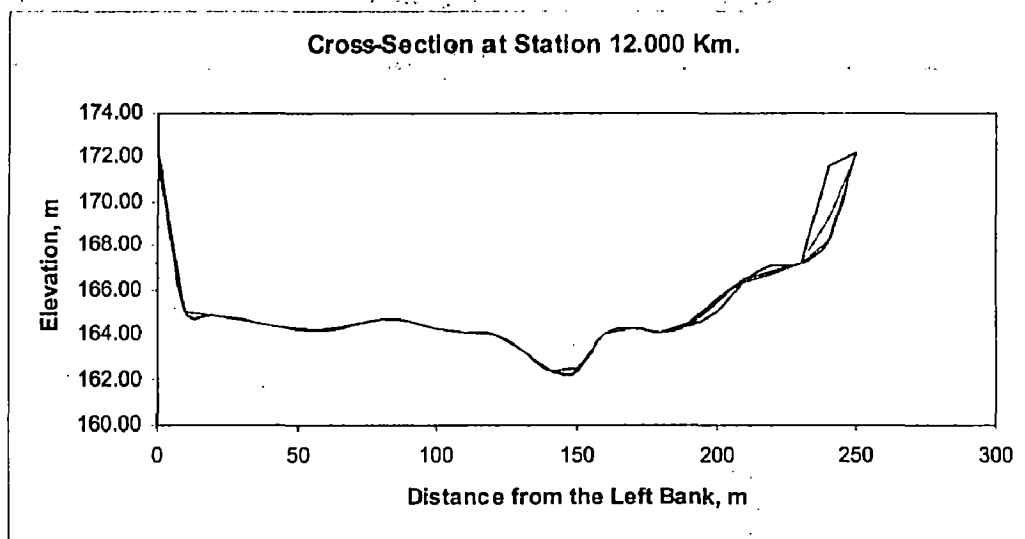


Fig. 5.2 Time Variation of Cross-section, No Significance Change

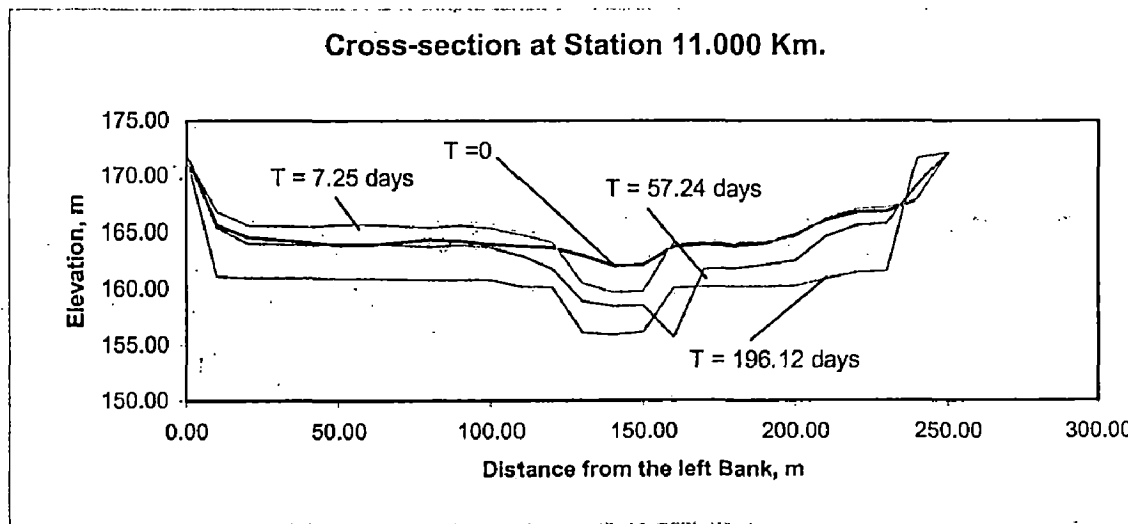


Fig. 5.3 Time Variation of Cross-section Near the Bend, Degradation of Channel

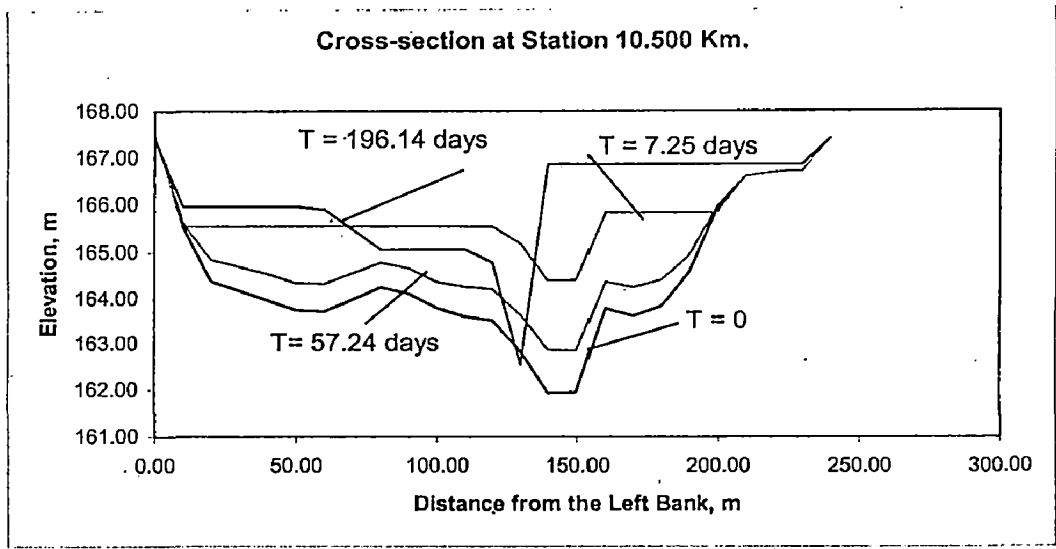


Fig. 5.4 Time Variation of Cross-section, Aggradation and Lateral migration of Channel

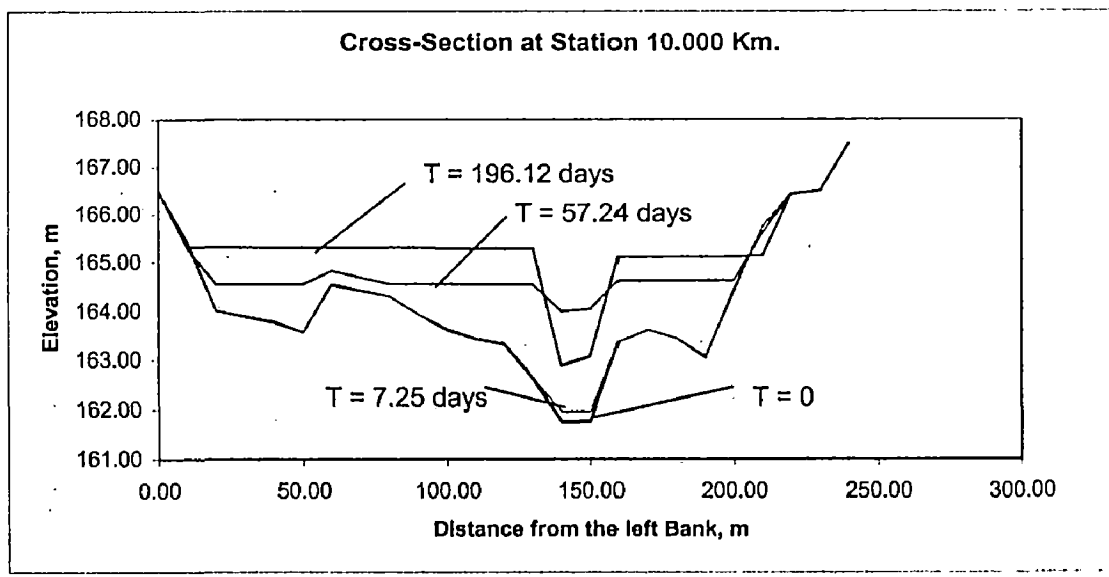


Fig. 5.5 Time Variation of Cross-section, Aggradation, Width Reduction

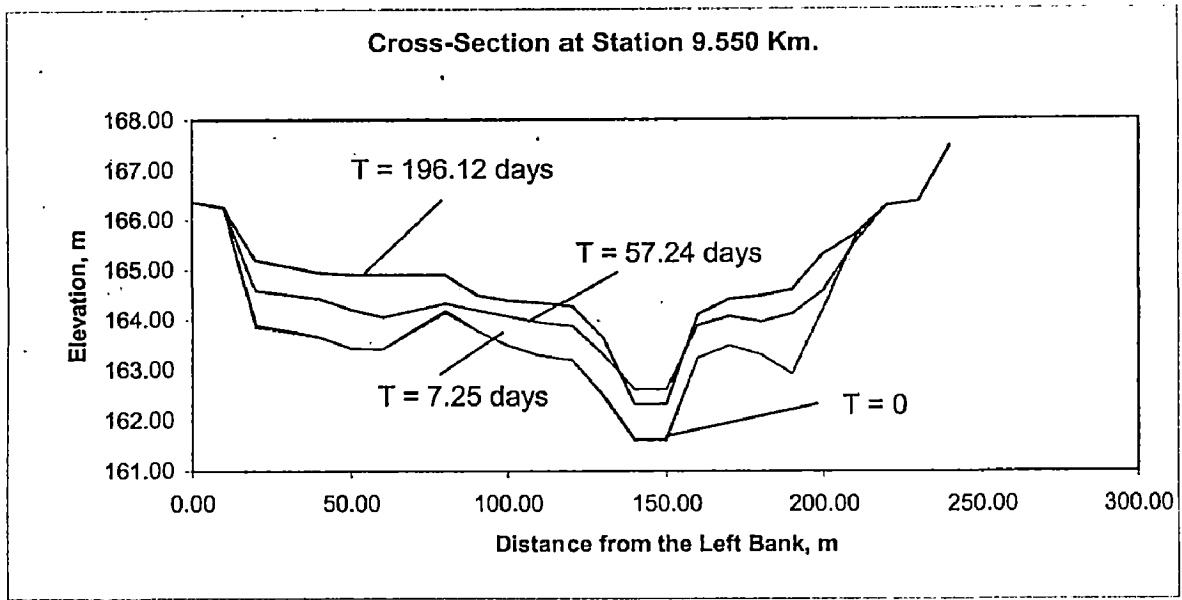


Fig. 5.6 Time Variation of Cross-section, Aggradation and Width Reduction

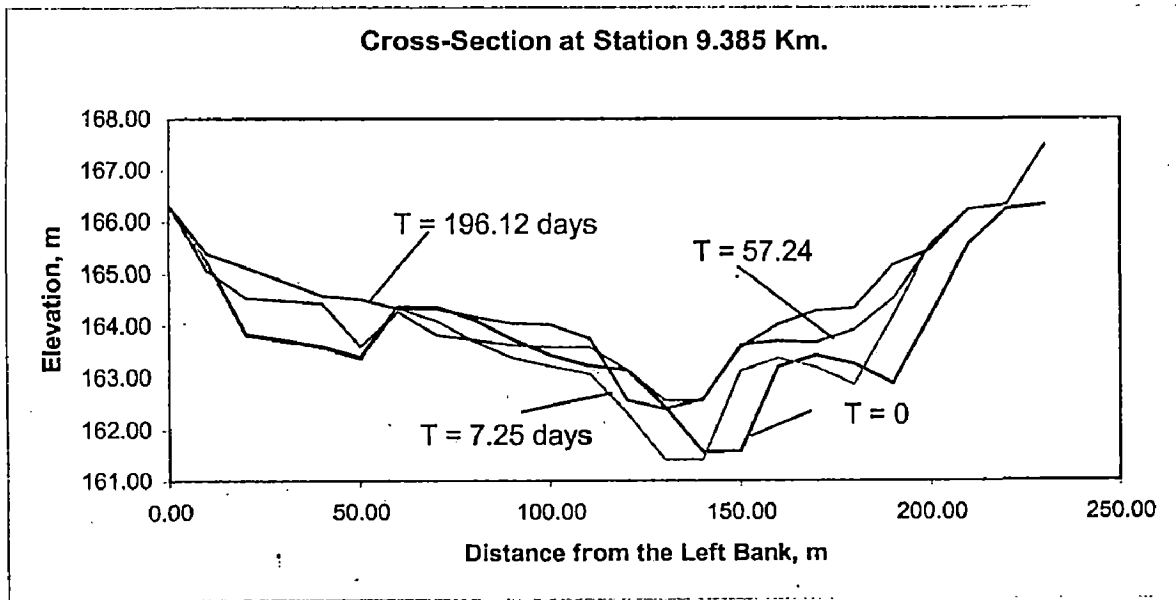


Fig. 5.7 Time Variation of Cross-section, Aggradation, Lateral Migration and Width Variation

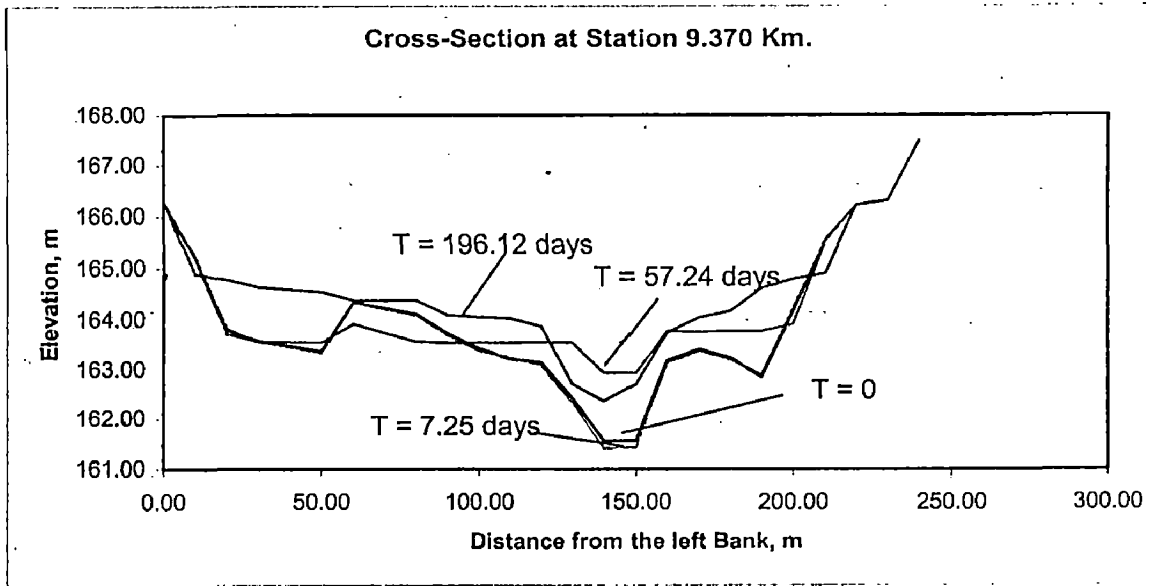


Fig. 5.8 Time Variation of Cross-section, Aggradation Width Variation of Channel

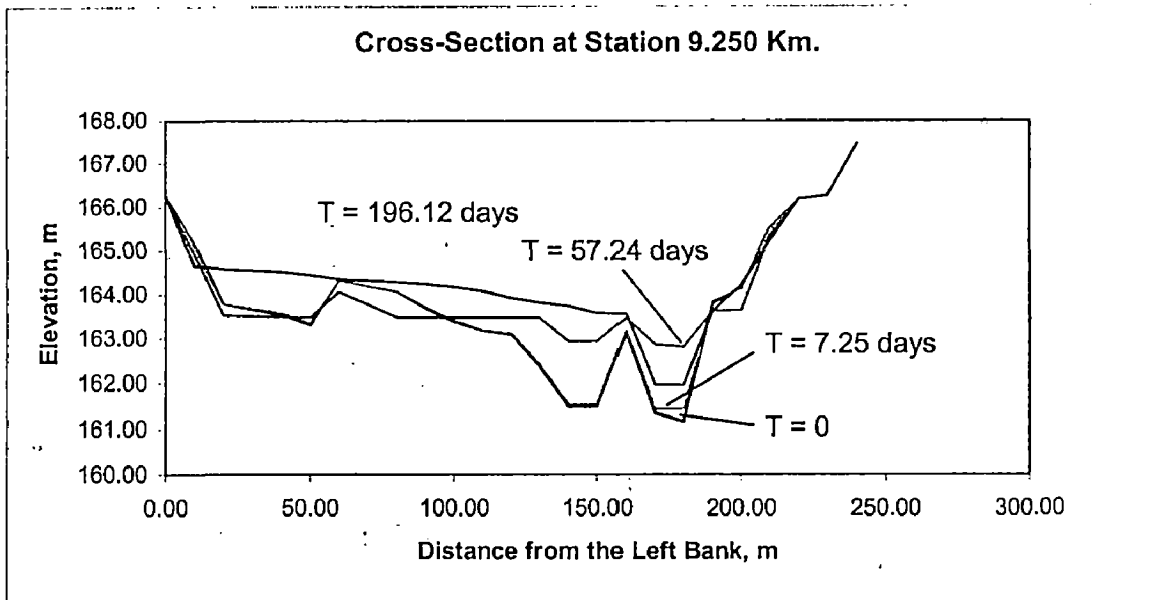


Fig. 5.9 Time Variation of Cross-section, Aggradation, Width Variation and Lateral Migration of Channel

Changes in Width: Changes in width occur currently with variations in channel-bed elevations and are characterized by gradual widening at those initially narrow sections, notably sections 11.0, 9.385 and 9.37 Km., and reduction in width initially wide sections, notably sections at 10.5, 10.0, and 9.55 Km.. By the study of initial and final channelbed profiles, one can find that widening occurs at a section is generally, through bank erosion whereas, width reduction is due to sand bar formation along the bank(s) (see Fig. 5.2 to 5.9).

The changes in channel width and channel-bed elevation may be illustrated by the simulation time variation of cross-sectional profile at stations 10.0 Km.. Initially this section is in ridge and gullies (or small channels) both the sides. There is no change in the first flood but gullies are filled in the second flood followed by gradual deepening by gully erosion. Similar effects are observed at section 9.55 Km..

Lateral Migration of Channel: Lateral migration of channel is simulated by the model at sections 10.50, 9.385 and 9.25 Km (Fig. 5.4, 5.7 and 5.9).

Change in Sediment and Hydraulic Parameters: The flood and sediment routing in erodible channels is closely related to river-channel changes as illustrated by the time and spatial variations of the velocity and, sediment load (see Fig. 5.10 to 5.12).

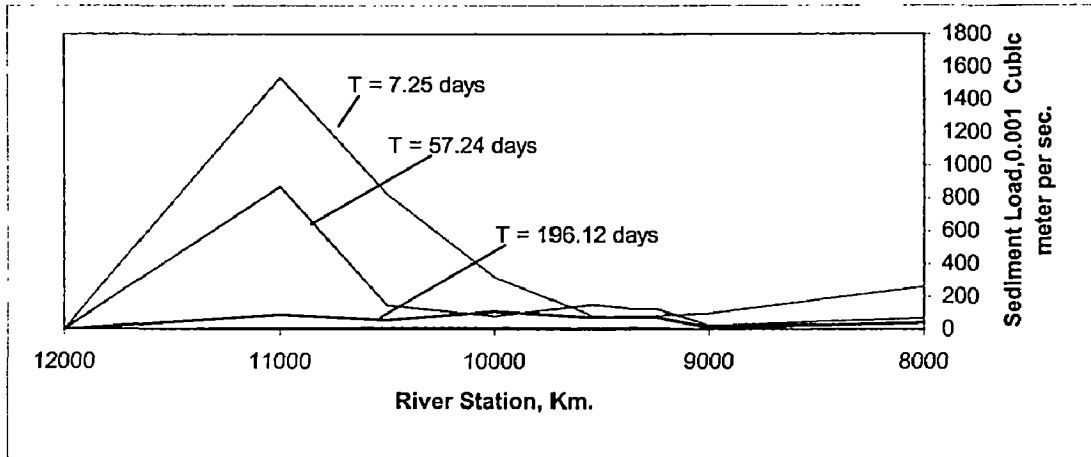


Fig. 5.10 Time and Spatial Variation of Sediment Load

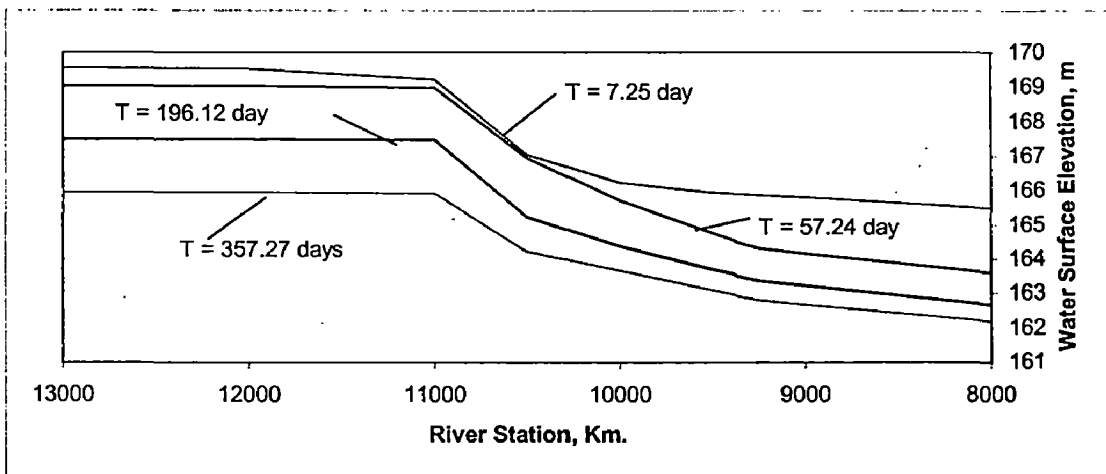


Fig. 5.11 Time and Spatial Variation of Water Surface Profiles

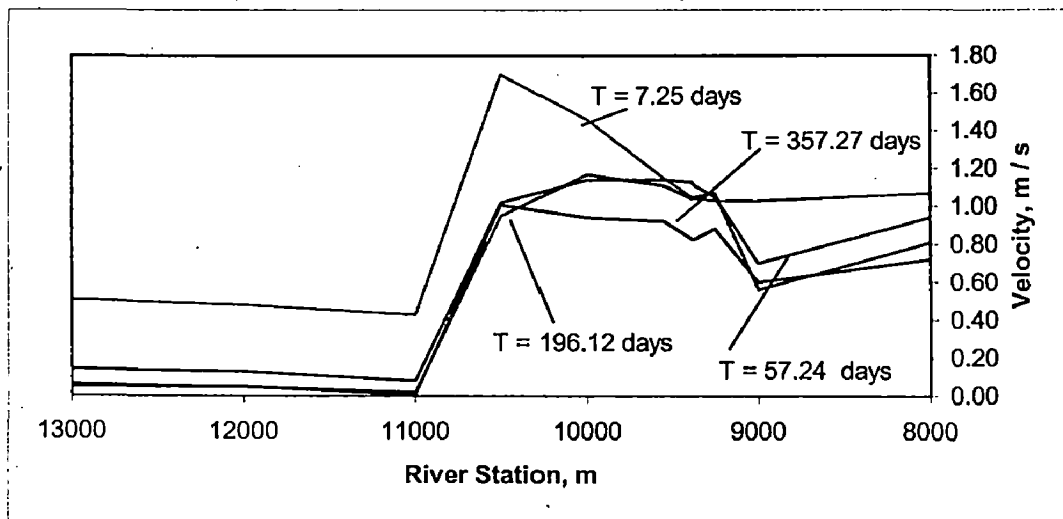


Fig. 5.12 Time and Spatial Variations of Velocity

The pronounced spatial variations in velocity and sediment load at the first flood are associated with the uneven river channel configuration, at depressions velocity and sediment load substantially lower, and downstream of the bends the velocity decrease and sediment load decrease substantially because of sediment deposition in the downstream reach. At the subsequent floods river channel is readjusted and another state of equilibrium is established. Low velocity at station 11.0 and 9.250 Km. (Fig. 5.3, 5.9 and 5.12) are due to high flow resistance.

5.7.2. Changes in Sediment Size and Hydraulic Sorting

Variation of sediment size due to hydraulic sorting as simulated, are not pronounced in this river reach. Certain trends can still be recognized (Table 5.1), including coarsening of the material during scour and reduction in size during deposition. Channel widening through bank erosion brings finer bank materials into the channel and hence contributes to a reduction in sediment size.

Table 5.1 Time and Spatial Variations of Grain Size

River Station (m)	d_{50} (mm)					
	T = 0	T = 7.25 days	T = 57.24 days	T = 63.499 days	T = 196.12 days	T = 357.27 days
8000	0.65	0.32	1.39	1.57	1.85	1.89
9000	0.77	0.9	1.13	1.17	1.24	1.38
9250	1.01	1.01	1.82	1.91	2.06	2.23
9370	1.15	1.21	2.12	2.17	2.36	2.42
9385	1.18	1.32	2.26	2.26	2.52	2.45
9550	1.4	1.73	2.52	2.48	2.83	2.7
10000	2.19	2.2	2.86	2.76	3.19	3.22
10500	2.19	2.64	3.15	3.09	3.29	3.31
11000	2.19	3.21	3.32	3.32	3.32	3.32
12000	2.19	2.19	2.19	2.19	2.19	2.19
13000	2.19	2.19	2.19	2.19	2.19	2.19

5.7.3. Streambed Variation in Relation to Power Expenditure

Changes in river-channel configuration are accompanied by changes in flow resistance and hence the rate of energy (or power) expenditure. The γQS product represents the rate of energy expenditure per unit channel length. Since there is no spatial variation in Q , the spatial variation of γQS may be represented by the spatial variation of energy gradient.

Table 5.2 Time and Spatial Variation of Energy Gradient (or Power)

River Station	Energy Gradient (S) in 1/10000					
	T = 0	T = 7.25 days	T = 57.24 days	T = 63.499 days	T = 196.12 days	T = 357.27 days
(m)						
8000	1.1	2.9	8.5	8.2	7.2	6.3
9000	2.7	2.9	3.4	3.4	4.2	3.3
9250	0.5	2.8	14.9	14.3	10.3	9.8
9370	3.6	2.9	16.9	15.6	14.4	11
9385	3.6	3	17.1	15.5	13.3	10.3
9550	3.9	4.1	18.5	18.5	13.8	11.5
10000	3.4	11.5	29.3	14.9	13.2	11.8
10500	4.9	23.9	21.3	20.08	20.4	10.4
11000	3.7	6.44	70.2	72	89.9	99.2
12000	3.3	0.2	0.000	0.000	0.000	0.000
13000	3.8	0.2	0.000	0.000	0.000	0.000

Simulated streambed variations (or river channel changes) are associated with the gradual reduction of the spatial variation of energy gradient along the channel subject to the physical constraint of rigid banks. The adjustment in river channel configuration is closely related to the change in power expenditure and that can be illustrated by the sequential changes in cross-sectional profile at station 11.0 Km.. Initially energy gradient is comparable to those of its adjacent sections, because of bend (the channel section is

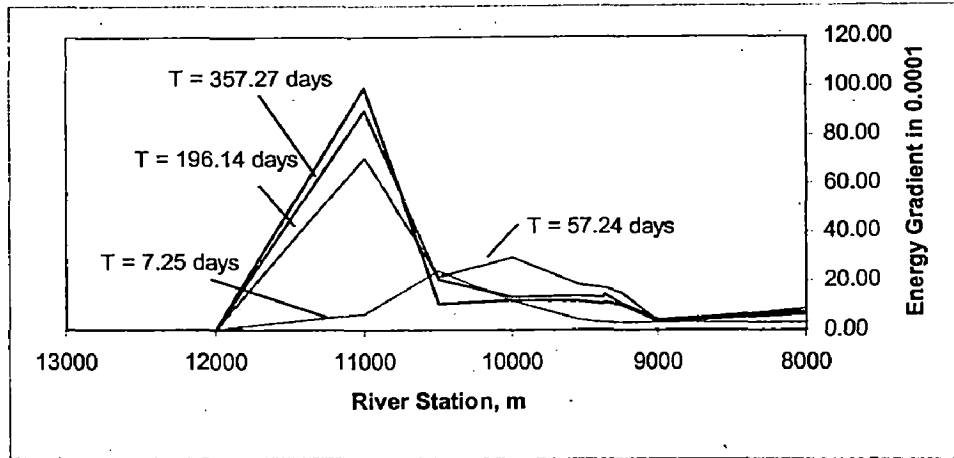


Fig. 5.13 Time and Spatial Variations of Energy Gradient (Power Expenditure)

During sedimentation energy released (at 10.50 Km., Fig. 8.3) and during erosion there is more expenditure of energy (10.0 and 9.25 Km. Fig. 8.5 and 8.9).

5.7.4. Water Surface Profiles

Water Surface profiles simulated by FLUVIAL-12 different time steps are comparable to each other (see Fig. 5.11), and are smooth except at sections 11.0 and 10.5 Km.. This is primarily because of change in bed elevations at these sections. The model predicts subcritical flow in the entire study reach (see table 5.3). The water surface elevation upstream of the section 11.0 Km. is higher because of high flow resistance.

Table 5.3 Time and Spatial Variations of Froude Number

River Station (m)	Froude Number Fr					
	T = 0	T = 7.25	T = 57.24	T = 63.499	T = 196.14	T = 357.27
8000	0.15	0.22	0.31	0.31	0.29	0.27
9000	0.2	0.21	0.22	0.22	0.24	0.22
9250	0.1	0.21	0.38	0.38	0.33	0.32
9370	0.22	0.21	0.4	0.39	0.37	0.34
9385	0.22	0.21	0.4	0.39	0.36	0.33
9550	0.23	0.24	0.41	0.4	0.37	0.34
10000	0.21	0.35	0.49	0.36	0.36	0.34
10500	0.24	0.46	0.43	0.68	0.41	0.3
11000	0.22	0.06	0.01	0.01	0.0004	0
12000	0.21	0.07	0.02	0.03	0.01	0.01
13000	0.22	0.08	0.02	0.03	0.01	0.02

5.8. Streambed Variation Study for Babai River

Streambed variation of Babai River (located in the same district as that of Man River about 35.0 Km west) was also simulated during the present study as described below:

5.8.1. Physical Conditions

The study reach of the river is about twelve kilometers long about four kilometer downstream of Babai Weir Cum-Bridge across the National Highway. The channel has non-uniform bed slope and bed material size decreases uniformly, $d_{50} = 4.13$ mm at 15.0 Km. to 1.89 mm at 2.0 Km.. The study reach is the sand quarry site and is distorted due to sand mining for the construction of Babai Irrigation Project.

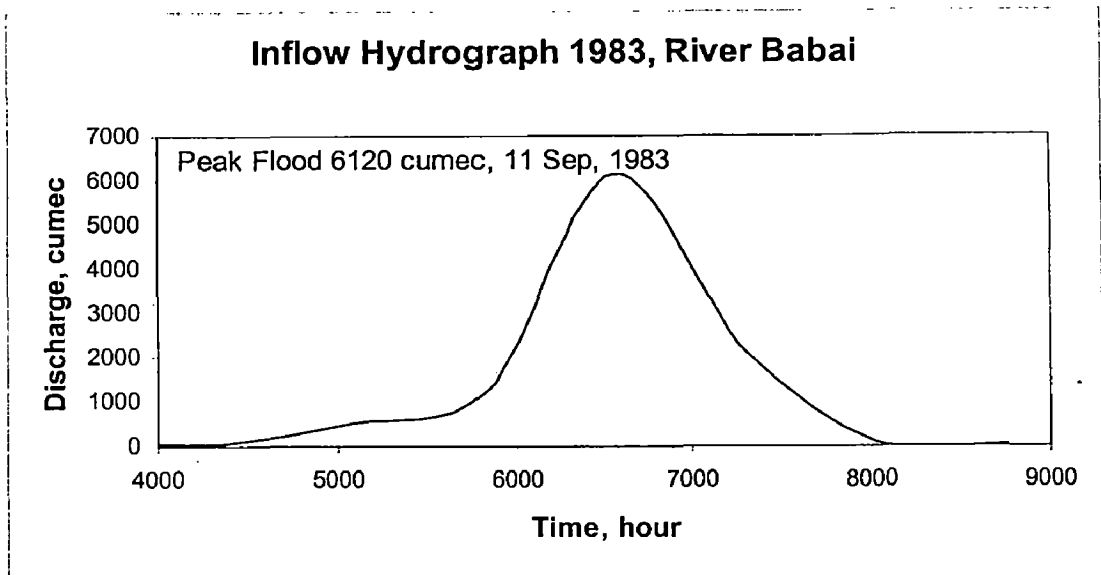


Fig. 5.14 Inflow hydrograph of Babai River

5.8.2. Simulation and Results

The mathematical model FLUVIAL-12 was used to simulate river channel variations. Engelund-Hansen total load equation was used to compute the sediment movement. Manning's roughness coefficient $n = 0.04$ was selected for the main channel irregularity and 0.05 for over bank flow. Factors 0.3 and 0.1 were selected as contraction and expansion losses, respectively. Bank erodibility factor was taken as 0.5. The simulated results are given below:

5.8.3. Changes in River Channel Configuration

Changes in river channel configuration are observed which is characterized by changes in longitudinal channel-bed slope due to aggradation and degradation, width variation, and lateral migration of channel.

Longitudinal Channel-bed Profile: Changes in longitudinal channel-bed profile are characterized by aggradation in borrow pits, and degradation at sand mounds and higher grounds, and gradual formation of a more or less smooth channel-bed profile at the end of the peak floods. Longitudinal channel bed variations are observed at all the sections (Fig.5.15 to 5.23), viz., degradation is observed at stations 3.0, 4.0 and 12.0 Km. (Fig. 5.15, 5.22 and 5.23) and aggradation at other stations (Fig. 5.16 to 5.21). Longitudinal channel-bed profile change is induced by the irregularities in the initial channelbed

profile because river tries to attain uniform bed slope by filling in borrow pits and degrading mounds.

Changes in Width: Changes in width occur currently with variations in channel-bed elevations are characterized by gradual widening at narrow section, notably section at 8.0 Km.(Fig. 5.18) and reduction in width initially wide sections, at 12.0, 10.0, and 3.0 Km. (Fig. 5.15, 5.16 and 5.23). By observations of the initial and final channel-bed profiles, one can find that widening at a section is generally, through bank erosion whereas, width reduction is due to sand bar formation along the bank(s) (see Fig. 5.15 to 5.23).

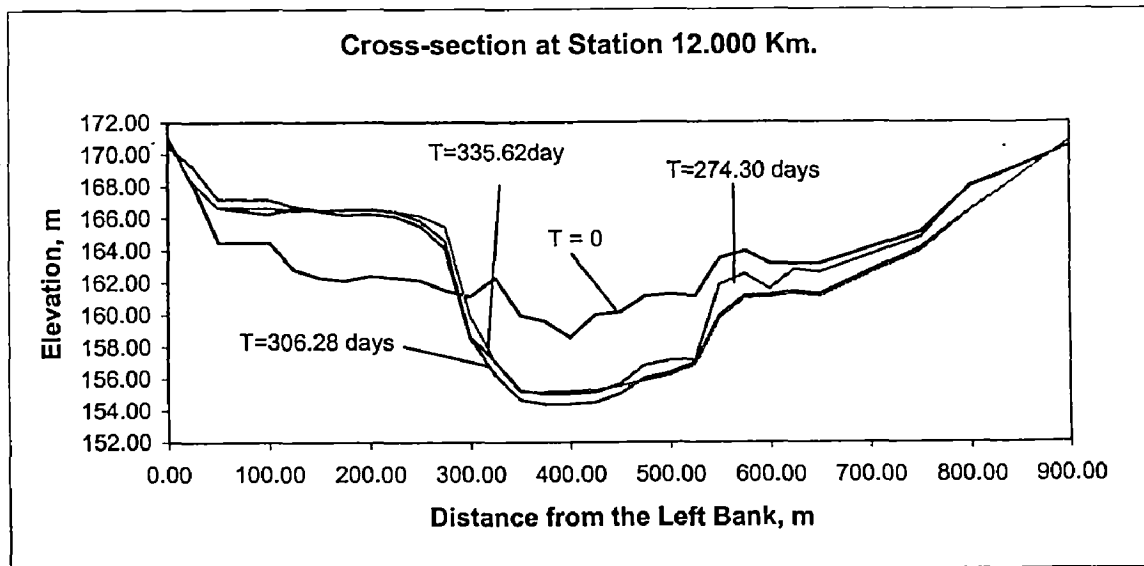


Fig. 5.15 Time Variation of Cross section, Degradation and Width Reduction

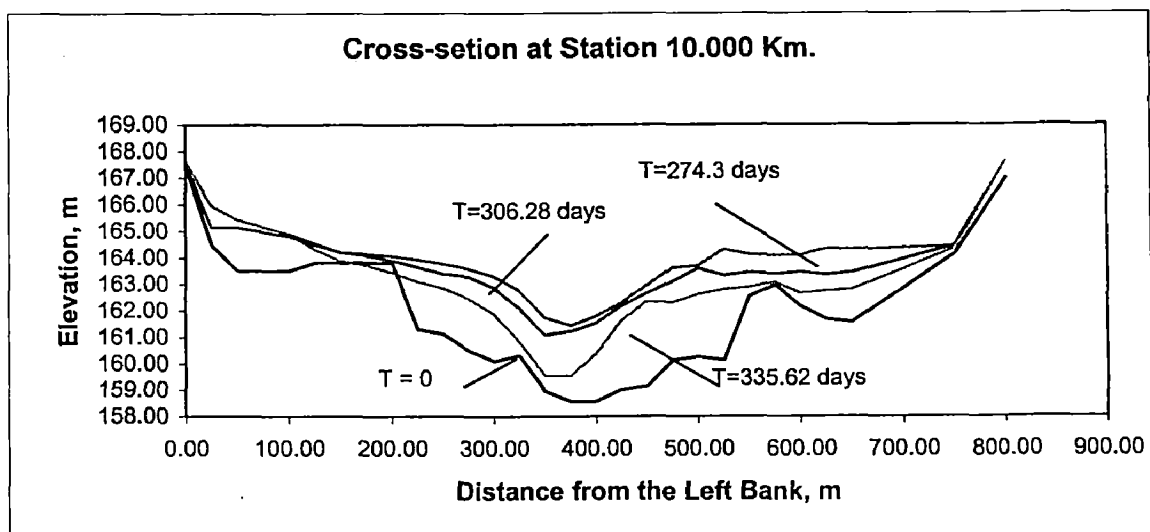


Fig. 5.16 Time Variation of Cross-section, Aggradation and Width Reduction

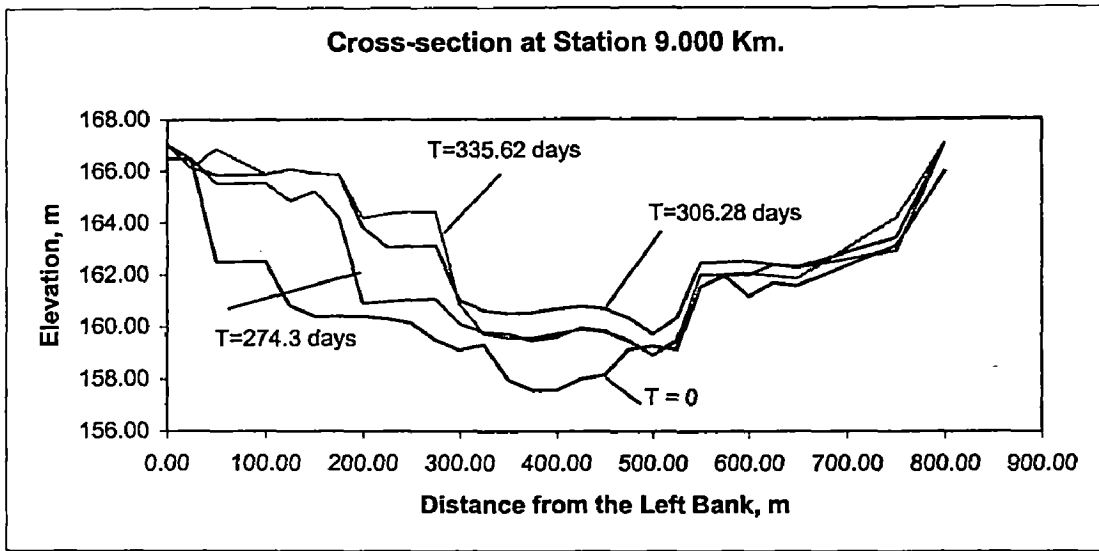


Fig. 5.17 Time Variation of Cross-section, Aggradation and Lateral Migration of Channel

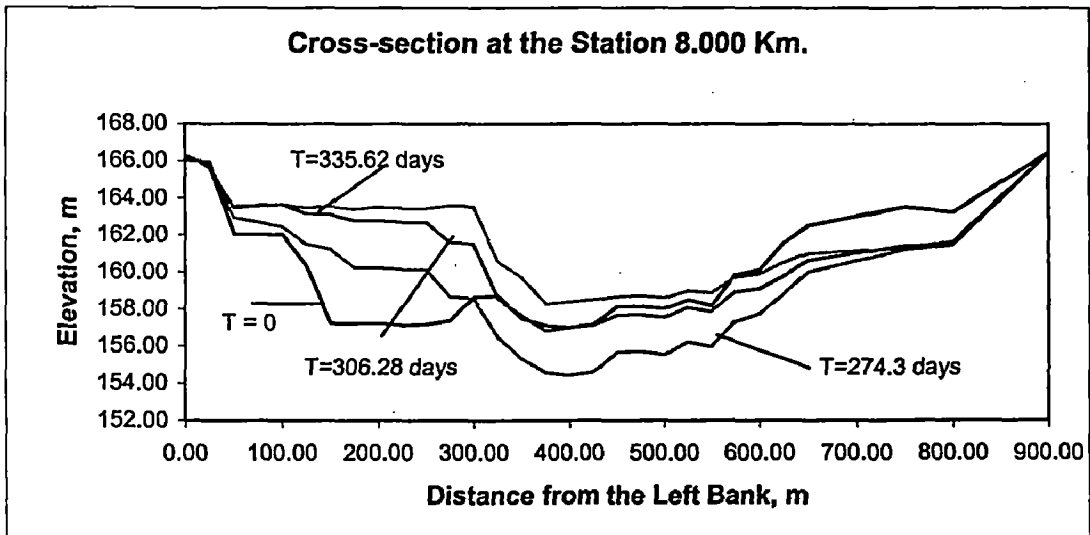


Fig. 5.18 Time Variation of Cross-section, Aggradation, Widening and Lateral Migration of Channel

Lateral Migration of Channel: Lateral migration of channel is simulated by the model at sections 9.0, 8.0 and 4.0 Km. (Fig. 5.16, 5.17 and 5.22).

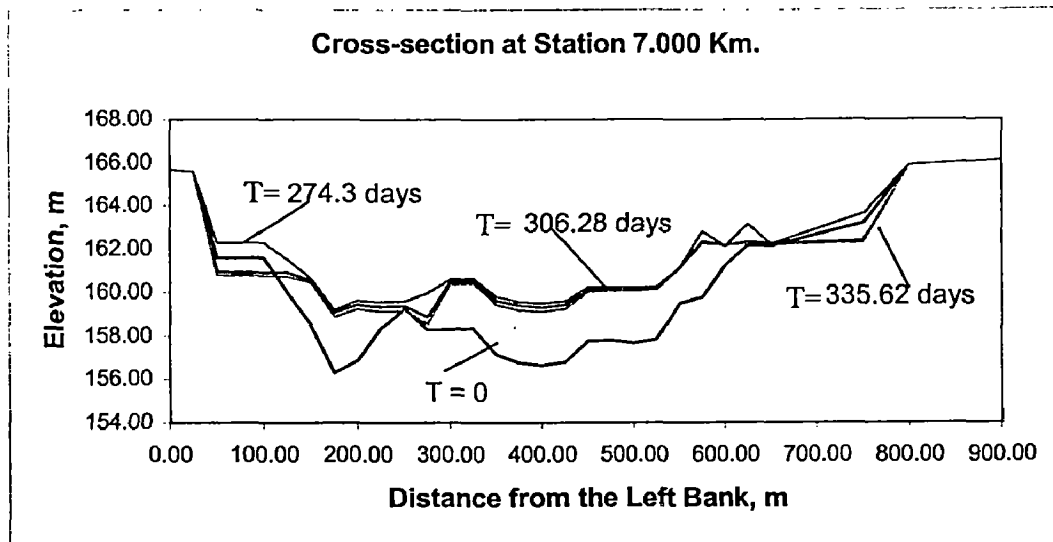


Fig. 5.19 Time Variation of Cross-section, Aggradation

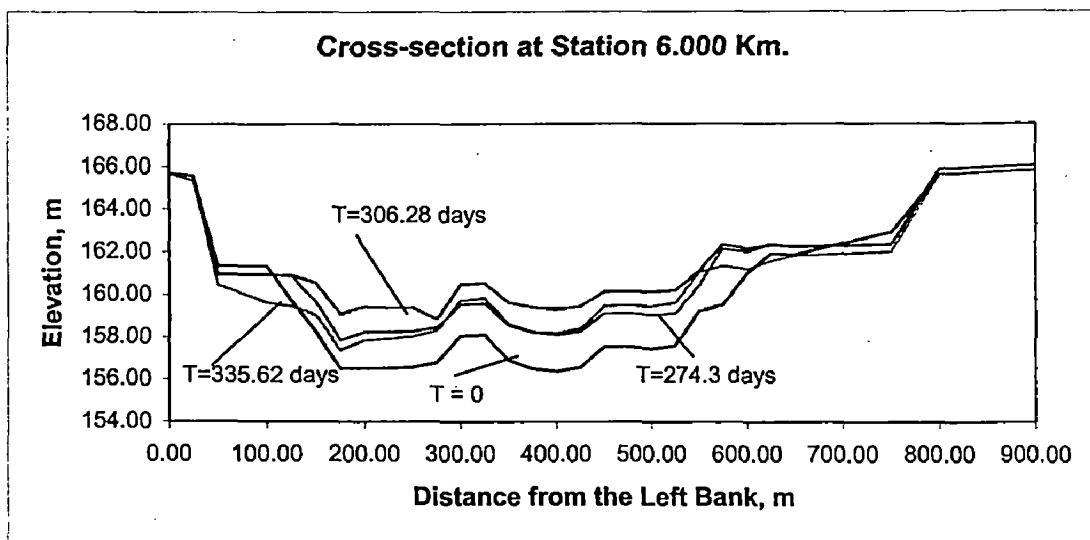


Fig. 5.20 Time Variation of Cross-section, Aggradation

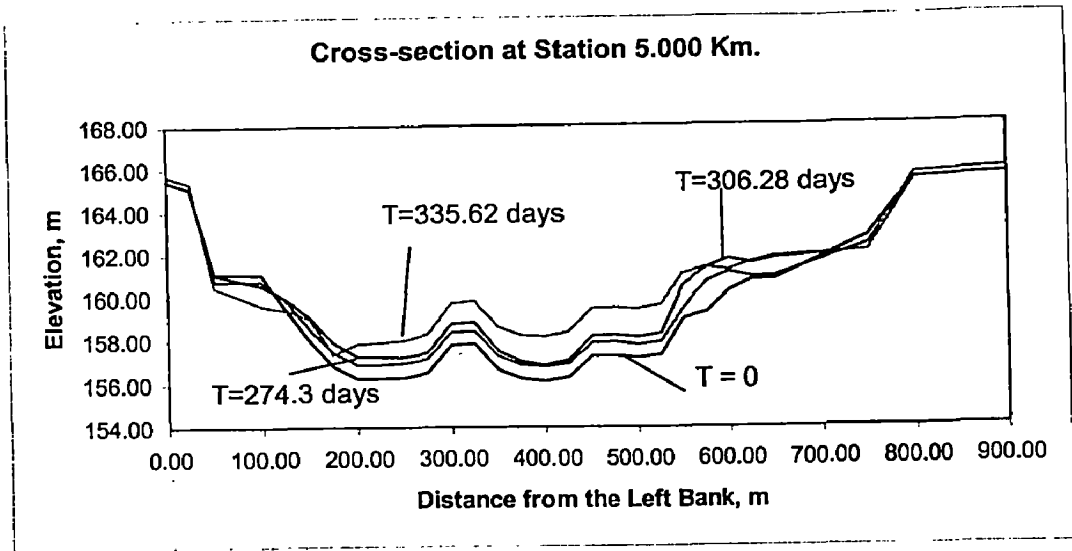


Fig. 5.21 Time Variation of Cross-section, Aggradation

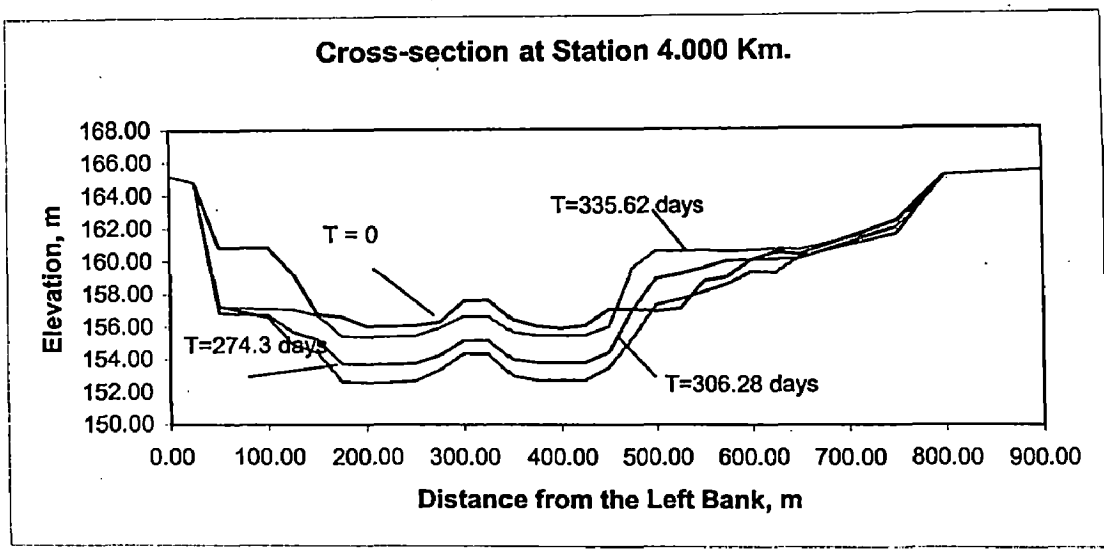


Fig. 5.22 Time Variation of Cross-section, Degradation and Lateral Migration of Channel

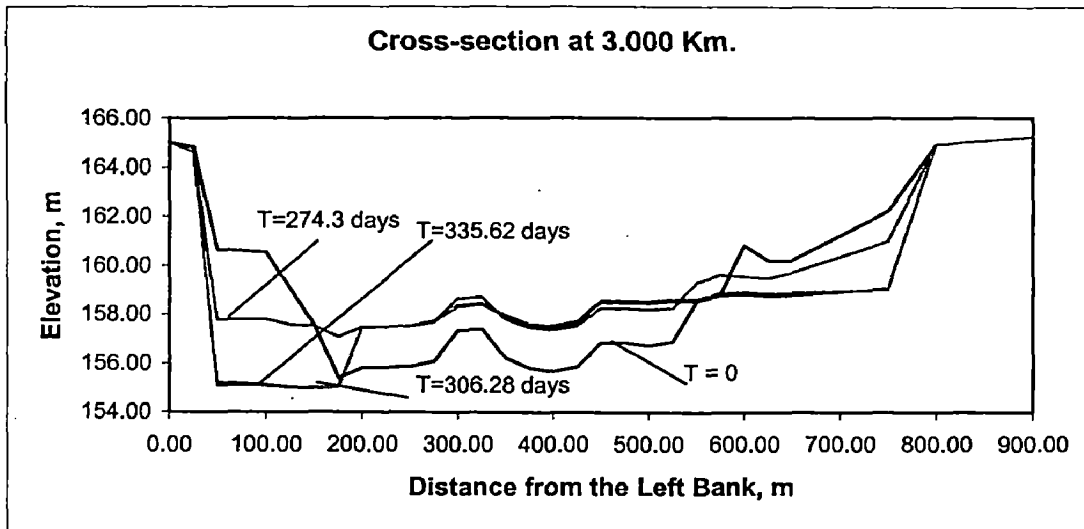


Fig.5.23 Time Variation of Cross-section, Degradation, Width Reduction and Lateral Migration of the Channel

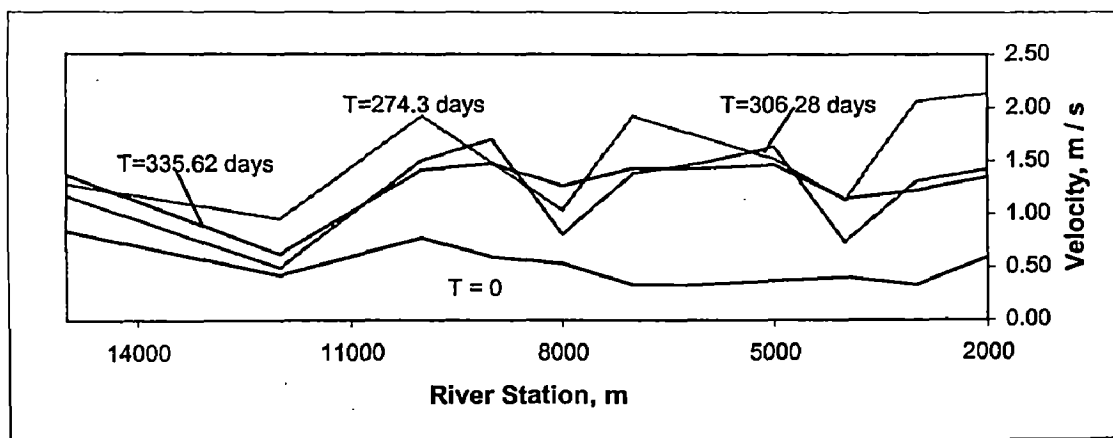


Fig. 5.24 Time and Spatial Variation of Velocity

5.8.4. Change in Sediment Load and Hydraulic Parameters

The flood and sediment routing in erodible channels is related to streambed variations which may be illustrated by the time and spatial variations of the velocity and, sediment load (see Fig. 5.24 and 5.25).

The spatial variations in velocity and sediment load at the first flood are associated with the uneven river channel configuration. At depressions and borrow pits, velocity and sediment load are substantially lower, and just after the bends the velocity decreased and sediment load also substantially reduce because of sediment deposition in the downstream reach. Low velocities at station 12.0, 8.0 and 4.0 Km. (Fig 5.24 and 5.25) are due to high flow resistance at these stations because resistance is increased on sand dunes.

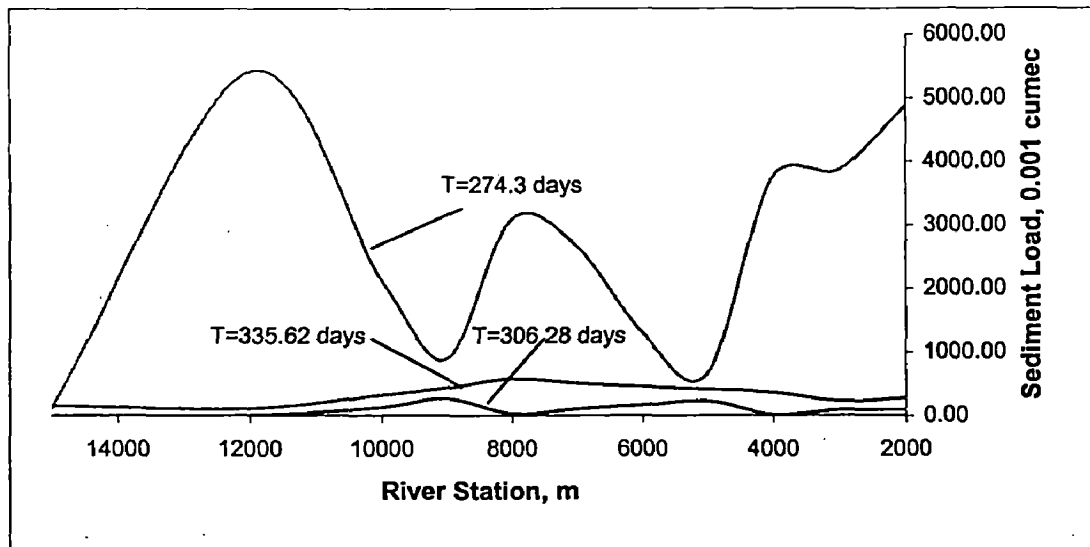


Fig. 5.25 Time and Spatial Variation of Sediment Load

5.8.5. Changes in Sediment Size and Hydraulic Sorting

Variation of sediment size due to hydraulic sorting as simulated, are pronounced in this river reach. Armoring effects can be recognized (see Fig 5.26), including coarsening of the material during scour and reduction in size during deposition. Channel widening through bank erosion brings finer bank materials into the channel and hence contributes to a reduction in sediment size.

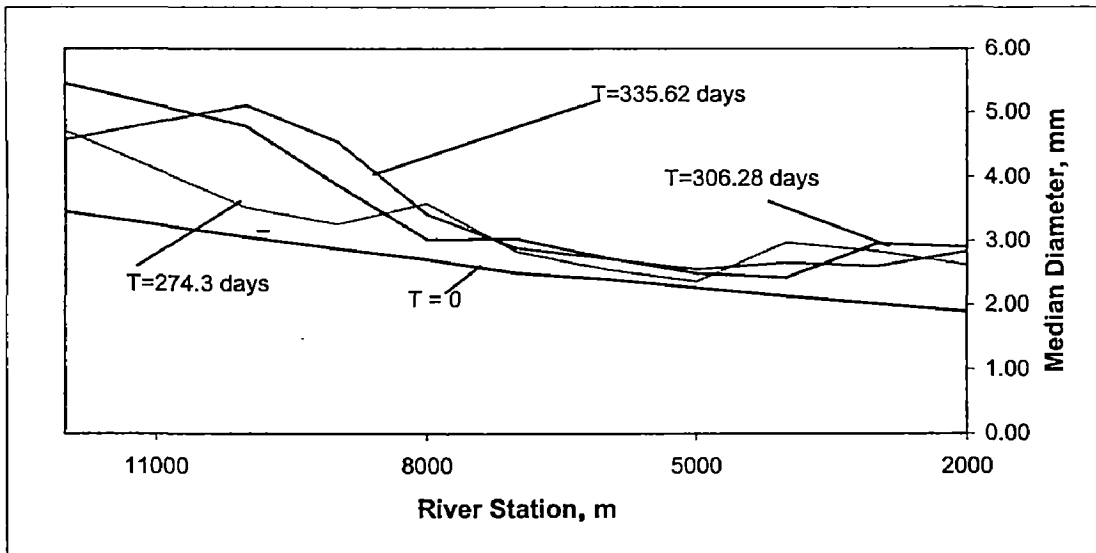


Fig. 5.26 Time and Spatial Variation of Median Size Diameter d_{50}

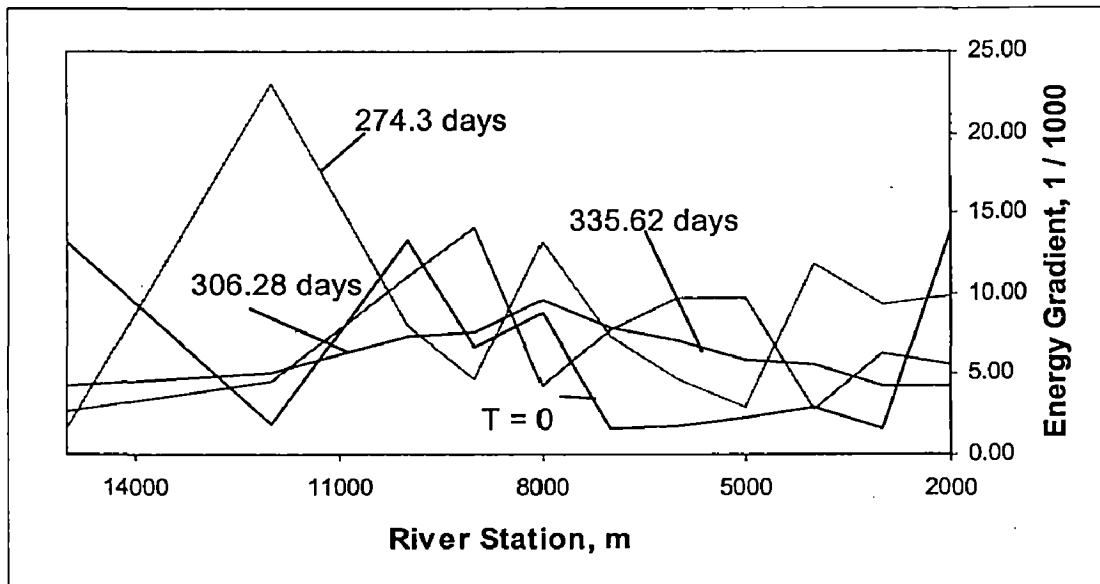


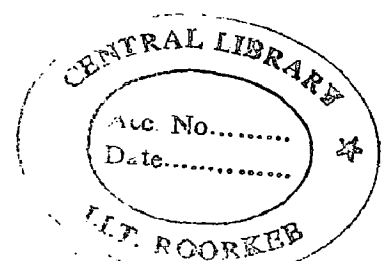
Fig. 5.27 Time and Spatial Variations of Energy Gradient

5.8.6. Streambed Variation in Relation to Power Expenditure

As stated in section 5.6.3 changes in river-channel configuration are accompanied by changes in flow resistance and hence the rate of energy (or power) expenditure. Simulated streambed variations (or river channel changes) are associated with the gradual reduction of the spatial variation of energy gradient along the channel subject to the physical constraint of rigid banks. There is a marked spatial variation of energy gradient during high flows due to sand dune formation. Subsequently, spatial variation of energy gradient becomes smoother (see Fig. 5.27). Initially energy gradient is highly undulating, because of uneven geometric gradient of the channel-bed and more energy is consumed at high flow resistance zones. The adjustment in river channel configuration is closely related to the change in power expenditure which can be illustrated by the sequential changes in cross-sectional profile at stations 12.0, 10.0, 8.0 and 4.0 Km.(Fig 5.15, 5.16 and 5.18). Higher value of power expenditure at any space and time indicate that there is degradation, and low energy expenditure indicates the aggradation.

5.8.7. Water Surface Profiles

Water Surface profiles simulated by FLUVIAL-12 different time steps are comparable to each other (see Fig. 5.28) in this river also, and are smooth. The model predicts subcritical flow in the entire study reach (see table 5.4).



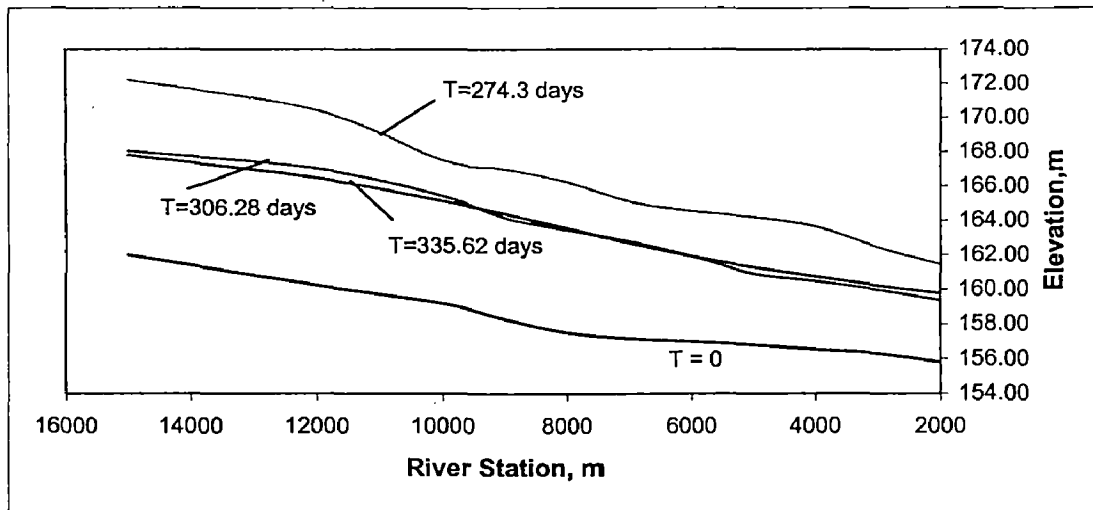


Fig. 5.28 Time and Spatial Variation of Water Surface Profile

Table 5.4 Time and Spatial Variations of Froude Number

River Station (m)	Froude Number			
	T=0	T = 274.3 days	T= 306.28 days	T = 335.62 days
2000	0.36	0.34	0.27	0.24
3000	0.16	0.33	0.28	0.24
4000	0.20	0.14	0.11	0.20
5000	0.18	0.21	0.33	0.27
6000	0.16	0.26	0.33	0.29
7000	0.16	0.30	0.30	0.30
8000	0.30	0.13	0.13	0.26
9000	0.27	0.21	0.37	0.28
10000	0.36	0.31	0.34	0.29
12000	0.16	0.11	0.07	0.08
15000	0.35	0.17	0.20	0.24

5.8.8. Flow Resistance

A prominent change in flow resistance can be illustrated from the result simulated by the model in Fig. 5.29. High flow resistance is observed at the sections that are degraded namely, 12.0, 8.0 and 4.0 Km.

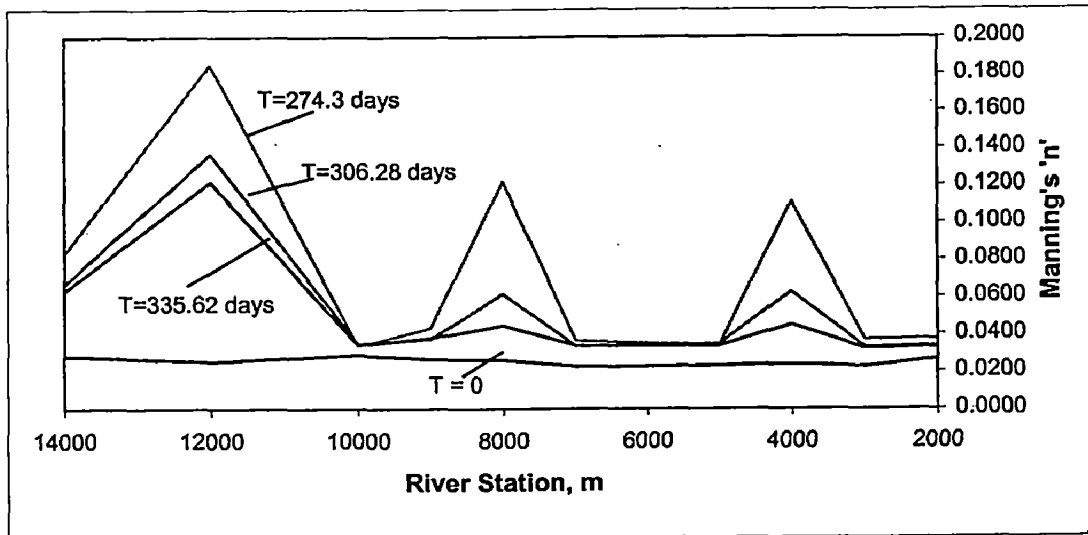


Fig. 5.29 Time and Spatial Variation of Manning's 'n'

Very high flow resistance at these stations during high floods may be due higher erosion of channel geometry and over bank flow and dune formation at the time.

5.9. Simulation of General and Local Scours

5.9.1. General

In the chapter three and four, the theoretical background of general and local scours were discussed, respectively, and in the chapter seven the models that are employed in the simulation studies of these scour quantities, (HEC-RAS and WSPRO) were discussed. In this chapter results of simulation studies are presented on general and local scours employing HEC-RAS and WSPRO. A hypothetical bridge is considered to exist across the River Maan at station 9.385 Km. as mentioned in section 5.5.2.

5.9.2. Data Required

The following data are required to simulate general and local scours:

1. Topographic survey data of the bridge site and river reach
2. Hydrologic data of the stream (inflow hydrograph, stage discharge curve, 100 or 500 years flood discharge etc.)
3. Geo-technical study data of the foundation
4. Geomorphology of the river (flow pattern, tendency of river meander, sediment transport characteristics, d_{50} and d_{90} , long-term aggradation and degradation study data etc.)
5. Hydraulic design data (Manning's coefficient of roughness, expansion and contraction coefficients, angle of attack of flow to the abutments, and other pier and abutment coefficients)
6. Geometric data of the bridge
7. Debris and ice formation records if any.

For scour calculation purpose 500 years floods or 1.7 times 100 years flood is recommended by HEC-18. However, it is common practice to use 1.2 to 1.3 times 100 years flood in scour depth computation. But in this study 550 cumec has been considered as catastrophic discharge (Fig.5.1). Sediment data given in the table 5.5.2 has been used. The physical conditions are described in the section 5.5.2 earlier and the bridge site is in the straight reach of the river. All the geometric data has been assumed as shown in computer software interface. For the determination of different coefficients, Tables 2.1 to 2.7 has been used.

5.9.3. Scour Depth Simulation Using HEC-RAS

5.9.3.1. Geometric Data Editor

The geometric data are entered through geometric data editor which look like below:

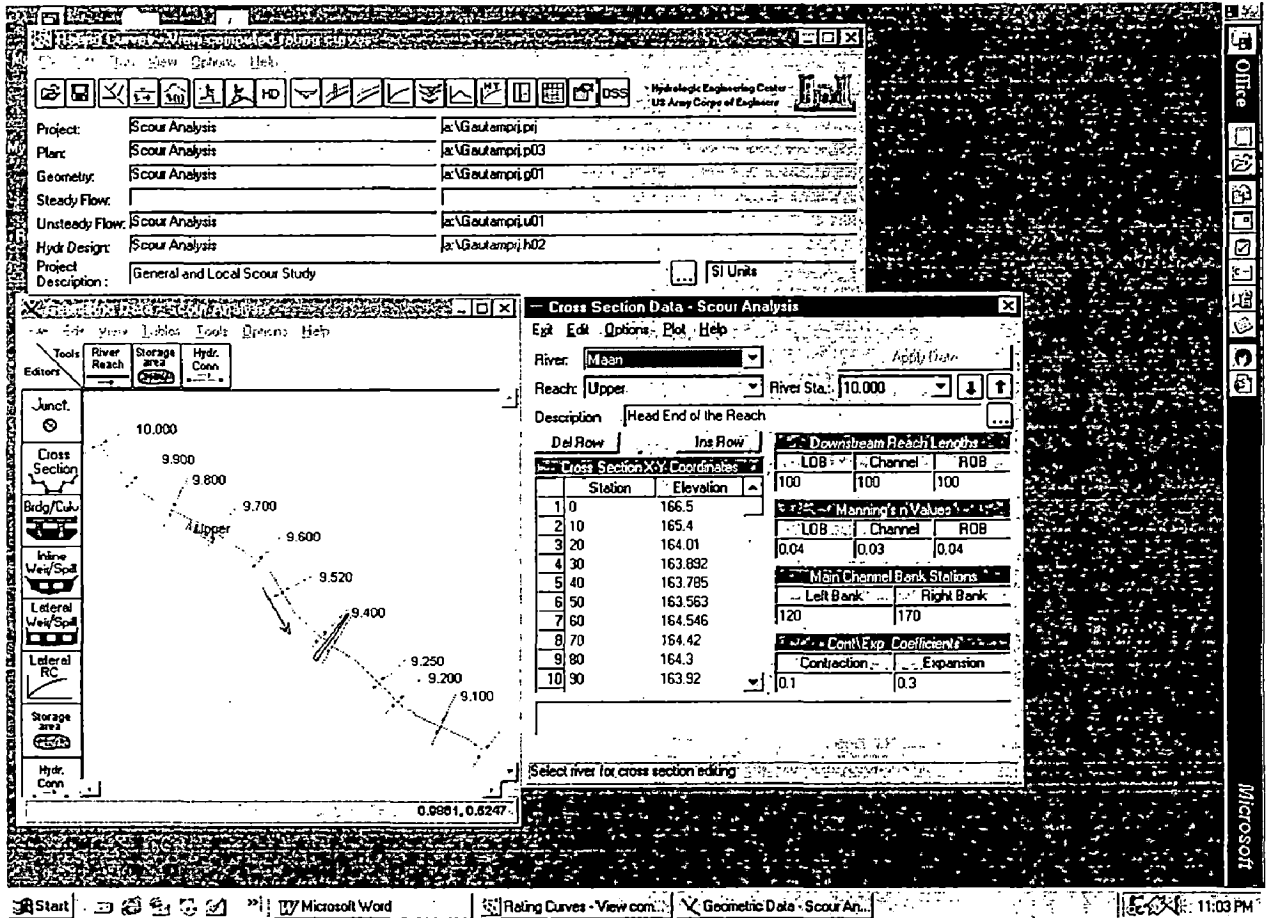


Fig. 5.30 River Schematic Drawn in Geometric Data Editor

1. All the geometric data in the form of (x,y) co-ordinates are entered in the vertical columns from upstream end of the river reach to the downstream end of the reach for each river station taking left bank of section as zero facing downstream (Fig.5.30).
2. Distance between cosecutive left over bank (LOB), main channel and right over bank (ROB) are entered.
3. Manning's n value for LOB, Main channel and ROB are entered.
4. Expansion and contraction coefficients are entered.
5. Data are applied and cross-section is automatically, drawn by the model. Process is repeated for all the cross-sections.

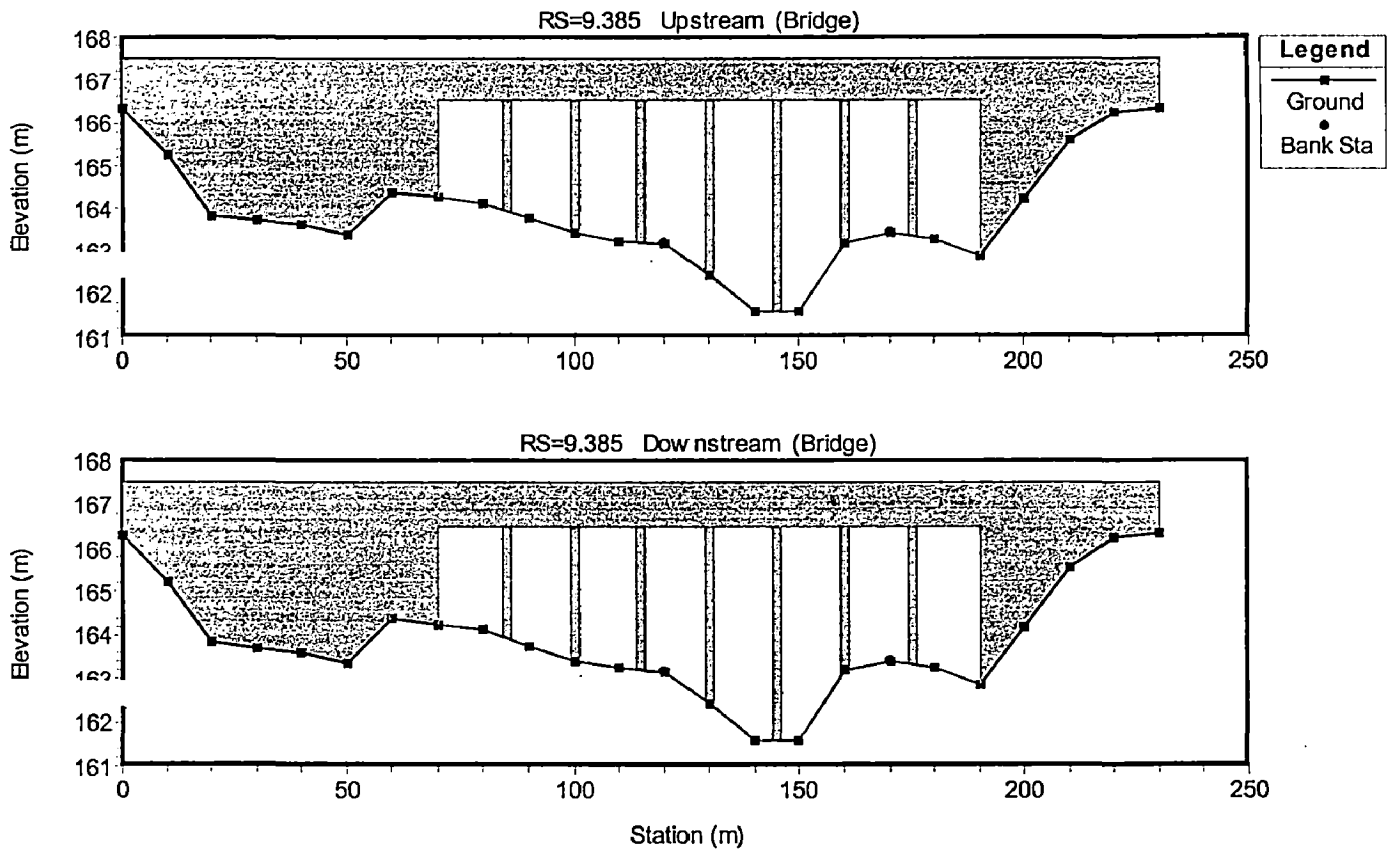


Fig. 5.31 Upstream and Downstream Cross-section of the Bridge

5.9.3.2. Entering Bridge Data

Bridge data viz., pier and abutment geometry, bridge deck low chord and high chord levels, selection of bridge modeling approach e.g., low flow, pressure flow or FHWA WSPRO method, discharge coefficient for a given flow condition are selected and entered through Bridge and Culvert Editor window. After entering the bridge geometric data the software automatically plots the cross-section profile through bridge from the upstream and downstream unconstricted cross-sections, which have already been entered through geometric cross-section data editor.

5.9.3.3. Unsteady Flow Data

Unsteady flow data, viz., inflow hydrograph, upstream and downstream boundary conditions, initial flow conditions, flow change locations, known water surface levels if any and stage discharge curve, simulation time steps are entered through Unsteady Flow Data Editor as shown below (Fig. 5.32). In this study upstream boundary condition is inflow hydrograph and downstream boundary approximate friction slope (or geometric slope of the channel). Inflow hydrograph plotted by the model is shown below in Fig. 5.32.

5.9.3.4. Unsteady Flow Analysis

Unsteady flow is analyzed through unsteady flow analysis editor window. In this window, stage and flow output locations, flow distribution locations, flow roughness factors, seasonal roughness factors, calculation option and tolerances and method of computations are selected as desired by user. After selecting the desired values the variables unsteady flow analysis is accomplished.

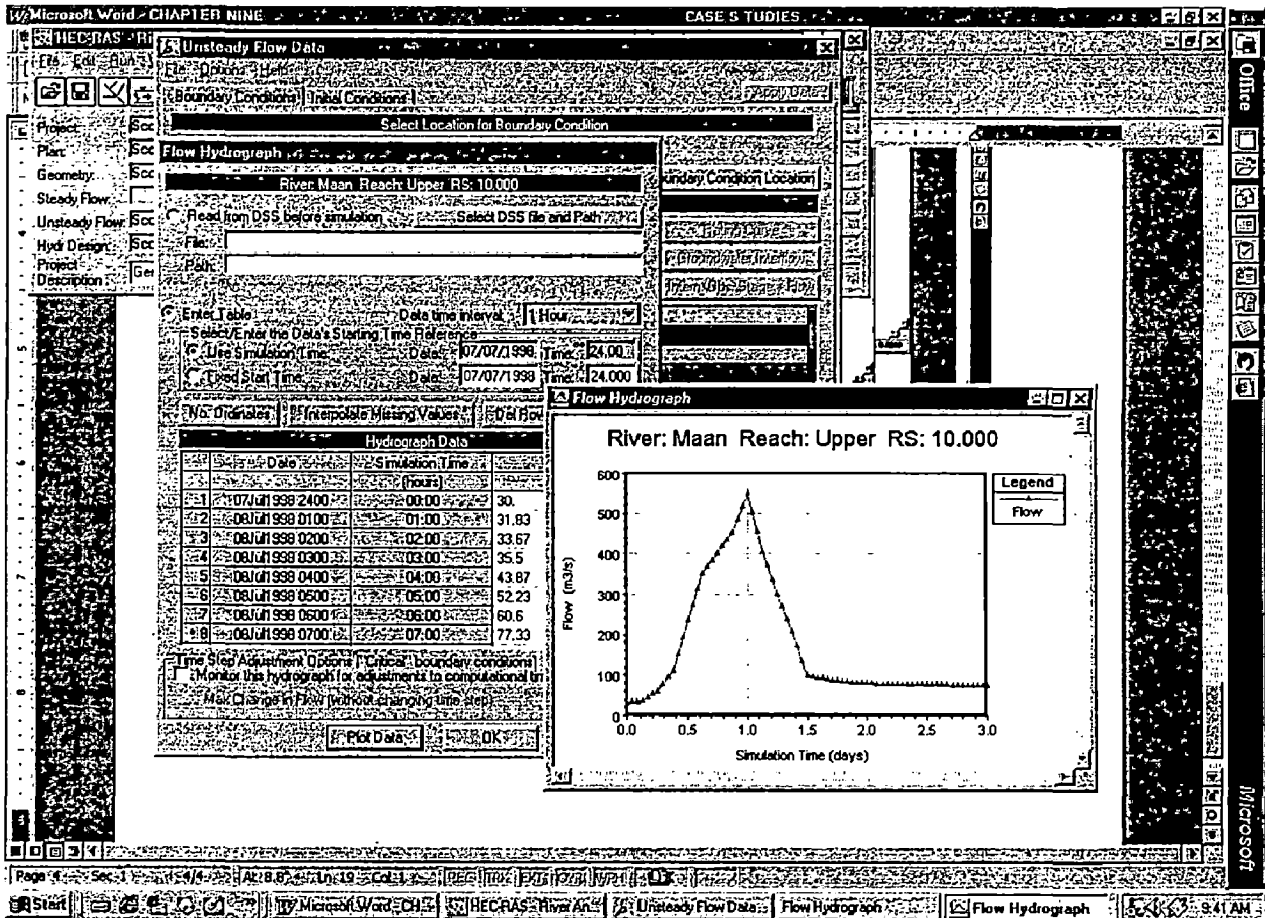


Fig. 5.32 Unsteady Flow Data Editor and Flood Hydrograph Plotted by HEC-RAS

5.9.4. Hydraulic Design Functions

To compute general (contraction) scour we have to enter only median sediment diameter d_{50} to impose sediment transport conditions (see equation (2.1) and Tables 2.1 and 2.2), d_{50} is selected from the simulation results obtained in table 5.1 or field data, here it was taken to be 1.15 mm. On selection of default option, system selects maximum scour depth under live-bed or clear water conditions.

For the computation of local scour around pier either CSU equation (2.17) under clear water condition, or Froehlich's equation (2.34), under live-bed condition is used. To select k_1 value in equation (2.17) we have to supply pier nose shape (rounded here), k_2 factor for angle of attack it was chosen to be 1. The coefficient k_4 for armoring is calculated from equation (2.24), where d_{90} was assumed to be 3.1 mm and k_3 is selected by the system from the sediment data or user can impose from known sand dune height

condition in the field. The mathematical model HEC-RAS computes abutment scour, using Froehlich's equation (2.34) under live-bed condition or HIRE equation (2.35) under clear water condition. To determine k_1 abutment was assumed to be vertical with no wing-walls, and for k_2 angle of attack was assumed to be 90° . After entering the above data, scour depth is computed as shown in Fig.5.34.

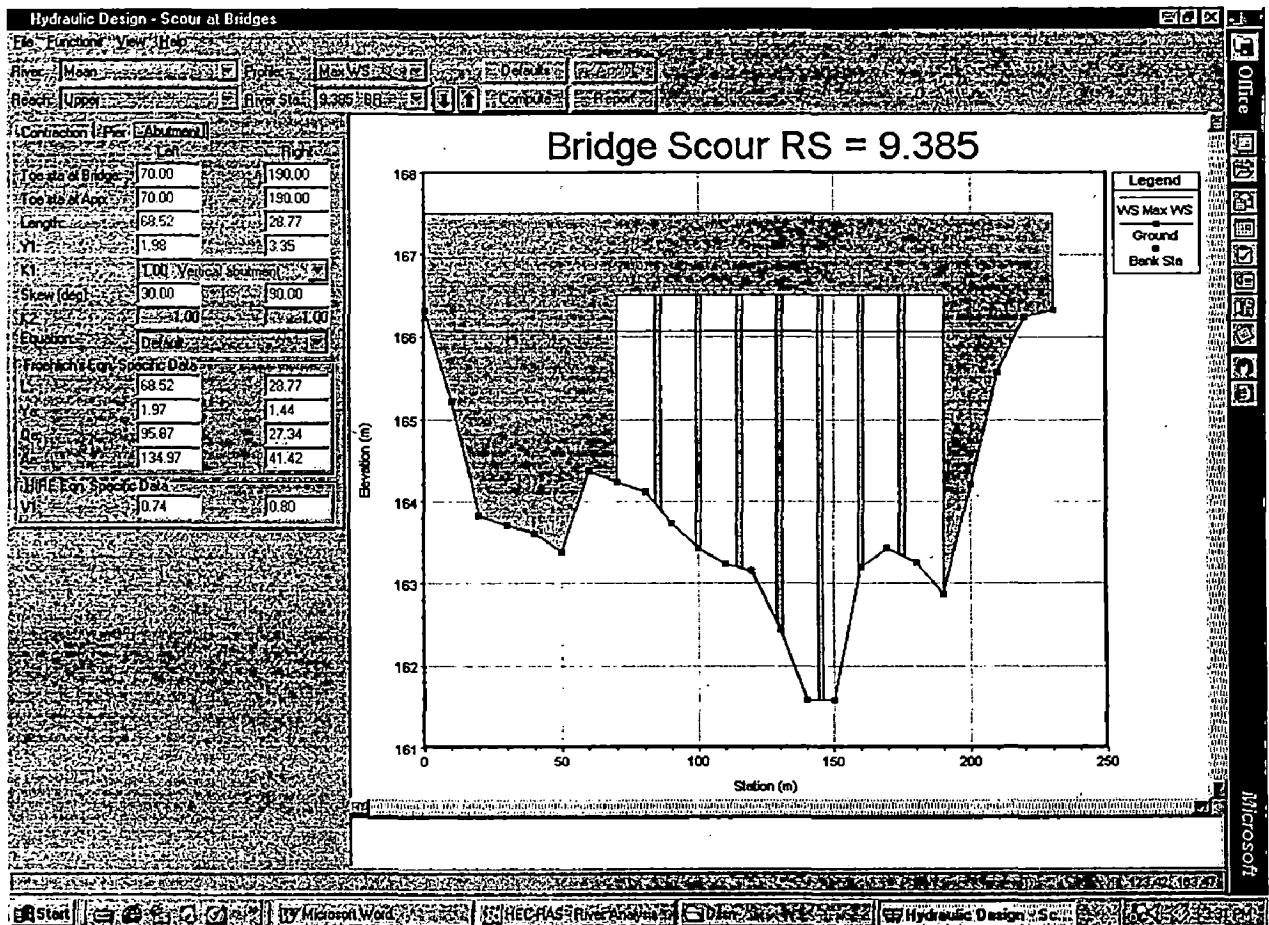


Fig. 5.33 Hydraulic Design Function

Table 5.5 Time and Discharge Variation of Contraction Scour

Time (hour)	Discharge (cumec)	Contraction Scour Depth (m)		
		Left	Channel	Right
0.00	30.00	0.00	0.02	0.00
3.00	42.13	0.00	0.04	0.00
6.00	81.09	0.00	0.17	0.00
9.00	107.77	0.00	0.32	0.00
12.00	300.00	0.66	0.75	0.68
15.00	346.62	0.45	0.96	0.75
18.00	399.00	0.63	1.09	0.41
21.00	546.00	0.39	1.42	0.42
24.00	550.00	0.39	1.42	0.42

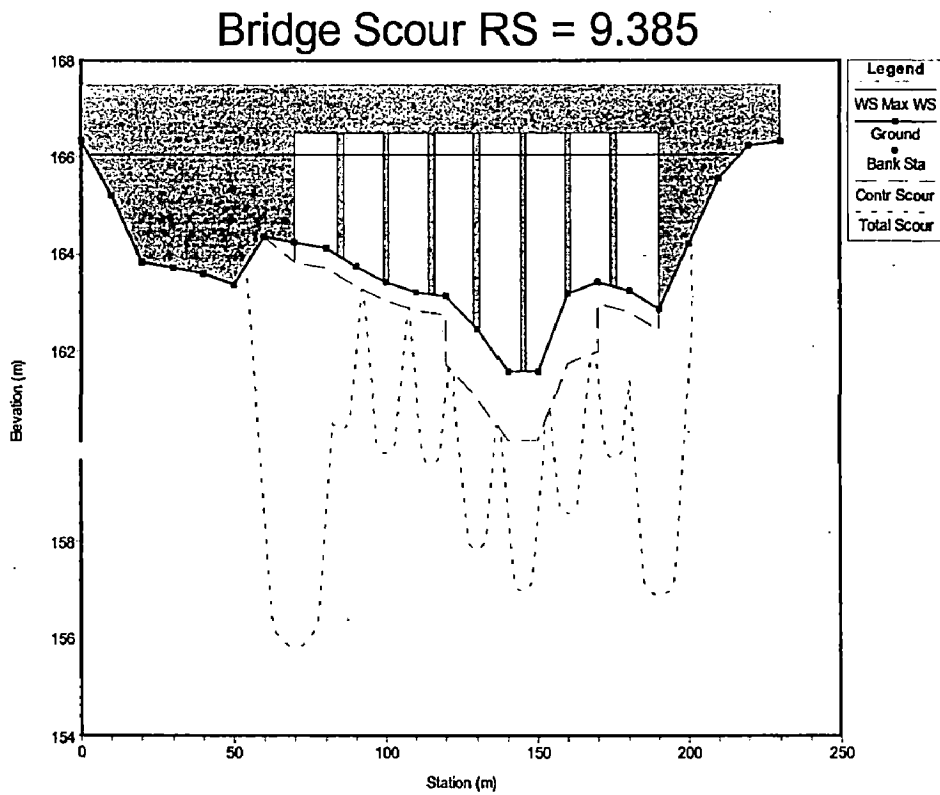


Fig. 5.34 Plot of General and Local Scour Depth

Table 5.6 Time and Discharge Variation of Abutment Scour Depth

Time (hour)	Discharge (cumec)	Local Scour Depth (m)		Total Abutment Scour (m)	
		Left	Right	Left	Right
0.00	30.00	0.77	0.77	0.77	0.77
3.00	42.13	0.94	0.94	0.94	0.94
6.00	81.09	1.39	1.39	1.39	1.39
9.00	107.77	2.10	2.10	2.10	2.10
12.00	300.00	2.74	3.48	3.40	4.16
15.00	346.62	4.89	4.89	5.34	5.64
18.00	399.00	5.78	4.46	6.41	4.87
21.00	546.00	7.99	7.99	8.38	5.02
24.00	550.00	7.99	7.99	8.38	5.96

Table 5.7 Time and Discharge Variation of Pier Scour Depth

Time (hour)	Discharge (cumec)	Pier Scour Depth (m)			Total Pier Scour (m)		
		Left	Channel	Right	Left	Channel	Right
0.00	30.00	2.01	2.01	2.01	2.01	2.03	2.01
3.00	42.13	2.05	2.05	2.05	2.05	2.09	2.05
6.00	81.09	2.26	2.26	2.26	2.26	2.43	2.26
9.00	107.77	2.80	2.80	2.80	3.46	3.55	2.80
12.00	300.00	2.76	2.76	2.76	3.42	3.51	3.44
15.00	346.62	2.89	2.89	2.89	3.34	3.85	3.64
18.00	399.00	2.90	2.90	2.90	3.53	3.99	3.31
21.00	546.00	3.15	3.15	3.15	3.54	4.57	3.57
24.00	550.00	3.15	3.15	3.15	3.54	4.57	3.57

5.9.5. Scour Depth under Steady Flow Conditions

General and local scour depths under steady flow condition were simulated using HEC-RAS at peak flood. The scour depths were simulated under subcritical, super critical and mixed flow conditions by computing conveyance in HEC-2 mode. The results were different from those of steady flow simulation. The results are given below.

Table 5.8 Scour Depth under Steady Flow Conditions

Contraction Scour, (m)			Pier Scour, (m)	Abutment Scour, (m)	
Left OB	Channel	Right OB	All	Left OB	Right OB
1.17	1.70	0.40	3.48	8.60	5.48

5.9.6. FHWA WSPRO Method

This is a computer program to compute water surface profiles and local and general scour. This method is also based on the methodology given in HEC-18, Evaluating Scour at Bridges, Richardson and Davis, (1995) like HEC-RAS. Data input system is very similar to HEC-2 with the difference that geometric data are entered in form (x, y) co-ordinate freely. This program is based on MS-DOS command. WSPRO method uses for class A flow condition, i.e., the flow through the bridge is always subcritical. As mentioned earlier WSPRO is a steady flow model. The method of computation of conveyance different, therefore, simulated results are different than those of HEC-RAS. Simulated scour depths for the peak discharge 550 cumec is given below (see Table 5.8 and Fig.5.35).

Table 5.9 Scour Depths Simulated by WSPRO

Scour Depth, (m)						
Abutment		Pier			Contraction	
Left OB	Right OB	Left OB	Channel	Right OB	Clear-water	Live-bed
3.01	5.89	5.75	5.75	7.71	3.63	0.91

SUMMARY AND CONCLUSIONS

6.1. Water Surface Profiles

Estimation of correct water surface profile always has been a challenge for hydraulic engineers for flood plain encroachment assessment, flood forecasting, fixing of bridge deck elevations, estimation of embankment height etc. Water surface profiles simulated by the models used, are shown in Fig.6.1. The profile simulated by the FLUVIAL-12 are quite smooth, whereas water surface profiles simulated by the HEC-RAS and WSPRO have shown undulations. This reflects that FLUVIAL-12 estimates, water surface profile more accurately.

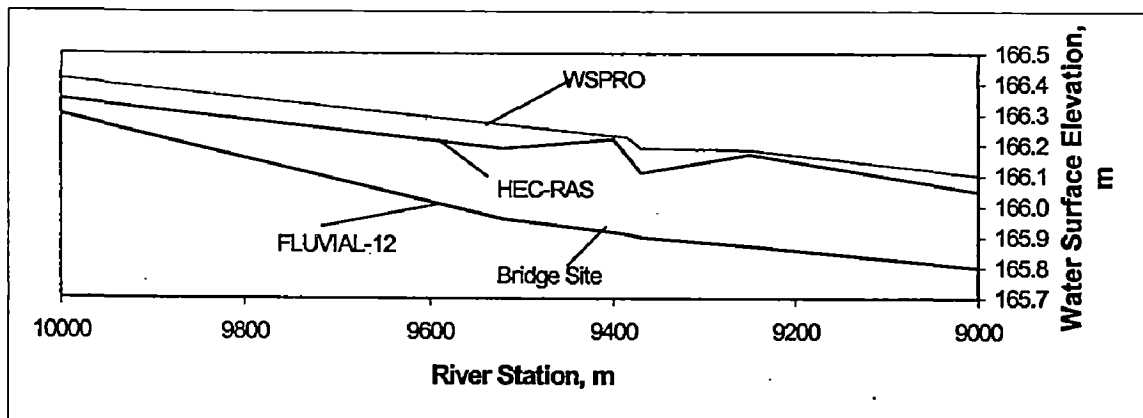


Fig. 6.1 Spatial Variations of Water Surface Profiles of Maan River at Peak Flood

6.2. Total Sediment Transport Rate

Total sediment transport rate of a river is related to erodibility of channel boundaries and sediment load from its watershed along with other hydraulic parameters and sediment characteristics. The sediment transport rate at the sections where boundaries are mobile are higher than the other sections. The maximum sediment transport rate in Maan River of 1.534 cubic meter per second was simulated by the model at the station 11.0 Km.. In Babai River, 5.416, 4.878, 3.749 and 3.094 cubic meter per second were simulated at stations 12.0, 2.0, 4.0 and 8.0, respectively.

6.3. Energy Gradient and Power Expenditure

The quantity (γQS_f) represents power expenditure by the flow per unit length of channel. Because Q is spatially constant in the study reach, therefore, variation of S_f represents energy expenditure by the flow. From the comparison of energy gradient simulated by the above models (see Table 6.1), HEC-RAS and WSPRO simulate almost uniform energy expenditure in the Maan River. The power expenditure rate can not be uniform in a river like Maan which is highly distorted. The channel boundaries are potentially changeable therefore, flow resistance varies with time and space. High power expenditure in high floods at stations 10.0 and 9.55 is because of high flow resistance due to sand-dune formation in the channel bed.

Table 6.1 Spatial Variation of Energy Gradient in Maan River at Peak Floods

River Station (m)	Maximum Energy Gradient S_f in 1/10000			
	HEC-RAS, Unsteady	HEC-RAS, Steady	WSPRO	FLUVIAL-12
10000	3.300	3.340	3.000	23.900
9550	3.050	2.370	3.000	11.500
9400	3.040	2.240	3.000	4.100
9385	3.230	2.210	3.000	3.000
9370	3.420	2.330	3.000	2.800
9250	3.410	2.710	3.000	2.800
9000	3.320	3.110	3.000	2.900

6.4. Variation in Streambed Profile

The initial stream profile at thalweg was smooth, subsequently when discharge increases the river tries to readjust its boundaries to maintain its cargo of sediment according to the capacity the flow. Consequently, The streambed profile gets changed with time and space (Fig. 6.2).

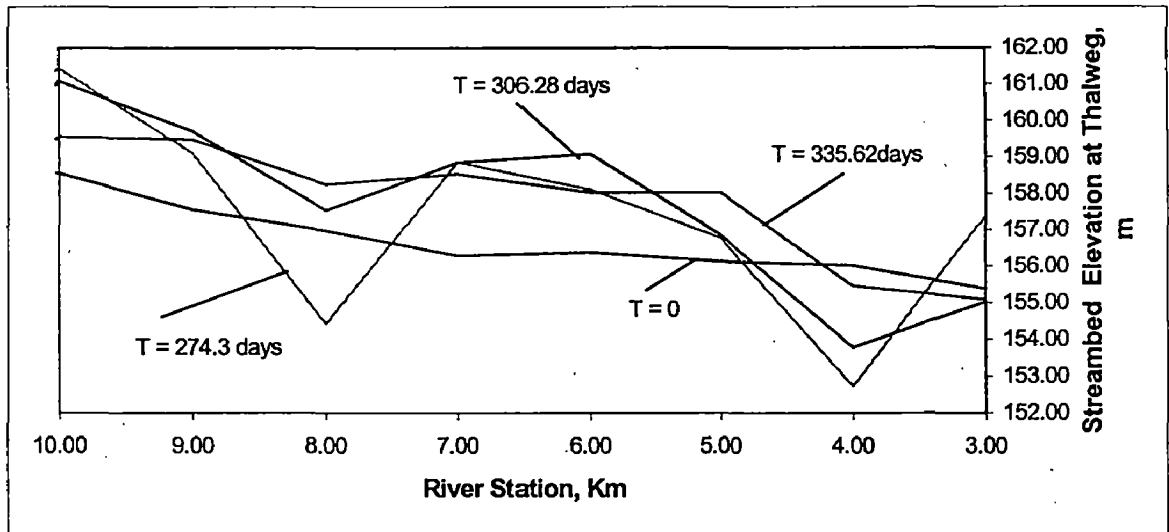


Fig. 6.2 Time and Spatial Variation of Streambed of Babai River Simulated by FLUVIAL-12

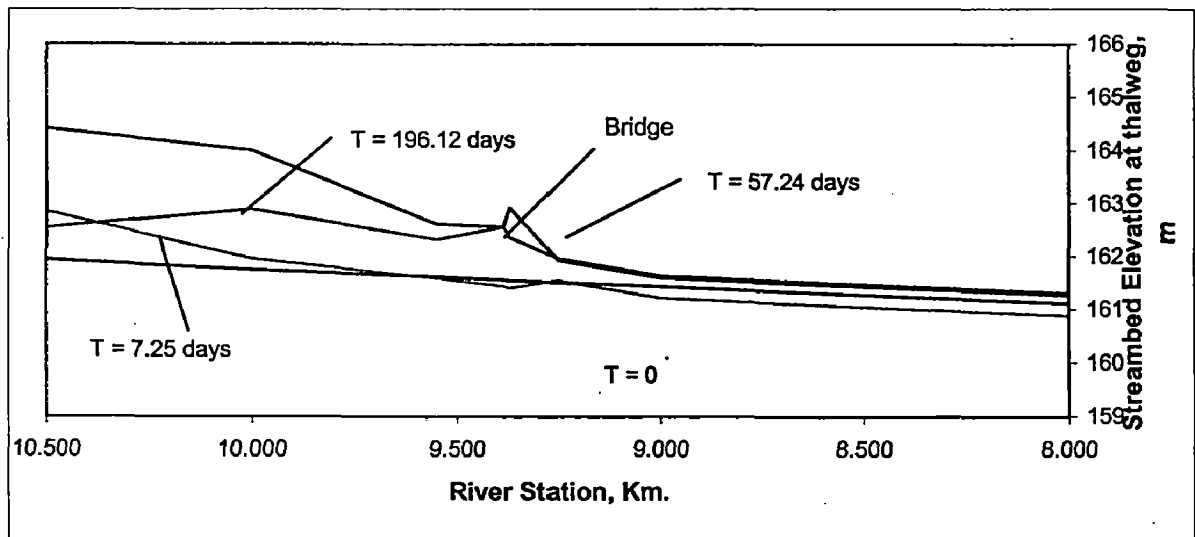


Fig. 6.3 Time and Spatial Variation of Streambed of Maan River Simulated by FLUVIAL-12

6.5. Scour Depths

To estimate general and local scour values, a hypothetical bridge was assumed to exist at station 9.385 Km. of Maan River and all the bridge geometric data were assumed. Estimation of bridge scour depths requires four cross-sections. In this study, upstream uncontracted, bridge upstream (BU), bridge downstream (BD) and downstream expanded sections, were taken at stations 9.520 (one bridge distance from the upstream end of the bridge), 9.400, 9.370 and 9.250 Km.. Median sediment diameter $d_{50} = 1.15$ mm, $d_{90} = 3.1$ mm, Bridge pier width exposed to the flow, $a = 2.5$ m, bridge opening, $L_b = 120$ m, eight equal spans of 15m each and angle of attack to the abutment by the flow $= 90^\circ$ were assumed in design data. With these design data general scour and local scours at bridge pier and abutment were simulated using the HEC-RAS (steady and unsteady flow) and WSPRO and the results are given below.

Table 6.2 Maximum Contraction Scour Depths

Maximum Contraction Scour, (m)						Mathematical Model Used
Live-bed			Clear-water			
Left OB	Channel	Right OB	Left OB	Channel	Right OB	
0.91	0.91	0.91	3.63	3.63	3.63	WSPRO
1.17	1.70	0.40	1.05	3.71	1.44	HEC-RAS Steady
0.63	1.42	0.75	1.19	4.27	1.60	HEC-RAS Unsteady

Table 6.3 Maximum Abutment Scour Depths

Maximum Abutment Scour, (m)					
HEC-RAS Steady Flow		HEC-RAS Unsteady Flow		WSPRO	
Left OB	Right OB	Left OB	Right OB	Left OB	Right OB
8.94	5.52	8.74	5.54	5.89	3.01

Table 6.4 Maximum Pier Scour Depths

Maximum Pier Scour, (m)		
HEC-RAS Unsteady Flow	HEC-RAS Steady Flow	WSPRO
3.15	3.53	7.71

The model HEC-RAS simulated abutment scour depth as maximum, whereas the model WSPRO simulated pier scour depth as maximum, this difference may be because of the fact that the WSPRO and HEC-RAS use different methods in scour depth computation.

6.6. Conclusions

The mathematical model FLUVIAL-12 is an erodible-boundary model, it has been employed to simulate flood and sediment routing and associated river channel changes in many rivers in USA, Taiwan, and Malasiya [16]. It has been reported that simulated results using this model are supported by field observation and measurements [27]. In this study this model was employed to simulate streambed variation of Maan and Babai Rivers of Western Nepal for the highest floods that were experienced and recorded so far in these rivers into the study reach. These rivers are highly disturbed due to sand and gravel mining activities in different reach of the rivers. In general observation, the simulated results are very close to the field conditions though they could not be verified quantitatively, due to lack of measured data.

The FLUVIAL-12 model has simulated inter-related changes in streambed profile, channel width and bed topography induced by the channel curvature. From the view of streambed variations, the following conclusion can be drawn.

- (1). The model FUVIAL-12 is capable to simulate all the components of streambed variations, effects of curvature and hydraulic parameters more accurately. Therefore, it can be used for modeling mobile boundary channels.

- (2). The models HEC-RAS and WSPRO are can be used for simulating general and local scour depths around bridge pier and abutments, losses through hydraulic structures, conveyance, energy gradient, velocity and water surface profile computation. However, the HEC-RAS seems to be better because it has many options. The HEC-RAS can be used for modeling relatively rigid boundary streams.
- (3). Water surface profiles simulated by the FLUVIAL-12 are quite smooth even near bridges also. Whereas water surface profiles simulated by the HEC-RAS and WSPRO has shown undulation near bridges. Therefore, flood level computations by using FLUVIAL-12 more seems more accurate.
- (4). The HEC-RAS and FUVIAL-12 are unsteady flow simulation models. Whereas, the WSPRO is steady flow simulation model. The HEC-RAS has option of steady flow simulation also.

REFERENCES

1. Garde, R. J. and Ranga Raju, K. G. Mechanics of Sediment Transport and Alluvial Stream Problems. Third Edition, 2000 New Age International (P) Limited Publishers, New Delhi.
2. Hoffmans, G. J. C. M. and Verheij, H. J. (1977), Delft Hydraulics, Delft. 'Scour Manual', A. A. Balkema / Rotterdam / Bookfield, Netherlands.
3. Garde, R. J. et al. (1961). Study of Scour Around Spur-Dikes. JHD, Proc. ASCE Nov. (1961).
4. Kothyari, U. C. and Ranga Raju, K. G. (1992). Temporal Variation of Scour Around Bridge Piers. JHD, ASCE, August, 1992.
5. Jain, S. C. and Fisher, E. E. (1980). Scour Around Bridge Piers at High Velocities. JHD, ASCE,
6. Melville, B. W. (1998). Piers and Abutment Scour. JHD, ASCE, July, 1998.
7. Ettema, R. and Raudkivi, A. J. (1980). School of Engineering Report No. 218. Deptt. of Civil Engg. Univ. of Auckland, Newzealand, Feb. 1980.
8. Chang, H. H. Fluvial Process in River Engineering, John Wiley and Sons, New York, (1988), Ch.5 and 14.
9. Shen H.W., V. R. Schnelder and S. S. Karaki, Local Scour Around Bridge Piers. JHD, Proc. ASCE, Nov. 1969.
10. Laursen, E. M. and A. Toch, Scour Around Bridge Piers and Abutments. Iowa, Highway Research Bulletin No., May 1956.
11. Karaki, S. S., Hydraulic Model Studies of Spur Dikes for Highway Bridge Openings Report NO. CER59- SSK36, Colorado State University, 1959
12. Ackers, P. and White W.R. Sediment Transport New Approach and Analysis. JHD, Proc. ASCE Nov. 1973.
13. Chow, V. T. Open Channel Hydraulics, International Student Edition, 1959, McGRAW-Hill Book Company, NY, USA.
14. Chow, V. T., Maidment, D. R. and Mays L. W. Applied Hydrology, 1988. McGraw-Hill Book Company, New York.

15. Cunge, J. A., Holly, F. M. Jr. and Verwey, A. Practical Aspects of Computational River Hydraulics, Pitman Advanced Publishing Program, London 1980.
16. Chang, H. H. A Generalized Computer Program, "FLUVIAL12" , Mathematical Model for Erodible Channel , User's Manual 1998. San Diego Univ. California, USA.
17. Guidelines for Calibration and Application of Computer Program HEC-6. Training Document No. 19, Feb. 1981, US Corps of Army Engineers, HEC.
18. Arneson, L. A., Shearman, J. O. and Jones, J. S. Evaluating Scour at Bridge (1998), Using WSPRO, FHWA, US Deptt. of Transportation, USA.
19. HEC-RAS River Analysis System, User's Manual (1986). US Army Corps of Engineers, HEC, Davis, CA.
20. Hydrologic Engineering Center Circular No. 18. Publication No. FHWA NHI 01- 001, May, 2001, US Department of Transportation, Federal Highway Authority.
21. HEC-2 Manual, 1992, US Army Corps of Engineers.
22. Laursen Emmet M., "Pier and Abutment Scour: Integrated Approach", JHD, ASCE, July, 1998.
23. Chang, H. H., Modeling of River Channel Changes, JHD, ASCE, Vol. 110, No.2, Feb., 1984.
24. MIKE11 Comprehensive 1-D Dynamic Flow Model. Danish Hydraulic Institute (DHI), Denmark.
25. Barkau, R.L, 1993, "UNET One-dimensional Unsteady Flow Through a Full Open Channels". Report CPD-66 US Army Corps of Engineers (USACE), Hydrologic Engineering Center (HEC), Davis, CA.
26. J. G., Arcement, Jr. and V. R. Schneider, (USGS), 1997, "Guide for Selecting Manning's Roughness Coefficient for Natural Channels and Flood Plains", USGS Water Supply Paper 2339.
27. Chang, H. H., Mathematical model for Erodible Channels, JHD, ASCE, Vol. 108, No.HY5, May, 1982.

APPENDIX -A

```

1*****
*   FLUVIAL-12   SIMULATION OF RIVER HYDRAULICS,   *
*   SEDIMENT TRANSPORT AND RIVER CHANNEL CHANGES *
*   FOR INSTRUCTION USE ONLY                       *
*****
  
```

07 November, 2002

THIS PROGRAM IS DEVELOPED AND FURNISHED BY HOWARD H. CHANG AND IS ACCEPTED AND USED BY THE RECIPIENT

UPON THE EXPRESS UNDERSTANDING THAT THE DEVELOPER MAKES NO WARRANTIES, EXPRESS OR IMPLIED, CONCERNING

THE ACCURACY, COMPLETENESS, RELIABILITY, USABILITY, OR SUITABILITY FOR ANY PARTICULAR PURPOSE OF THE

INFORMATION AND DATA CONTAINED IN THIS PROGRAM OR FURNISHED IN CONNECTION THEREWITH, AND THE DEVELOPER

SHALL BE UNDER NO LIABILITY WHATSOEVER TO ANY PERSON BY REASON OF ANY USE MADE THEREOF.

T1	ANALYSIS OF STREAM BED VARIATIONS						
T2	STUDY OF SIMULATION MODEL						
T3	PEAK Q = 550 CUMEC						
G1	0.00	8736.00	604800.00	3.00	0.50	1.00	0.04
168.00	4704.00	13.00					
G2	11.00	53.00	0.00	0.00	0.00	0.00	0.00
0.00	0.00	0.00					
G2	30.00	0.00	550.00	168.00	150.00	336.00	205.00
504.00	75.60	672.00					
G2	75.90	840.00	102.00	1008.00	147.80	1176.00	100.50
1344.00	225.60	1512.00					
G2	105.60	1680.00	88.85	1848.00	68.50	2016.00	63.50
2184.00	55.30	2352.00					
G2	52.30	2520.00	45.10	2688.00	39.65	2856.00	40.60
3024.00	41.20	3192.00					
G2	40.10	3360.00	41.70	3548.00	39.60	3696.00	38.50
3864.00	37.99	4032.00					
G2	37.40	4200.00	37.12	4368.00	36.24	4536.00	31.46
4704.00	28.60	4872.00					
G2	27.50	5040.00	25.63	5208.00	24.75	5376.00	22.94
5544.00	20.73	5712.00					
G2	18.63	5880.00	15.46	6048.00	14.32	6216.00	13.75
6384.00	13.20	6552.00					
G2	12.32	6720.00	11.64	6888.00	11.21	7056.00	10.34
7224.00	10.11	7392.00					
G2	9.23	7560.00	8.94	7728.00	8.25	7896.00	8.12
8084.00	10.98	8232.00					
G2	12.63	8400.00	15.23	8568.00	27.50	8736.00	
G3	0.00	1.00	0.00	25.00	1.00	0.00	0.00
0.00	0.00	0.00					
GS	0.17	5.20	0.41	0.20	0.74	0.20	1.16
0.20	2.46	0.20					

NC	0.04	0.03	0.04	0.10	0.30	0.00	0.00
0.00	0.00	0.00					
X1	8000.00	23.00	0.00	0.00	0.00	0.00	500.00
0.00	0.00	1.00					
XF	0.00	0.00	0.00	0.00	0.00	0.00	0.00
5.00	0.00	0.00					
GR	165.85	0.00	164.75	10.00	163.36	20.00	163.13
40.00	162.91	50.00					
GR	163.89	60.00	163.65	80.00	163.27	90.00	162.96
100.00	162.76	110.00					
GR	162.68	120.00	161.98	130.00	161.10	140.00	161.11
150.00	162.72	160.00					
GR	162.95	170.00	162.78	180.00	162.40	190.00	163.73
200.00	165.10	210.00					
GR	165.77	220.00	165.85	230.00	166.96	240.00	
X1	9000.00	23.00	0.00	0.00	0.00	0.00	1000.00
0.00	0.00	1.00					
XF	0.00	0.00	0.00	0.00	0.00	0.00	0.00
5.00	0.00	0.00					
GR	166.18	0.00	165.08	10.00	163.69	20.00	163.46
40.00	163.24	50.00					
GR	164.22	60.00	163.98	80.00	163.60	90.00	163.29
100.00	163.09	110.00					
GR	163.01	120.00	162.31	130.00	161.43	140.00	161.44
150.00	163.05	160.00					
GR	163.28	170.00	163.11	180.00	163.11	190.00	162.73
200.00	164.06	210.00					
GR	165.43	220.00	166.10	230.00	166.18	240.00	
GS	0.19	0.20	0.42	0.20	0.77	0.20	1.19
0.20	2.59	0.20					
X1	9250.00	23.00	0.00	0.00	0.00	0.00	250.00
0.00	0.00	0.00					
XF	0.00	0.00	0.00	0.00	0.00	0.00	0.00
5.00	0.00	0.00					
GR	166.26	0.00	165.16	10.00	163.77	20.00	163.54
40.00	163.32	50.00					
GR	164.30	60.00	164.06	80.00	163.68	90.00	163.37
100.00	163.17	110.00					
GR	163.09	120.00	162.39	130.00	161.51	140.00	161.52
150.00	163.13	160.00					
GR	161.36	170.00	161.19	180.00	163.81	190.00	164.14
200.00	165.51	210.00					
GR	166.18	220.00	166.26	230.00	167.46	240.00	
X1	9370.00	23.00	0.00	0.00	0.00	0.00	120.00
0.00	0.00	0.00					
XF	0.00	0.00	0.00	0.00	0.00	0.00	0.00
0.00	0.00	0.00					
GR	166.30	0.00	165.20	10.00	163.81	20.00	163.58
40.00	163.36	50.00					
GR	164.34	60.00	164.10	80.00	163.72	90.00	163.41
100.00	163.21	110.00					
GR	163.13	120.00	162.43	130.00	161.55	140.00	161.56
150.00	163.17	160.00					
GR	163.40	170.00	163.23	180.00	162.85	190.00	164.18
200.00	165.55	210.00					
GR	166.22	220.00	166.30	230.00	167.48	240.00	

GS	0.39	0.20	0.71	0.20	1.15	0.20	1.65
0.20	3.14	0.20					
X1	9385.00	23.00	0.00	0.00	0.00	0.00	30.00
0.00	0.00	0.00					
XF	0.00	0.00	0.00	0.00	0.00	0.00	0.00
0.00	0.00	0.00					
GR	166.31	0.00	165.21	10.00	163.82	20.00	163.59
40.00	163.37	50.00					
GR	164.35	60.00	164.11	80.00	163.73	90.00	163.42
100.00	163.22	110.00					
GR	163.14	120.00	162.44	130.00	161.56	140.00	161.57
150.00	163.18	160.00					
GR	163.41	170.00	163.24	180.00	162.86	190.00	164.19
200.00	165.56	210.00					
GR	166.23	220.00	166.31	230.00	167.48	240.00	
X1	9550.00	23.00	0.00	0.00	0.00	0.00	165.00
0.00	0.00	0.00					
XF	0.00	0.00	0.00	0.00	0.00	0.00	0.00
0.00	0.00	0.00					
GR	166.36	0.00	166.26	10.00	163.87	20.00	163.65
40.00	163.42	50.00					
GR	163.41	60.00	164.16	80.00	163.78	90.00	163.47
100.00	163.28	110.00					
GR	163.19	120.00	162.49	130.00	161.62	140.00	161.62
150.00	163.23	160.00					
GR	163.47	170.00	163.29	180.00	162.91	190.00	164.25
200.00	165.61	210.00					
GR	166.28	220.00	166.36	230.00	167.46	240.00	
X1	10000.00	23.00	0.00	0.00	0.00	0.00	450.00
0.00	0.00	0.00					
XF	0.00	0.00	0.00	0.00	0.00	0.00	0.00
0.00	0.00	0.00					
GR	166.50	0.00	165.40	10.00	164.01	20.00	163.78
40.00	163.56	50.00					
GR	164.55	60.00	164.30	80.00	163.92	90.00	163.61
100.00	163.42	110.00					
GR	163.33	120.00	162.63	130.00	161.75	140.00	161.76
150.00	163.37	160.00					
GR	163.60	170.00	163.43	180.00	163.05	190.00	164.38
200.00	165.75	210.00					
GR	166.42	220.00	166.50	230.00	167.50	240.00	
GS	1.20	0.20	1.65	0.20	2.19	0.20	2.77
0.20	4.28	0.20					
X1	10500.00	23.00	0.00	0.00	0.00	0.00	500.00
0.00	0.00	0.00					
XF	0.00	0.00	0.00	0.00	0.00	0.00	0.00
0.00	0.00	0.00					
GR	166.49	0.00	165.54	10.00	164.39	20.00	163.98
40.00	163.75	50.00					
GR	163.73	60.00	164.25	80.00	164.12	90.00	163.80
100.00	163.61	110.00					
GR	163.52	120.00	162.83	130.00	161.94	140.00	161.95
150.00	163.79	160.00					
GR	163.62	170.00	163.84	180.00	164.57	190.00	165.94
200.00	166.61	210.00					
GR	166.69	220.00	166.72	230.00	167.42	240.00	

X1	11000.00	23.00	0.00	0.00	0.00	0.00	500.00
0.00	0.00	0.00					
XF	0.00	0.00	1.00	0.00	0.00	0.00	0.00
0.00	0.00	0.00					
GR	166.15	0.00	165.70	10.00	164.55	20.00	164.14
40.00	163.91	50.00					
GR	163.89	60.00	164.41	80.00	164.28	90.00	163.96
100.00	163.77	110.00					
GR	163.68	120.00	162.99	130.00	162.10	140.00	162.11
150.00	163.72	160.00					
GR	163.95	170.00	163.78	180.00	164.00	190.00	164.73
200.00	166.10	210.00					
GR	166.77	220.00	166.85	230.00	167.88	240.00	
X1	12000.00	23.00	0.00	0.00	0.00	0.00	1000.00
0.00	0.00	0.00					
XF	0.00	0.00	1500.00	0.00	0.00	0.00	0.00
0.00	0.00	0.00					
GR	166.97	0.00	165.02	10.00	164.87	20.00	164.46
40.00	164.23	50.00					
GR	164.21	60.00	164.73	80.00	164.60	90.00	164.28
100.00	164.09	110.00					
GR	164.00	120.00	163.31	130.00	162.42	140.00	162.43
150.00	164.04	160.00					
GR	164.27	170.00	164.10	180.00	164.32	190.00	165.05
200.00	166.42	210.00					
GR	167.09	220.00	167.17	230.00	168.20	240.00	
X1	13000.00	23.00	0.00	0.00	0.00	0.00	1000.00
0.00	0.00	0.00					
XF	0.00	0.00	1.00	0.00	0.00	0.00	0.00
0.00	0.00	0.00					
GR	167.30	0.00	166.35	10.00	165.20	20.00	164.79
40.00	164.56	50.00					
GR	164.54	60.00	165.06	80.00	164.93	90.00	164.61
100.00	164.42	110.00					
GR	164.33	120.00	163.64	130.00	162.75	140.00	162.76
150.00	164.60	160.00					
GR	164.43	170.00	164.65	180.00	164.65	190.00	165.38
200.00	166.75	210.00					
GR	167.42	220.00	167.50	230.00	168.53	240.00	
GS	1.20	0.20	1.65	0.20	2.19	0.20	2.77
0.20	4.28	0.20					
EJ	0.00	0.00	0.00	0.00	0.00	0.00	0.00
0.00	0.00	0.00					

1

TI

INITIAL BED MATERIAL COMPOSITION

SECTION	SIZE	FRACTION	SIZE	FRACTION	SIZE	FRACTION	SIZE
FRACTION	SIZE	FRACTION	MM	MM	MM	MM	MM
8000.00	0.17	5.200	0.41	0.200	0.74	0.200	1.16
0.200	2.46	0.200					
9000.00	0.19	0.200	0.42	0.200	0.77	0.200	1.19
0.200	2.59	0.200					

9250.00	0.31	0.200	0.60	0.200	1.01	0.200	1.48
0.200	2.95	0.200					
9370.00	0.39	0.200	0.71	0.200	1.15	0.200	1.65
0.200	3.14	0.200					
9385.00	0.41	0.200	0.74	0.200	1.18	0.200	1.69
0.200	3.19	0.200					
9550.00	0.55	0.200	0.92	0.200	1.40	0.200	1.93
0.200	3.45	0.200					
10000.00	1.20	0.200	1.65	0.200	2.19	0.200	2.77
0.200	4.28	0.200					
10500.00	1.20	0.200	1.65	0.200	2.19	0.200	2.77
0.200	4.28	0.200					
11000.00	1.20	0.200	1.65	0.200	2.19	0.200	2.77
0.200	4.28	0.200					
12000.00	1.20	0.200	1.65	0.200	2.19	0.200	2.77
0.200	4.28	0.200					
13000.00	1.20	0.200	1.65	0.200	2.19	0.200	2.77
0.200	4.28	0.200					

THE ENGELUND-HANSEN SEDIMENT FORMULA IS USED

1

TIME = 0.00 HRS DT = 100 SECS TIME STEP = 0

SECTION	W.S.ELEV.	WIDTH	DEPTH	Q	V	SLOPE	D50
QS/Q	FR	MANNING N					
	M	M	M	CMS	MPS		MM
1000 PPM							
8000.00	163.13	113.2	2.03	30	0.39	0.00011	0.19
0.18	0.15	0.211E-01					
9000.00	163.30	107.9	1.87	30	0.48	0.00027	0.77
0.05	0.20	0.238E-01					
9250.00	163.34	87.4	2.15	30	0.33	0.00005	1.01
0.00	0.10	0.216E-01					
9370.00	163.34	84.7	1.79	30	0.55	0.00036	1.15
0.05	0.22	0.253E-01					
9385.00	163.36	84.9	1.80	30	0.55	0.00036	1.18
0.05	0.22	0.253E-01					
9550.00	163.42	92.9	1.80	30	0.55	0.00039	1.40
0.04	0.23	0.253E-01					
10000.00	163.58	91.4	1.83	30	0.53	0.00034	2.19
0.02	0.21	0.255E-01					
10500.00	163.76	84.5	1.82	30	0.59	0.00049	2.19
0.04	0.24	0.264E-01					
11000.00	163.98	106.5	1.88	30	0.51	0.00037	2.19
0.02	0.22	0.253E-01					

12000.00	164.33	110.2	1.91	30	0.49	0.00033	2.19
0.02	0.21	0.250E-01					
13000.00	164.66	110.8	1.91	30	0.51	0.00038	2.19
0.02	0.22	0.253E-01					

1

TIME = 7.25 DAYS DT = 12.1 HRS TIME STEP = 39

SECTION	W.S.ELEV.	WIDTH	DEPTH	Q	V	SLOPE	D50
QS/Q	FR	MANNING N					
	M	M	M	CMS	MPS		MM
1000 PPM							
8000.00	165.50	212.9	4.40	546	1.07	0.00029	0.32
0.48	0.22	0.285E-01					
9000.00	165.80	222.0	4.37	546	1.03	0.00029	0.90
0.18	0.21	0.293E-01					
9250.00	165.87	212.2	4.52	546	1.03	0.00028	1.01
0.16	0.21	0.295E-01					
9370.00	165.90	211.9	4.62	546	1.04	0.00029	1.21
0.14	0.21	0.298E-01					
9385.00	165.91	213.4	4.44	546	1.05	0.00030	1.32
0.13	0.21	0.299E-01					
9550.00	165.96	204.4	4.05	546	1.15	0.00041	1.73
0.16	0.24	0.310E-01					
10000.00	166.23	215.5	3.30	546	1.46	0.00115	2.20
0.58	0.35	0.336E-01					
10500.00	167.03	234.4	2.69	546	1.70	0.00239	2.68
1.51	0.46	0.354E-01					
11000.00	169.20	239.7	11.40	546	0.43	0.00644	3.21
2.81	0.06	0.551E+00					
12000.00	169.52	239.6	7.12	546	0.48	0.00002	2.19
0.00	0.07	0.243E-01					
13000.00	169.54	239.5	6.79	546	0.51	0.00002	2.19
0.00	0.08	0.247E-01					

ID

10 SECTION 12000.00 TIME = 7.25 DAYS WS = 169.52 WIDTH = 239.6

DZ	Z	DZ	TDZ	Y	Z	DZ	TDZ	Y	Z
	TDZ	Y							
169.58	0.00	0.00	0.0	165.00	0.00	-0.02	10.0		
164.85	0.00	-0.02	20.0						
164.44	0.00	-0.02	40.0	164.21	0.00	-0.02	50.0		
164.21	0.00	0.00	60.0						
164.70	0.00	-0.03	80.0	164.58	0.00	-0.02	90.0		
164.26	0.00	-0.02	100.0						
164.08	0.00	-0.01	110.0	163.97	0.00	-0.03	120.0		
163.29	0.00	-0.02	130.0						
162.40	0.00	-0.02	140.0	162.46	0.00	0.03	150.0		
163.99	0.00	-0.05	160.0						
164.24	0.00	-0.03	170.0	164.08	0.00	-0.02	180.0		
164.37	0.00	0.05	190.0						
165.60	0.00	0.55	200.0	166.48	0.00	0.06	210.1		
166.81	0.00	-0.28	220.1						

167.16 0.00 -0.01 230.0 169.58 0.00 0.00 240.0

ID
9 SECTION 11000.00 TIME = 7.25 DAYS WS = 169.20 WIDTH
= 239.7

DZ	Z	DZ	TDZ	Y	Z	DZ	TDZ	Y	Z
	TDZ	Y							
	169.26	0.00	0.00	0.0	165.02	-0.12	-0.68	10.0	
164.91	-0.12	0.36	20.0						
	164.93	-0.13	0.79	39.8	164.90	-0.13	0.99	50.0	
164.92	-0.13	1.03	60.0						
	164.83	-0.13	0.42	80.0	164.88	-0.13	0.60	90.0	
164.86	-0.13	0.90	100.0						
	163.56	-0.13	-0.21	110.5	163.31	-0.13	-0.37	120.6	
157.93	-0.05	-5.06	132.5						
	157.74	-0.05	-4.36	142.5	157.98	-0.05	-4.13	152.5	
163.10	-0.13	-0.62	160.5						
	163.49	-0.13	-0.46	170.5	163.42	-0.13	-0.36	180.6	
163.53	-0.13	-0.47	190.6						
	163.68	-0.13	-1.05	200.4	164.98	-0.13	-1.12	210.0	
165.55	-0.13	-1.22	220.0						
	165.66	-0.12	-1.19	230.0	169.26	0.00	0.00	240.0	

ID
8 SECTION 10500.00 TIME = 7.25 DAYS WS = 167.03 WIDTH
= 234.4

DZ	Z	DZ	TDZ	Y	Z	DZ	TDZ	Y	Z
	TDZ	Y							
	167.09	0.00	0.00	0.0	165.69	0.03	0.15	9.3	
165.61	0.03	1.22	19.8						
	165.58	0.03	1.60	40.0	165.57	0.03	1.82	50.0	
165.68	0.16	1.95	60.0						
	165.59	0.03	1.34	80.0	165.58	0.03	1.46	90.0	
165.60	0.03	1.80	100.0						
	165.66	0.03	2.05	110.0	165.60	0.03	2.08	120.0	
165.22	0.17	2.39	130.0						
	164.51	0.18	2.57	140.0	164.52	0.18	2.57	150.0	
165.82	0.16	2.03	160.0						
	165.79	0.16	2.17	170.0	165.84	0.16	2.00	180.0	
165.89	0.16	1.32	190.4						
	166.45	0.14	0.51	200.2	166.60	0.01	-0.01	210.0	
166.66	0.00	-0.03	220.0						
	166.68	0.00	-0.04	230.3	167.42	0.00	0.00	240.0	

ID
7 SECTION 10000.00 TIME = 7.25 DAYS WS = 166.23 WIDTH
= 215.5

DZ	Z	DZ	TDZ	Y	Z	DZ	TDZ	Y	Z
	TDZ	Y							
	166.50	0.00	0.00	0.0	165.28	-0.01	-0.12	9.7	
164.77	0.07	0.76	20.0						

164.65	0.07	0.87	40.0	164.48	0.08	0.92	50.0
165.16	0.06	0.61	60.0				
164.98	0.06	0.68	80.0	164.76	0.07	0.84	90.0
164.52	0.07	0.91	100.0				
164.38	0.08	0.96	110.0	164.31	0.08	0.98	120.0
163.75	0.09	1.12	130.0				
163.03	0.10	1.28	140.0	163.04	0.10	1.28	150.0
164.34	0.08	0.97	160.0				
164.51	0.07	0.91	170.0	164.38	0.08	0.95	180.0
164.08	0.08	1.03	190.0				
164.91	0.07	0.53	200.1	165.60	-0.02	-0.15	210.2
166.42	0.00	0.00	220.0				
166.50	0.00	0.00	230.0	167.50	0.00	0.00	240.0

ID
6 SECTION 9550.00 TIME = 7.25 DAYS WS = 165.96 WIDTH
= 204.4

DZ	Z	DZ	TDZ	Y	Z	DZ	TDZ	Y	Z
	TDZ	Y							
166.36	0.00	0.00	0.0	0.0	166.26	0.00	0.00	10.0	
163.86	0.02	-0.01	19.8						
163.83	0.02	0.18	40.0	163.70	0.06	0.28	50.0		
163.69	0.06	0.28	60.0						
164.13	0.02	-0.03	80.0	163.86	0.02	0.08	90.0		
163.75	0.06	0.28	100.0						
163.57	0.07	0.29	110.0	163.48	0.07	0.29	120.0		
162.82	0.07	0.33	130.0						
161.99	0.08	0.37	140.0	161.99	0.08	0.37	150.0		
163.52	0.07	0.29	160.0						
163.74	0.06	0.27	170.0	163.58	0.07	0.29	180.0		
163.22	0.07	0.31	190.0						
164.37	0.05	0.12	200.1	165.53	-0.01	-0.08	210.1		
166.28	0.00	0.00	220.0						
166.36	0.00	0.00	230.0	167.46	0.00	0.00	240.0		

ID
5 SECTION 9385.00 TIME = 7.25 DAYS WS = 165.91 WIDTH
= 213.4

DZ	Z	DZ	TDZ	Y	Z	DZ	TDZ	Y	Z
	TDZ	Y							
166.31	0.00	0.00	0.0	0.0	164.90	-0.04	-0.31	9.8	
163.81	0.01	-0.01	20.0						
163.56	0.01	-0.03	40.0	163.32	0.02	-0.05	50.0		
164.34	0.01	-0.01	60.0						
164.08	0.01	-0.03	80.0	163.67	0.01	-0.06	90.0		
163.33	0.01	-0.09	100.0						
163.11	0.02	-0.11	110.0	163.01	0.02	-0.13	120.0		
162.24	0.02	-0.20	130.0						
161.48	0.02	-0.08	140.0	161.48	0.02	-0.09	150.0		
163.06	0.02	-0.12	160.0						
163.32	0.02	-0.09	170.0	163.14	0.02	-0.10	180.0		
162.75	0.02	-0.11	190.0						

164.08	0.01	-0.11	200.0	165.33	-0.04	-0.23	210.1
166.23	0.00	0.00	220.0				
166.31	0.00	0.00	230.0	167.48	0.00	0.00	240.0

ID
 4 SECTION 9370.00 TIME = 7.25 DAYS WS = 165.90 WIDTH
 = 211.9

DZ	Z	DZ	TDZ	Y	Z	DZ	TDZ	Y	Z
	TDZ	Y							
	166.30	0.00	0.00	0.0	165.14	0.00	-0.06	10.0	
164.00	0.00	0.19	20.2						
	163.47	0.00	-0.11	40.0	163.23	0.00	-0.13	50.0	
164.25	0.00	-0.09	60.0						
	163.99	0.00	-0.11	80.0	163.58	0.00	-0.14	90.0	
163.25	0.00	-0.16	100.0						
	163.03	0.00	-0.18	110.0	162.93	0.00	-0.20	120.0	
162.17	0.00	-0.26	130.0						
	161.28	0.00	-0.27	140.0	161.28	0.00	-0.28	150.0	
162.98	0.00	-0.19	160.0						
	163.23	0.00	-0.17	170.0	163.06	0.00	-0.17	180.0	
162.69	0.00	-0.16	190.0						
	164.31	0.00	0.13	199.9	165.52	0.00	-0.03	210.0	
166.22	0.00	0.00	220.0						
	166.30	0.00	0.00	230.0	167.48	0.00	0.00	240.0	

ID
 3 SECTION 9250.00 TIME = 7.25 DAYS WS = 165.87 WIDTH
 = 212.2

DZ	Z	DZ	TDZ	Y	Z	DZ	TDZ	Y	Z
	TDZ	Y							
	166.26	0.00	0.00	0.0	165.05	0.00	-0.11	9.9	
163.70	0.00	-0.07	19.9						
	163.59	0.00	0.05	40.0	163.36	0.00	0.04	50.0	
164.21	0.00	-0.09	60.0						
	163.97	0.00	-0.09	80.0	163.69	0.00	0.01	90.0	
163.42	0.00	0.05	100.0						
	163.23	0.00	0.06	110.0	163.15	0.00	0.06	120.0	
162.47	0.00	0.08	130.0						
	161.61	0.00	0.10	140.0	161.62	0.00	0.10	150.0	
163.19	0.00	0.06	160.0						
	161.46	0.00	0.10	170.0	161.35	0.00	0.16	180.0	
163.84	0.00	0.03	190.0						
	163.96	0.00	-0.18	200.1	165.49	0.00	-0.02	210.0	
166.18	0.00	0.00	220.0						
	166.26	0.00	0.00	230.0	167.46	0.00	0.00	240.0	

1

TIME = 196.14 DAYS DT = 25.6 HRS TIME STEP = 668

SECTION	W.S.ELEV.	WIDTH	DEPTH	Q	V	SLOPE	D50
QS/Q	FR	MANNING N					

1000 PPM	M	M	M	CMS	MPS	MM	
8000.00	162.66	48.4	1.56	31	0.81	0.00072	1.85
0.15 0.29	0.286E-01						
9000.00	163.23	95.7	1.80	31	0.56	0.00042	1.24
0.06 0.24	0.255E-01						
9250.00	163.37	27.5	1.43	31	1.07	0.00103	2.06
0.32 0.33	0.312E-01						
9370.00	163.51	37.6	0.92	31	1.05	0.00144	2.36
0.38 0.37	0.311E-01						
9385.00	163.56	36.4	1.18	31	1.04	0.00133	2.52
0.31 0.36	0.310E-01						
9550.00	163.77	30.2	1.46	31	1.11	0.00138	2.83
0.32 0.37	0.319E-01						
10000.00	164.38	24.1	1.49	31	1.17	0.00132	3.19
0.33 0.36	0.328E-01						
10500.00	165.23	60.7	2.68	31	0.95	0.00204	3.29
0.35 0.41	0.312E-01						
11000.00	167.45	231.9	11.54	31	0.02	0.00899	3.32
0.23 0.00	0.184E+02						
12000.00	167.48	224.4	5.08	31	0.05	0.00000	2.19
0.00 0.01	0.126E-01						
13000.00	167.48	219.2	4.73	31	0.05	0.00000	2.19
0.00 0.01	0.130E-01						

ID
 10 SECTION 12000.00 TIME = 196.14 DAYS WS = 167.48 WIDTH
 = 224.4

DZ	Z	DZ	TDZ	Y	Z	DZ	TDZ	Y	Z
	171.62	0.00	0.00	0.0	165.00	0.00	-0.02	10.0	
164.85	0.00	-0.02	20.0						
	164.44	0.00	-0.02	40.0	164.21	0.00	-0.02	50.0	
164.21	0.00	0.00	60.0						
	164.70	0.00	-0.03	80.0	164.58	0.00	-0.02	90.0	
164.26	0.00	-0.02	100.0						
	164.08	0.00	-0.01	110.0	163.97	0.00	-0.03	120.0	
163.29	0.00	-0.02	130.0						
	162.40	0.00	-0.02	140.0	162.47	0.00	0.04	150.0	
163.98	0.00	-0.06	160.0						
	164.23	0.00	-0.04	170.0	164.08	0.00	-0.02	180.0	
164.40	0.00	0.08	190.0						
	165.62	0.00	0.57	200.0	166.45	0.00	0.03	210.1	
166.79	0.00	-0.30	220.1						
	167.16	0.00	-0.01	230.0	171.62	0.00	0.00	240.0	

ID
 9 SECTION 11000.00 TIME = 196.14 DAYS WS = 167.45 WIDTH
 = 231.9

DZ	Z	DZ	TDZ	Y	Z	DZ	TDZ	Y	Z
----	---	----	-----	---	---	----	-----	---	---

171.61	0.00	0.00	0.0	161.11	0.00	-4.59	10.0
160.98	0.00	-3.57	20.0				
160.95	0.00	-3.19	39.8	160.90	0.00	-3.01	50.0
160.89	0.00	-3.00	60.0				
160.79	0.00	-3.62	80.0	160.81	0.00	-3.47	90.0
160.79	0.00	-3.17	100.0				
160.18	0.00	-3.59	110.5	160.12	0.00	-3.56	120.6
156.07	0.00	-6.92	132.5				
155.91	0.00	-6.19	142.5	156.13	0.00	-5.98	152.5
160.07	0.00	-3.65	160.5				
160.17	0.00	-3.78	170.5	160.16	0.00	-3.62	180.6
160.19	0.00	-3.81	190.6				
160.25	0.00	-4.48	200.4	160.93	0.00	-5.17	210.0
161.46	0.00	-5.31	220.0				
161.57	0.00	-5.28	230.0	171.61	0.00	0.00	240.0

ID
8 SECTION 10500.00 TIME = 196.14 DAYS WS = 165.23 WIDTH
= 60.7

DZ	Z	DZ	TDZ	Y	Z	DZ	TDZ	Y	Z
	TDZ	Y							
167.41	0.00	0.00	0.0	165.96	0.00	0.42	7.0		
165.96	0.00	1.57	19.8						
165.96	0.00	1.98	40.0	165.96	0.00	2.21	50.0		
165.90	0.00	2.17	60.0						
165.06	-0.01	0.81	79.6	165.06	-0.01	0.94	90.0		
165.06	-0.01	1.26	100.0						
165.06	-0.01	1.45	110.0	164.79	0.00	1.27	120.0		
162.54	-0.01	-0.29	131.1						
166.86	0.00	4.92	140.0	166.86	0.00	4.91	150.2		
166.86	0.00	3.07	160.0						
166.86	0.00	3.24	170.0	166.86	0.00	3.02	180.0		
166.86	0.00	2.29	190.4						
166.86	0.00	0.92	200.2	166.86	0.00	0.25	210.0		
166.86	0.00	0.17	220.0						
166.86	0.00	0.14	231.7	167.42	0.00	0.00	240.0		

ID
7 SECTION 10000.00 TIME = 196.14 DAYS WS = 164.38 WIDTH
= 24.1

DZ	Z	DZ	TDZ	Y	Z	DZ	TDZ	Y	Z
	TDZ	Y							
166.50	0.00	0.00	0.0	165.32	0.00	-0.08	7.7		
165.32	0.00	1.31	20.0						
165.31	0.00	1.53	40.0	165.31	0.00	1.75	50.0		
165.31	0.00	0.76	60.0						
165.31	0.00	1.01	80.0	165.31	0.00	1.39	90.0		
165.28	0.00	1.67	100.0						
165.28	0.00	1.86	110.0	165.28	0.00	1.95	120.0		
165.28	0.00	2.65	130.0						
162.89	0.01	1.14	137.9	163.06	0.00	1.30	152.0		
165.11	0.00	1.74	160.0						

165.12	0.00	1.52	170.0	165.12	0.00	1.70	180.0
165.12	0.00	2.07	190.0				
165.12	0.00	0.74	200.1	165.14	0.00	-0.61	212.3
166.42	0.00	0.00	220.0				
166.50	0.00	0.00	230.0	167.50	0.00	0.00	240.0

ID
 6 SECTION 9550.00 TIME = 196.14 DAYS WS = 163.77 WIDTH
 = 30.2

DZ	Z	DZ	TDZ	Y	Z	DZ	TDZ	Y	Z
	TDZ	Y							
166.36	0.00	0.00	0.00	0.0	166.26	0.00	0.00	10.0	
165.20	0.00	1.33	20.3						
164.95	0.00	1.30	40.2		164.90	0.00	1.48	50.1	
164.91	0.00	1.50	60.1						
164.90	0.00	0.74	80.0		164.50	0.00	0.72	89.8	
164.38	0.00	0.91	100.0						
164.34	0.00	1.06	110.0		164.27	0.00	1.08	119.9	
163.63	0.00	1.14	130.5						
162.32	0.00	0.70	140.0		162.32	0.00	0.70	149.8	
164.11	0.00	0.88	160.2						
164.41	0.00	0.94	170.0		164.48	0.00	1.19	180.1	
164.61	0.00	1.70	189.9						
165.32	0.00	1.07	199.8		165.71	0.00	0.10	210.1	
166.28	0.00	0.00	220.0						
166.36	0.00	0.00	230.0		167.46	0.00	0.00	240.0	

ID
 5 SECTION 9385.00 TIME = 196.14 DAYS WS = 163.56 WIDTH
 = 36.4

DZ	Z	DZ	TDZ	Y	Z	DZ	TDZ	Y	Z
	TDZ	Y							
166.31	0.00	0.00	0.00	0.0	165.38	0.00	0.17	9.9	
165.13	0.00	1.31	20.5						
164.58	0.00	0.99	40.2		164.51	0.00	1.14	50.1	
164.33	0.00	-0.02	59.9						
164.31	0.00	0.20	80.1		164.16	0.00	0.43	89.8	
164.04	0.00	0.62	99.9						
164.02	0.00	0.80	110.1		163.76	0.00	0.62	120.0	
162.56	0.00	0.12	129.6						
162.40	0.02	0.84	140.0		162.58	0.00	1.01	150.4	
163.76	0.00	0.58	159.7						
164.02	0.00	0.61	170.0		164.28	0.00	1.04	179.8	
164.33	0.00	1.47	189.9						
165.15	0.00	0.96	199.7		165.45	0.00	-0.11	210.2	
166.23	0.00	0.00	220.0						
166.31	0.00	0.00	230.0		167.48	0.00	0.00	240.0	

ID
 4 SECTION 9370.00 TIME = 196.14 DAYS WS = 163.51 WIDTH
 = 37.6

DZ	Z	DZ	TDZ	Y	Z	DZ	TDZ	Y	Z
	TDZ	Y							
	166.30	0.00	0.00	0.0	164.90	0.00	-0.30	9.4	
164.79	0.00	0.98	20.3						
	164.64	0.00	1.06	40.1	164.54	0.00	1.18	49.9	
164.38	0.00	0.04	60.1						
	164.38	0.00	0.28	79.7	164.09	0.00	0.37	89.5	
164.05	0.00	0.64	99.4						
	164.03	0.00	0.82	110.1	163.86	0.00	0.73	119.8	
162.71	0.08	0.28	125.5						
	162.36	-0.24	0.81	140.0	162.70	0.07	1.14	154.1	
163.74	0.00	0.57	160.3						
	164.04	0.00	0.64	169.9	164.16	0.00	0.93	180.2	
164.61	0.00	1.76	190.0						
	164.79	0.00	0.61	199.9	164.90	0.00	-0.65	210.7	
166.22	0.00	0.00	220.0						
	166.30	0.00	0.00	230.0	167.48	0.00	0.00	240.0	

ID
 3 SECTION 9250.00 TIME = 196.14 DAYS WS = 163.37 WIDTH
 = 27.5

DZ	Z	DZ	TDZ	Y	Z	DZ	TDZ	Y	Z
	TDZ	Y							
	166.26	0.00	0.00	0.0	164.66	0.00	-0.50	9.5	
164.58	0.00	0.81	20.1						
	164.51	0.00	0.97	40.2	164.43	0.00	1.11	50.2	
164.34	0.00	0.04	60.1						
	164.28	0.00	0.22	80.0	164.23	0.00	0.55	90.0	
164.16	0.00	0.79	100.0						
	164.07	0.00	0.90	109.9	163.91	0.00	0.82	120.0	
163.81	0.00	1.42	130.0						
	163.72	0.00	2.21	140.5	163.57	0.00	2.05	150.9	
163.55	0.00	0.42	160.3						
	161.97	0.03	0.61	168.2	161.97	0.03	0.78	182.1	
163.62	0.00	-0.19	189.9						
	164.22	0.00	0.08	200.4	165.20	0.00	-0.31	210.2	
166.18	0.00	0.00	220.0						
	166.26	0.00	0.00	230.0	167.46	0.00	0.00	240.0	
1									
0.00000	2.19	0.00	0.01	0.117E-01					
	13000.00	165.34	180.6	2.59	8	0.05	0.00000	2.19	
0.00	0.02	0.129E-01							

APPENDIX -B

```
***** W S P R O *****
Federal Highway Administration - U. S. Geological Survey
Model for Water-Surface Profile Computations.
Run Date & Time: 11/17/** 11:48 am      Version V021297
Input File: LOCAL1.DAT      Output File: LOCAL1.OUT
```

```
-----*
T1      ANALYSIS OF STREAM BED VARIATIONS
T2      ESTIMATION OF SCOUR AT BRIDGE
T3      CONTRACTION, PIER AND ABUTMENT SCOUR CALCULATIONS
SI 1
```

Metric (SI) Units Used in WSPRO

Quantity	SI Unit	Precision
Length	meters	0.001
Depth	meters	0.001
Elevation	meters	0.001
Widths	meters	0.001
Velocity	meters/second	0.001
Discharge	cubic meters/second	0.001
Slope	meter/meter	0.001
Angles	degrees	0.01

Q 550

```
***      Processing Flow Data; Placing Information into Sequence 1
***
```

SK 0.0003

```
***** W S P R O *****
Federal Highway Administration - U. S. Geological Survey
Model for Water-Surface Profile Computations.
Input Units: Metric / Output Units: Metric
```

```
-----*
ANALYSIS OF STREAM BED VARIATIONS
ESTIMATION OF SCOUR AT BRIDGE
CONTRACTION, PIER AND ABUTMENT SCOUR CALCULATIONS
```

```
-----*
*      Starting To Process Header Record EXIT      *
-----*
```

```
XS  EXIT  9250 * * * 0.0003
GR      0,166.26  10,165.16  20,163.77  40,163.54  50,163.32
GR      60,164.30  80,164.06  90,163.68  100,163.37  110,163.17
GR      120,163.09  130,162.39  140,161.51  150,161.52
160,163.13
GR      170,163.36  180,163.19  190,162.81  200,164.14
210,165.51
GR      220,166.18  230,166.26  240,167.50
```

N 0.04 0.03 0.04
 SA 120 .170

*** Completed Reading Data Associated With Header Record EXIT

 *** Storing X-Section Data In Temporary File As Record Number 1

*** Data Summary For Header Record EXIT

SRD Location: 9250. Cross-Section Skew: .0 Error Code
 0
 Valley Slope: .00030 Averaging Conveyance By Geometric Mean.
 Energy Loss Coefficients -> Expansion: .50 Contraction: .00

X,Y-coordinates (23 pairs)					
X	Y	X	Y	X	Y
.000	166.260	10.000	165.160	20.000	163.770
40.000	163.540	50.000	163.320	60.000	164.300
80.000	164.060	90.000	163.680	100.000	163.370
110.000	163.170	120.000	163.090	130.000	162.390
140.000	161.510	150.000	161.520	160.000	163.130
170.000	163.360	180.000	163.190	190.000	162.810
200.000	164.140	210.000	165.510	220.000	166.180
230.000	166.260	240.000	167.500		

Minimum and Maximum X,Y-coordinates
 Minimum X-Station: .000 (associated Y-Elevation: 166.260
)
 Maximum X-Station: 240.000 (associated Y-Elevation: 167.500
)
 Minimum Y-Elevation: 161.510 (associated X-Station: 140.000
)
 Maximum Y-Elevation: 167.500 (associated X-Station: 240.000
)

Roughness Data (3 SubAreas)		
SubArea	Roughness Coefficient	Horizontal Breakpoint
1	.040	---
	---	120.000
2	.030	---
	---	170.000
3	.040	---

 * Finished Processing Header Record EXIT *

-----*
 ANALYSIS OF STREAM BED VARIATIONS
 ESTIMATION OF SCOUR AT BRIDGE
 CONTRACTION, PIER AND ABUTMENT SCOUR CALCULATIONS

-----*
 * Starting To Process Header Record FULLV *

XS FULLV 9385

*** Completed Reading Data Associated With Header Record FULLV

 *** No Roughness Data Input, Propagating From Previous Section

 *** Storing X-Section Data In Temporary File As Record Number 2

*** Data Summary For Header Record FULLV

 SRD Location: 9385. Cross-Section Skew: .0 Error Code
 0
 Valley Slope: .00030 Averaging Conveyance By Geometric Mean.
 Energy Loss Coefficients -> Expansion: .50 Contraction: .00

X,Y-coordinates (23 pairs)					
X	Y	X	Y	X	Y
.000	166.300	10.000	165.201	20.000	163.811
40.000	163.580	50.000	163.361	60.000	164.340
80.000	164.100	90.000	163.721	100.000	163.411
110.000	163.211	120.000	163.130	130.000	162.430
140.000	161.550	150.000	161.561	160.000	163.171
170.000	163.400	180.000	163.230	190.000	162.850
200.000	164.180	210.000	165.550	220.000	166.221
230.000	166.300	240.000	167.540		

Minimum and Maximum X,Y-coordinates
) Minimum X-Station: .000 (associated Y-Elevation: 166.300
)
) Maximum X-Station: 240.000 (associated Y-Elevation: 167.540
)
) Minimum Y-Elevation: 161.550 (associated X-Station: 140.000
)
) Maximum Y-Elevation: 167.540 (associated X-Station: 240.000
)

Roughness Data (3 SubAreas)		
SubArea	Roughness Coefficient	Horizontal Breakpoint
1	.040	---
	---	120.000
2	.030	---
	---	170.000
3	.040	---

* Finished Processing Header Record FULLV *

***** W S P R O *****

Federal Highway Administration - U. S. Geological Survey
 Model for Water-Surface Profile Computations.
 Input Units: Metric / Output Units: Metric

ANALYSIS OF STREAM BED VARIATIONS
 ESTIMATION OF SCOUR AT BRIDGE
 CONTRACTION, PIER AND ABUTMENT SCOUR CALCULATIONS

* Starting To Process Header Record BRDG *

```
BR BRDG 9385
BL 1 120 70 190
BC 166.50
CD 2 10 1 167.50
AB 161.56 161.56
PD 0 161.56,2.0,1 161.56,2.0,1 161.56,2.0,1 161.56,2.0,1
PD 161.56,2.0,1 161.56,2.0,1 161.56,2.0,1
N 0.040 0.030 0.040
SA 120 170
```

*** Completed Reading Data Associated With Header Record BRDG ***

+++072 NOTICE: X-coordinate # 2 increased to eliminate vertical segment.

+++072 NOTICE: X-coordinate #15 increased to eliminate vertical segment.

*** Storing Bridge Data In Temporary File As Record Number 3 ***

*** Data Summary For Bridge Record BRDG ***

SRD Location: 9385. Cross-Section Skew: .0 Error Code

0

Valley Slope: ***** Averaging Conveyance By Geometric Mean.
 Energy Loss Coefficients -> Expansion: .50 Contraction: .00

X,Y-coordinates (16 pairs)					
X	Y	X	Y	X	Y
70.000	166.500	70.100	164.220	80.000	164.100
90.000	163.721	100.000	163.411	110.000	163.211
120.000	163.130	130.000	162.430	140.000	161.550
150.000	161.561	160.000	163.171	170.000	163.400
180.000	163.230	190.000	162.850	190.100	166.500
70.000	166.500				

Minimum and Maximum X,Y-coordinates

Minimum X-Station: 70.000 (associated Y-Elevation: 166.500)

Maximum X-Station: 190.100 (associated Y-Elevation: 166.500)

Minimum Y-Elevation: 161.550 (associated X-Station: 140.000)

Maximum Y-Elevation: 166.500 (associated X-Station: 70.000)

Roughness Data (3 SubAreas)

SubArea	Roughness Coefficient	Horizontal Breakpoint
1	.040	---
	---	120.000
2	.030	---
	---	170.000
3	.040	---

Discharge coefficient parameters

BRTYPE	BRWTH	EMBSS	EMBELV	UserCD
2	10.000	1.00	167.500	*****

Pressure flow elevations

AVBCEL	PFElev
166.500	166.500

Abutment Parameters

ABSLPL	ABSLPR	XTOELT	YTOELT	XTOERT	YTOERT
161.560	161.560	70.000	164.220	190.000	162.850

Bridge Length and Bottom Chord component input data

BRLEN	LOCOPT	XCONLT	XCONRT	BCELEV	BCSLP	BCXSTA
120.000	1	70.000	190.000	166.500	.0000	130.000

Pier/Pile Data (7 Group(s))

Code Indicates Bridge Uses Piers

Group	Elevation	Gross Width	Number
1	161.560	2.000	1
2	161.560	2.000	1
3	161.560	2.000	1
4	161.560	2.000	1
5	161.560	2.000	1
6	161.560	2.000	1
7	161.560	2.000	1

```

*-----*
*           Finished Processing Header Record BRDG           *
*-----*
***** W S P R O *****
Federal Highway Administration - U. S. Geological Survey
Model for Water-Surface Profile Computations.
Input Units: Metric / Output Units: Metric
*-----*

```

ANALYSIS OF STREAM BED VARIATIONS
ESTIMATION OF SCOUR AT BRIDGE
CONTRACTION, PIER AND ABUTMENT SCOUR CALCULATIONS

```

*-----*
*           Starting To Process Header Record APPR           *
*-----*

```

XS APPR 9520

```

*** Completed Reading Data Associated With Header Record APPR
***
*** No Roughness Data Input, Propagating From Previous Section
***
*** Storing X-Section Data In Temporary File As Record Number 4
***

```

```

*** Data Summary For Header Record APPR
***
SRD Location:      9520.   Cross-Section Skew:   .0   Error Code
0
Valley Slope:     .00030   Averaging Conveyance By Geometric Mean.
Energy Loss Coefficients -> Expansion:   .50   Contraction:   .00

```

X,Y-coordinates (23 pairs)

X	Y	X	Y	X	Y
.000	166.341	10.000	165.241	20.000	163.851
40.000	163.621	50.000	163.401	60.000	164.381
80.000	164.141	90.000	163.761	100.000	163.451
110.000	163.251	120.000	163.171	130.000	162.471
140.000	161.591	150.000	161.601	160.000	163.211
170.000	163.441	180.000	163.271	190.000	162.891
200.000	164.221	210.000	165.591	220.000	166.261
230.000	166.341	240.000	167.581		

Minimum and Maximum X,Y-coordinates

```

) Minimum X-Station:      .000   ( associated Y-Elevation: 166.341
)
) Maximum X-Station:     240.000 ( associated Y-Elevation: 167.581
)
) Minimum Y-Elevation:   161.591 ( associated X-Station: 140.000
)
) Maximum Y-Elevation:   167.581 ( associated X-Station: 240.000
)

```

Roughness Data (3 SubAreas)		
SubArea	Roughness Coefficient	Horizontal Breakpoint
1	.040	---
	---	120.000
2	.030	---
	---	170.000
3	.040	---

Bridge datum projection(s): XREFLT XREFRT FDSTLT FDSTRT

```

*-----*
*       Finished Processing Header Record APPR       *
*-----*
***** W S P R O *****
Federal Highway Administration - U. S. Geological Survey
Model for Water-Surface Profile Computations.
Input Units: Metric / Output Units: Metric
*-----*

```

ANALYSIS OF STREAM BED VARIATIONS
 ESTIMATION OF SCOUR AT BRIDGE
 CONTRACTION, PIER AND ABUTMENT SCOUR CALCULATIONS

```

DA BRDG
DP BRDG 115 * 2.0
DP BRDG * 115 2.0
DC 0 BRDG * 115 * * 8.0
DC 1 BRDG 115 190 * * 1.15 6.0
EX

```

```

*=====*
*       Summary of Boundary Condition Information       *
*=====*

```

#	Reach Discharge	Water Surface Elevation	Friction Slope	Flow Regime
1	550.00	*****	.0003	Sub-Critical

```

*=====*
*       Beginning 1 Profile Calculation(s)           *
*=====*
***** W S P R O *****
Federal Highway Administration - U. S. Geological Survey
Model for Water-Surface Profile Computations.
Input Units: Metric / Output Units: Metric
*-----*

```

ANALYSIS OF STREAM BED VARIATIONS
 ESTIMATION OF SCOUR AT BRIDGE
 CONTRACTION, PIER AND ABUTMENT SCOUR CALCULATIONS

<< Beginning Computations for Profile 1 >>

WSEL	VHD	Q	AREA	SRDL	LEW	
EGEL	HF	V	K	FLEN	REW	
CRWS	HO	FR #	SF	ALPHA	ERR	

Section: EXIT		166.186	.064	549.999	570.297	*****
.668						
Header Type: XS		166.250	*****	.964	31732.38	*****
220.791						
SRD: 9250.000		164.402	*****	.222	*****	1.351

Section: FULLV		166.227	.064	549.999	570.355	135.000
.666						
Header Type: FV		166.291	.040	.964	31733.76	135.000
220.851						
SRD: 9385.000		164.444	.000	.222	.0003	1.351
.001						

<<< The Preceding Data Reflect The "Unconstricted" Profile >>>

Section: APPR		166.267	.064	549.999	570.407	134.999
.664						
Header Type: AS		166.331	.040	.964	31736.66	134.999
220.877						
SRD: 9520.000		164.484	.000	.222	.0003	1.351
.001						

<<< The Preceding Data Reflect The "Unconstricted" Profile >>>

<<< The Following Data Reflect The "Constricted" Profile >>>
<<< Beginning Bridge/Culvert Hydraulic Computations >>>

WSEL	VHD	Q	AREA	SRDL	LEW	
EGEL	HF	V	K	FLEN	REW	
CRWS	HO	FR #	SF	ALPHA	ERR	

Section: BRDG		166.172	.160	549.999	376.193	135.000
70.014						
Header Type: BR		166.333	.055	1.462	23837.87	135.000
190.090						
SRD: 9385.000		164.523	.027	.320	*****	1.476
.000						

Specific Bridge Information		C	P/A	PFELEV	BLEN	XLAB
XRAB						
Bridge Type 2	Flow Type 1	-----	-----	-----	-----	-----

Pier/Pile Code	0	.8232	.025	166.499	119.999	69.999
189.999						

Unconstricted Full Valley Section Water Surface Elevation:
166.227

Downstream Bridge Section Water Surface Elevation:
166.172

Bridge DrawDown Distance:

.055

```

-----
-----
WSEL      VHD      Q      AREA      SRDL      LEW
EGEL      HF      V      K      FLEN      REW
CRWS      HO      FR #      SF      ALPHA      ERR
-----
Section: APPR      166.330      .062      549.999      584.395      124.999
.098
Header Type: AS      166.392      .052      .941      32495.43      130.692
228.653
SRD: 9520.000      164.484      .006      .221      .0003      1.377
.000

```

** Change in Approach Section Water Surface Elevation: .063 **

```

Approach Section APPR Flow Contraction Information
M( G )      M( K )      KQ      XLKQ      XRKQ      OTEL
-----
.455      .226      25141.2      64.210      184.287      166.330
-----

```

<<< End of Bridge Hydraulics Computations >>>

<< Completed Computations of Profile 1 >>

```

***** W S P R O *****
Federal Highway Administration - U. S. Geological Survey
Model for Water-Surface Profile Computations.
Input Units: Metric / Output Units: Metric
*-----*
```

ANALYSIS OF STREAM BED VARIATIONS
 ESTIMATION OF SCOUR AT BRIDGE
 CONTRACTION, PIER AND ABUTMENT SCOUR CALCULATIONS

*** Abutment Scour Calculations for Header Record BRDG ***

Constants and Input Variables

```

*-----*
Adjustment Factor      (K1):      .55
Flow Angle of Attack Factor (K2):      1.00
Factor of Safety      (FS):      1.00
*-----*
```

#	Abtmnt Side	Scour Depth	X-Statn	A-Prime	Ya	Qe	Overbank Froude #
1	Left	5.889	70.000	70.000	2.111	102.831	.153
	Right	3.011	190.000	50.000	.927	22.044	.158

***** W S P R O *****
 Federal Highway Administration - U. S. Geological Survey
 Model for Water-Surface Profile Computations.
 Input Units: Metric / Output Units: Metric

ANALYSIS OF STREAM BED VARIATIONS
 ESTIMATION OF SCOUR AT BRIDGE
 CONTRACTION, PIER AND ABUTMENT SCOUR CALCULATIONS

*** Pier Scour Calculations for Header Record BRDG ***

Constants and Input Variables

Pier Width: 6.562

 Pier Shape Factor (K1): 1.00
 Flow Angle of Attack Factor (K2): 1.00
 Bed Condition Factor (K3): 1.10
 Bed Material Factor (K4): 1.00
 Velocity Multiplier (VM): 1.00
 Depth Multiplier (YM): 1.00

Stations -- #	Scour Depth	---- Localized Hydraulic Properties ----					Froude #	-- X- Left
		Flow	WSE	Depth	Velocity	Right		
1	7.705	434.442	166.179	4.629	2.079	.309	115.000	
190.091								

***** W S P R O *****
 Federal Highway Administration - U. S. Geological Survey
 Model for Water-Surface Profile Computations.
 Input Units: Metric / Output Units: Metric

ANALYSIS OF STREAM BED VARIATIONS
 ESTIMATION OF SCOUR AT BRIDGE
 CONTRACTION, PIER AND ABUTMENT SCOUR CALCULATIONS

*** Pier Scour Calculations for Header Record BRDG ***

Constants and Input Variables

Pier Width: 6.562

 Pier Shape Factor (K1): 1.00
 Flow Angle of Attack Factor (K2): 1.00
 Bed Condition Factor (K3): 1.10
 Bed Material Factor (K4): 1.00
 Velocity Multiplier (VM): 1.00
 Depth Multiplier (YM): 1.00

```

      Scour   ---- Localized Hydraulic Properties ----   -- X-
Stations --
#   Depth   Flow      WSE      Depth  Velocity Froude #   Left
Right
-----
1   5.750   115.970  166.179  3.009   1.205    .222    70.014
115.000
-----

```

```

***** W S P R O *****
Federal Highway Administration - U. S. Geological Survey
Model for Water-Surface Profile Computations.
Input Units: Metric / Output Units: Metric
*-----*

```

ANALYSIS OF STREAM BED VARIATIONS
 ESTIMATION OF SCOUR AT BRIDGE
 CONTRACTION, PIER AND ABUTMENT SCOUR CALCULATIONS

*** Live-Bed Contraction Scour Calculations for Header Record BRDG

Constants and Input Variables

```

*-----*
Bed Material Transport Mode Factor (k1):   .64
Total Pier Width Value (Pw):   8.000
*-----*

```

```

      Scour   -- Flow --           -- Width --           --- X-Limits ---
#   Depth   Contract Approach  Contract Approach  Side  Contract
Approach
-----
1   .912    115.846   94.421   37.000   45.000  Left:   70.000
70.000
..... Approach Channel Depth:   2.614 ..... Right: 115.000
115.000
-----

```

***** W S P R O *****
 Federal Highway Administration - U. S. Geological Survey
 Model for Water-Surface Profile Computations.
 Input Units: Metric / Output Units: Metric

-----*
 ANALYSIS OF STREAM BED VARIATIONS
 ESTIMATION OF SCOUR AT BRIDGE
 CONTRACTION, PIER AND ABUTMENT SCOUR CALCULATIONS

*** Clear-Water Contraction Scour for Header Record BRDG ***

Constants and Input Variables

 Bed Material D50 Value (D50): 1.0000
 Pier Width Value (Pw): 6.000

#	Scour Depth	-- Flow --		-- Width --		--- X-Limits ---	
		Contract	Approach	Contract	Approach	Side	Contract
1	3.626	441.266	341.583	69.000	75.000	Left:	115.000
	115.000 Approach Channel Depth:		3.635	Right:	190.000
	190.000						

ER

***** Normal end of WSPRO execution.

 ***** Elapsed Time: 0 Minutes 1 Seconds

```

* Weir Submerg          *          * Froude # Chl          *
  0.04 *          0.04 *
* Weir Max Depth (m)   *          * Specif Force (m3)   *
  609.29 *          609.50 *
* Min El Weir Flow (m) *          * Hydr Depth (m)     *
  3.01 *          3.01 *
* Min El Prs (m)       *          * W.P. Total (m)     *
  154.14 *          154.16 *
* Delta EG (m)         *          * Conv. Total (m3/s) *
  15541.0 *          15546.4 *
* Delta WS (m)         *          * Top Width (m)      *
  106.00 *          106.00 *
* BR Open Area (m2)    *          * Frctn Loss (m)     *
  0.01 *          0.01 *
* BR Open Vel (m/s)    *          * C & E Loss (m)     *
  0.00 *          0.05 *
* Coef of Q            *          * Shear Total (N/m2) *
  25.01 *          25.00 *
* Br Sel Method        *Energy only * Power Total (N/m s) *
  42.86 *          42.83 *

```

Profile Output Table - Standard Table 1

```

* Reach          * River Sta *      Q Total *Min Ch El *W.S. Elev
*Crit W.S. *E.G. Elev *E.G. Slope * Vel Chnl *Flow Area *Top
Width *Froude # Chl *
*
*          *          *          (m3/s) *          (m) *          (m) *
*          *          *          (m/s) *          (m2) *          (m) *
*

```

```

* Upper          * 10.000    *          550.10 * 161.75 * 166.35 *
* 166.41 * 0.000329 *          1.45 * 552.12 * 217.44 *
0.24 *
* Upper          * 9.900     *          549.40 * 161.73 * 166.31 *
* 166.38 * 0.000329 *          1.45 * 551.36 * 217.41 *
0.24 *
* Upper          * 9.800     *          548.71 * 161.70 * 166.28 *
* 166.35 * 0.000330 *          1.45 * 550.73 * 217.33 *
0.24 *
* Upper          * 9.700     *          548.01 * 161.67 * 166.25 *
* 166.31 * 0.000330 *          1.45 * 550.09 * 217.27 *
0.24 *
* Upper          * 9.600     *          547.32 * 161.64 * 166.21 *
* 166.28 * 0.000330 *          1.45 * 549.46 * 217.20 *
0.24 *
* Upper          * 9.520     *          546.76 * 161.61 * 166.19 *
164.48 * 166.25 * 0.000305 *          1.40 * 550.28 * 217.29 *
0.23 *
* Upper          * 9.400     *          545.93 * 161.58 * 166.22 *
164.45 * 166.29 * 0.000304 *          1.41 * 564.33 * 218.83 *
0.23 *
* Upper          * 9.385     *          Bridge *          *          *
*          *          *          *          *          *
*
* Upper          * 9.370     *          545.93 * 161.57 * 166.11 *
* 166.18 * 0.000342 *          1.47 * 541.91 * 216.36 *
0.24 *

```

```

* Upper      * 9.250      *      545.10 * 161.53 * 166.07 *
*      166.14 * 0.000341 *      1.47 * 541.72 * 216.34 *
0.24 *
* Upper      * 9.200      *      544.76 * 161.52 * 166.05 *
*      166.12 * 0.000343 *      1.47 * 540.13 * 216.16 *
0.24 *
* Upper      * 9.100      *      544.08 * 161.49 * 166.02 *
*      166.09 * 0.000344 *      1.47 * 539.17 * 216.05 *
0.24 *
* Upper      * 9.000      *      543.40 * 161.42 * 165.98 *
164.30 * 166.05 * 0.000332 *      1.45 * 545.56 * 216.72 *
0.24 *

```

Profile Output Table - Standard Table 2

```

* Reach      * River Sta * E.G. Elev *W.S. Elev * Vel Head
*Frctn Loss *C & E Loss * Q Left *Q Channel * Q Right *Top
Width *
*
*      *      *      (m) *      (m) *      (m) *
(m) *      (m) * (m3/s) * (m3/s) * (m3/s) * (m) *
*****
* Upper      * 10.000      *      166.41 * 166.35 * 0.07 *
*      *      203.42 * 272.60 * 74.08 * 217.44 *
* Upper      * 9.900      *      166.38 * 166.31 * 0.07 *
*      *      203.12 * 272.36 * 73.92 * 217.41 *
* Upper      * 9.800      *      166.35 * 166.28 * 0.07 *
*      *      202.78 * 272.10 * 73.83 * 217.33 *
* Upper      * 9.700      *      166.31 * 166.25 * 0.07 *
*      *      202.44 * 271.85 * 73.72 * 217.27 *
* Upper      * 9.600      *      166.28 * 166.21 * 0.07 *
*      *      202.10 * 271.60 * 73.62 * 217.20 *
* Upper      * 9.520      *      166.25 * 166.19 * 0.06 *
0.00 *      0.00 * 203.69 * 261.36 * 81.71 * 217.29 *
* Upper      * 9.400      *      166.29 * 166.22 * 0.06 *
0.01 *      0.03 * 203.46 * 268.80 * 73.66 * 218.83 *
* Upper      * 9.385      *      Bridge *      *      *
*      *      *      *      *      *
* Upper      * 9.370      *      166.18 * 166.11 * 0.07 *
*      *      200.60 * 272.01 * 73.32 * 216.36 *
* Upper      * 9.250      *      166.14 * 166.07 * 0.07 *
*      *      200.26 * 271.62 * 73.21 * 216.34 *
* Upper      * 9.200      *      166.12 * 166.05 * 0.07 *
*      *      199.93 * 271.69 * 73.14 * 216.16 *
* Upper      * 9.100      *      166.09 * 166.02 * 0.07 *
*      *      199.55 * 271.49 * 73.04 * 216.05 *
* Upper      * 9.000      *      166.05 * 165.98 * 0.07 *
*      *      200.13 * 270.21 * 73.07 * 216.72 *

```

Profile Output Table - Bridge Only

```

* Reach      * River Sta * E.G. US. *Min El Prs *BR Open Area *
Prs O WS * Q Total *Min El Weir Flow * Q Weir * Delta EG *
*
*      *      *      (m) *      (m) *      (m2) *
(m) * (m3/s) * (m) * (m3/s) * (m) *
*****
* Upper      * 9.385      *      166.29 * 166.50 * 364.02 *
*      545.93 *      167.50 *      * 0.11 *

```

```

*****
Profile Output Table - Four XS Culvert
*****
* Reach      * River Sta  *   E.G. Elev *W.S. Elev * Vel Head
*Frctn Loss *C & E Loss *   Q Left *Q Channel *  Q Right *Top
Width *
*
*          *          *          (m) *          (m) *          (m) *
*        (m) *        (m) *        (m3/s) *        (m3/s) *        (m3/s) *        (m) *
*****
*          *          *          *          *          *          *          *
*          *          *          *          *          *          *          *
*****

```

```

Bridge Scour Data
River = Maan
Reach = Upper
Riv Sta = 9.385
Profile = 08JUL1998 0900

```

Contraction Scour

	Left	Channel	Right
Input Data			
Average Depth (m):	0.56	1.79	0.90
Approach Velocity (m/s):	0.35	0.88	0.43
Br Average Depth (m):	0.59	1.74	0.98
BR Opening Flow (m3/s):	11.26	85.18	10.58
BR Top WD (m):	37.66	44.00	18.00
Grain Size D50 (m):	0.0012	0.0012	0.0012
Approach Flow (m3/s):	17.14	79.10	11.53
Approach Top WD (m):	88.57	50.00	30.00
K1 Coefficient:	0.590	0.590	0.590
Results			
Scour Depth Ys (m):	0.00	0.32	0.00
Critical Velocity (m/s):	0.58	0.71	0.63
Equation:	Clear	Live	Clear

Pier Scour

All piers have the same scour depth

Input Data	
Pier Shape:	Round nose
Pier Width (m):	2.00
Grain Size D50 (m):	0.00120
Depth Upstream (m):	2.53
Velocity Upstream (m/s):	1.09
K1 Nose Shape:	1.00
Pier Angle:	0.00
Pier Length (m):	7.50
K2 Angle Coef:	1.00
K3 Bed Cond Coef:	1.10
Grain Size D90 (m):	0.00300
K4 Armouring Coef:	1.00
Results	
Scour Depth Ys (m):	2.48
Froude #:	0.22
Equation:	CSU equation

Abutment Scour

Left	Right
------	-------

Input Data

Station at Toe (m):	70.00	190.00
Toe Sta at appr (m):	70.00	190.00
Abutment Length (m):	42.11	10.00
Depth at Toe (m):	-0.04	1.33
K1 Shape Coef:	1.00	Vertical abutment
Degree of Skew (degrees):	90.00	90.00
K2 Skew Coef:	1.00	1.00
Projected Length L' (m):	42.11	10.00
Avg Depth Obstructed Ya (m):	0.44	0.67
Flow Obstructed Qe (m3/s):	5.40	2.31
Area Obstructed Ae (m2):	18.63	6.70

Results

Scour Depth Ys (m):	2.10
Qe/Ae = Ve:	0.34
Froude #:	0.13
Equation:	Default Froehlich

Combined Scour Depths

Pier Scour + Contraction Scour (m):

Left Bank:	2.48
Channel:	2.80
Right Bank:	2.48

Right abutment scour + contraction scour (m): 2.10

Bridge Scour Data

River = Maan
 Reach = Upper
 Riv Sta = 9.385
 Profile = 07JUL1998 2400

Contraction Scour

	Left	Channel	Right
Input Data			
Average Depth (m):	0.13	1.00	0.22
Approach Velocity (m/s):	0.13	0.61	0.19
Br Average Depth (m):	0.11	1.01	0.22
BR Opening Flow (m3/s):	0.22	29.13	0.65
BR Top WD (m):	13.64	40.55	14.00
Grain Size D50 (m):	0.0012	0.0012	0.0012
Approach Flow (m3/s):	0.28	28.88	0.84
Approach Top WD (m):	16.81	47.47	20.35
K1 Coefficient:	0.590	0.590	0.590
Results			
Scour Depth Ys (m):	0.00	0.02	0.00
Critical Velocity (m/s):	0.46	0.64	0.50
Equation:	Clear	Clear	Clear

Pier Scour

All piers have the same scour depth

Input Data

Pier Shape:	Round nose
Pier Width (m):	2.00
Grain Size D50 (m):	0.00120

Depth Upstream (m): 1.70
 Velocity Upstream (m/s): 0.75
 K1 Nose Shape: 1.00
 Pier Angle: 0.00
 Pier Length (m): 7.50
 K2 Angle Coef: 1.00
 K3 Bed Cond Coef: 1.10
 Grain Size D90 (m): 0.00300
 K4 Armouring Coef: 1.00

Results

Scour Depth Ys (m): 2.01
 Froude #: 0.18
 Equation: CSU equation

Abutment Scour

	Left	Right
Input Data		
Station at Toe (m):	70.00	190.00
Toe Sta at appr (m):	70.00	190.00
Abutment Length (m):	0.00	3.73
Depth at Toe (m):	-0.88	0.49
K1 Shape Coef:	1.00 - Vertical abutment	
Degree of Skew (degrees):	90.00	90.00
K2 Skew Coef:	1.00	1.00
Projected Length L' (m):	0.00	3.73
Avg Depth Obstructed Ya (m):		0.25
Flow Obstructed Qe (m3/s):		0.19
Area Obstructed Ae (m2):		0.93

Results

Scour Depth Ys (m): 0.77
 Qe/Ae = Ve: 0.20
 Froude #: 0.13
 Equation: Default Froehlich

Combined Scour Depths

Pier Scour + Contraction Scour (m):
 Left Bank: 2.01
 Channel: 2.03
 Right Bank: 2.01

Right abutment scour + contraction scour (m): 0.77

Bridge Scour Data

River = Maan
 Reach = Upper
 Riv Sta = 9.385
 Profile = 08JUL1998 0300

Contraction Scour

	Left	Channel	Right
Input Data			
Average Depth (m):	0.17	1.06	0.28
Approach Velocity (m/s):	0.16	0.62	0.21
Br Average Depth (m):	0.19	1.03	0.27
BR Opening Flow (m3/s):	0.64	33.05	1.28

	BR Top WD (m):	17.00	44.00	18.00
	Grain Size D50 (m):	0.0012	0.0012	0.0012
	Approach Flow (m ³ /s):	0.73	32.87	1.48
	Approach Top WD (m):	26.65	50.00	24.52
	K1 Coefficient:	0.590	0.590	0.590
Results	Scour Depth Ys (m):	0.00	0.04	0.00
	Critical Velocity (m/s):	0.48	0.65	0.52
	Equation:	Clear	Clear	Clear

Pier Scour

All piers have the same scour depth

Input Data

Pier Shape:	Round nose
Pier Width (m):	2.00
Grain Size D50 (m):	0.00120
Depth Upstream (m):	1.80
Velocity Upstream (m/s):	0.78
K1 Nose Shape:	1.00
Pier Angle:	0.00
Pier Length (m):	7.50
K2 Angle Coef:	1.00
K3 Bed Cond Coef:	1.10
Grain Size D90 (m):	0.00300
K4 Armouring Coef:	1.00

Results

Scour Depth Ys (m):	2.05
Froude #:	0.18
Equation:	CSU equation

Abutment Scour

	Left	Right
Input Data		
Station at Toe (m):	70.00	190.00
Toe Sta at appr (m):	70.00	190.00
Abutment Length (m):	3.87	4.52
Depth at Toe (m):	-0.77	0.60
K1 Shape Coef:	1.00 - Vertical abutment	
Degree of Skew (degrees):	90.00	90.00
K2 Skew Coef:	1.00	1.00
Projected Length L' (m):	3.87	4.52
Avg Depth Obstructed Ya (m):	0.05	0.30
Flow Obstructed Qe (m ³ /s):	0.01	0.31
Area Obstructed Ae (m ²):	0.19	1.37

Results

Scour Depth Ys (m):	0.94
Qe/Ae = Ve:	0.23
Froude #:	0.13
Equation:	Default Froehlich

Combined Scour Depths

Pier Scour + Contraction Scour (m):	
	Left Bank:2.05
	Channel: 2.10
	Right Bank:2.05

Right abutment scour + contraction scour (m):0.94

Bridge Scour Data

River = Maan
Reach = Upper
Riv Sta = 9.385
Profile = 08JUL1998 0600

Contraction Scour

	Left	Channel	Right
Input Data			
Average Depth (m):	0.28	1.36	0.55
Approach Velocity (m/s):	0.24	0.74	0.31
Br Average Depth (m):	0.36	1.32	0.56
BR Opening Flow (m3/s):	3.14	51.25	4.06
BR Top WD (m):	26.10	44.00	18.00
Grain Size D50 (m):	0.0012	0.0012	0.0012
Approach Flow (m3/s):	4.09	50.23	4.55
Approach Top WD (m):	60.51	50.00	26.77
K1 Coefficient:	0.590	0.590	0.590
Results			
Scour Depth Ys (m):	0.00	0.17	0.00
Critical Velocity (m/s):	0.52	0.68	0.58
Equation:	Clear	Live	Clear

Pier Scour

All piers have the same scour depth

Input Data

Pier Shape: Round nose
Pier Width (m): 2.00
Grain Size D50 (m): 0.00120
Depth Upstream (m): 2.09
Velocity Upstream (m/s): 0.93
K1 Nose Shape: 1.00
Pier Angle: 0.00
Pier Length (m): 7.50
K2 Angle Coef: 1.00
K3 Bed Cond Coef: 1.10
Grain Size D90 (m): 0.00300
K4 Armouring Coef: 1.00

Results

Scour Depth Ys (m): 2.26
Froude #: 0.20
Equation: CSU equation

Abutment Scour

	Left	Right
Input Data		
Station at Toe (m):	70.00	190.00
Toe Sta at appr (m):	70.00	190.00
Abutment Length (m):	26.05	6.77
Depth at Toe (m):	-0.48	0.89
K1 Shape Coef:	1.00 - Vertical	abutment
Degree of Skew (degrees):	90.00	90.00
K2 Skew Coef:	1.00	1.00
Projected Length L' (m):	26.05	6.77

Avg Depth Obstructed Ya (m) : 0.16 0.45
 Flow Obstructed Qe (m3/s) : 0.67 0.84
 Area Obstructed Ae (m2) : 4.06 3.07

Results

Scour Depth Ys (m) : 1.39
 Qe/Ae = Ve: 0.27
 Froude #: 0.13
 Equation: Default Froehlich

Combined Scour Depths

Pier Scour + Contraction Scour (m):
 Left Bank:2.26
 Channel: 2.43
 Right Bank:2.26

Right abutment scour + contraction scour (m):1.39

Bridge Scour Data

River = Maan
 Reach = Upper
 Riv Sta = 9.385
 Profile = 08JUL1998 1500

Contraction Scour

	Left	Channel	Right
Input Data			
Average Depth (m) :	1.60	3.01	1.77
Approach Velocity (m/s) :	0.63	1.23	0.70
Br Average Depth (m) :	1.70	2.94	2.18
BR Opening Flow (m3/s) :	74.22	227.76	43.57
BR Top WD (m) :	44.00	44.00	18.00
Grain Size D50 (m) :	0.0012	0.0012	0.0012
Approach Flow (m3/s) :	113.06	185.27	48.29
Approach Top WD (m) :	111.90	50.00	38.96
K1 Coefficient:	0.590	0.640	0.590
Results			
Scour Depth Ys (m) :	0.45	0.96	0.75
Critical Velocity (m/s) :	0.70	0.77	0.71
Equation:	Clear	Live	Clear

Pier Scour

All piers have the same scour depth

Input Data

Pier Shape: Round nose
 Pier Width (m) : 2.00
 Grain Size D50 (m) : 0.00120
 Depth Upstream (m) : 3.80
 Velocity Upstream (m/s) : 1.41
 K1 Nose Shape: 1.00
 Pier Angle: 0.00
 Pier Length (m) : 7.50
 K2 Angle Coef: 1.00
 K3 Bed Cond Coef: 1.10
 Grain Size D90 (m) : 0.00300
 K4 Armouring Coef: 1.00

Results

Scour Depth Ys (m): 2.93
 Froude #: 0.23
 Equation: CSU equation

Abutment Scour

	Left	Right
Input Data		
Station at Toe (m):	70.00	190.00
Toe Sta at appr (m):	70.00	190.00
Abutment Length (m):	61.90	18.96
Depth at Toe (m):	1.22	2.59
K1 Shape Coef:	1.00 - Vertical abutment	
Degree of Skew (degrees):	90.00	90.00
K2 Skew Coef:	1.00	1.00
Projected Length L' (m):	61.90	18.96
Avg Depth Obstructed Ya (m):	1.41	1.28
Flow Obstructed Qe (m3/s):	50.31	14.49
Area Obstructed Ae (m2):	87.46	24.35

Results

Scour Depth Ys (m):	4.89	4.40
Qe/Ae = Ve:	0.00	0.60
Froude #:	0.16	0.17
Equation:	HIRE	Froehlich

Combined Scour Depths

Pier Scour + Contraction Scour (m):
 Left Bank: 3.38
 Channel: 3.89
 Right Bank: 3.68

Left abutment scour + contraction scour (m): 5.34
 Right abutment scour + contraction scour (m): 5.15

Bridge Scour Data

River = Maan
 Reach = Upper
 Riv Sta = 9.385
 Profile = 08JUL1998 1800

Contraction Scour

	Left	Channel	Right
Input Data			
Average Depth (m):	1.78	3.22	1.88
Approach Velocity (m/s):	0.67	1.28	0.73
Br Average Depth (m):	1.91	3.15	2.38
BR Opening Flow (m3/s):	90.07	257.50	50.99
BR Top WD (m):	44.00	44.00	18.00
Grain Size D50 (m):	0.0012	0.0012	0.0012
Approach Flow (m3/s):	136.55	205.70	56.75
Approach Top WD (m):	113.81	50.00	41.03
K1 Coefficient:	0.590	0.640	0.590
Results			
Scour Depth Ys (m):	0.63	1.09	0.41
Critical Velocity (m/s):	0.71	0.78	0.72

Equation: Clear Live Live

Pier Scour

All piers have the same scour depth

Input Data

Pier Shape: Round nose
 Pier Width (m): 2.00
 Grain Size D50 (m): 0.00120
 Depth Upstream (m): 4.02
 Velocity Upstream (m/s): 1.45
 K1 Nose Shape: 1.00
 Pier Angle: 0.00
 Pier Length (m): 7.50
 K2 Angle Coef: 1.00
 K3 Bed Cond Coef: 1.10
 Grain Size D90 (m): 0.00300
 K4 Armouring Coef: 1.00

Results

Scour Depth Ys (m): 2.99
 Froude #: 0.23
 Equation: CSU equation

Abutment Scour

Left Right

Input Data

Station at Toe (m): 70.00 190.00
 Toe Sta at appr (m): 70.00 190.00
 Abutment Length (m): 63.81 21.03
 Depth at Toe (m): 1.44 2.81
 K1 Shape Coef: 1.00 - Vertical abutment
 Degree of Skew (degrees): 90.00 90.00
 K2 Skew Coef: 1.00 1.00
 Projected Length L' (m): 63.81 21.03
 Avg Depth Obstructed Ya (m): 1.58 1.36
 Flow Obstructed Qe (m3/s): 61.94 16.37
 Area Obstructed Ae (m2): 100.66 28.51

Results

Scour Depth Ys (m): 5.78 4.60
 Qe/Ae = Ve: 0.00 0.57
 Froude #: 0.16 0.16
 Equation: HIRE Froehlich

Combined Scour Depths

Pier Scour + Contraction Scour (m):

Left Bank: 3.62
 Channel: 4.08
 Right Bank: 3.40

Left abutment scour + contraction scour (m): 6.41

Right abutment scour + contraction scour (m): 5.01

Bridge Scour Data

River = Maan
 Reach = Upper
 Riv Sta = 9.385

Profile = Max WS

Contraction Scour

	Left	Channel	Right
Input Data			
Average Depth (m):	2.22	3.74	2.06
Approach Velocity (m/s):	0.78	1.40	0.81
Br Average Depth (m):	2.41	3.65	2.89
BR Opening Flow (m ³ /s):	135.10	339.18	71.64
BR Top WD (m):	44.00	44.00	18.00
Grain Size D50 (m):	0.0012	0.0012	0.0012
Approach Flow (m ³ /s):	203.69	261.36	81.71
Approach Top WD (m):	118.52	50.00	48.77
K1 Coefficient:	0.590	0.640	0.590
Results			
Scour Depth Ys (m):	1.19	4.27	1.60
Critical Velocity (m/s):			
Equation:	Clear	Clear	Clear

Pier Scour

All piers have the same scour depth

Input Data

Pier Shape:	Round nose
Pier Width (m):	2.00
Grain Size D50 (m):	0.00120
Depth Upstream (m):	4.56
Velocity Upstream (m/s):	1.58
K1 Nose Shape:	1.00
Pier Angle:	0.00
Pier Length (m):	7.50
K2 Angle Coef:	1.00
K3 Bed Cond Coef:	1.10
Grain Size D90 (m):	0.00300
K4 Armouring Coef:	1.00

Results

Scour Depth Ys (m):	3.15
Froude #:	0.24
Equation:	CSU equation

Abutment Scour

	Left	Right
Input Data		
Station at Toe (m):	70.00	190.00
Toe Sta at appr (m):	70.00	190.00
Abutment Length (m):	68.52	28.77
Depth at Toe (m):	1.98	3.35
K1 Shape Coef:	1.00 - Vertical abutment	
Degree of Skew (degrees):	90.00	90.00
K2 Skew Coef:	1.00	1.00
Projected Length L' (m):	68.52	28.77
Avg Depth Obstructed Ya (m):	1.97	1.44
Flow Obstructed Qe (m ³ /s):	95.87	27.34
Area Obstructed Ae (m ²):	134.97	41.42
Results		
Scour Depth Ys (m):	8.74	5.54
Qe/Ae = Ve:	0.71	0.66
Froude #:	0.16	0.18

Equation:

Froehlich Froehlich

Combined Scour Depths

Pier Scour + Contraction Scour (m):

Left Bank:4.34

Channel: 7.43

Right Bank:4.76

Left abutment scour + contraction scour (m):9.92

Right abutment scour + contraction scour (m):7.14